Microgravity- and shear stress-mediated regulation of E3 ligase NEDD4 and its substrate Cx43 in endothelial cells

Dissertation
to obtain academic degree
Doctor rerum naturalium
(Dr. rer. nat.)

submitted to the Department of Biology, Chemistry and Pharmacy
of the Freie Universität Berlin

by

Katarzyna Fiedorowicz
born in Bydgoszcz (Poland)

Berlin, March 2012

1st Reviewer: Prof. Dr. V. Haucke
2nd Reviewer: Prof. Dr. A.R. Pries

Date of disputation: 12.11.12

List of abbreviations

AP-1	Activator protein 1
ARE	Antioxidant responsive element
ADAMTS1	A disintegrin and metalloproteinase with thrombospondin motifs 1
ALLN	Acetyl-L-Leucyl-L-Leucyl-L-Norleucinal
APS	Ammonium persulfate
BAG-3	BCL2-associated athanogene 3
BSA	Bovine serum albumin
Bcl10	B-cell lymphoma/leukemia 10
Co-IP	Co-immunoprecipitation
Cx	Connexin
DAP	1,4 Bis(acryl) piperazine
DMEM	Dulbecco's Modified Eagle Medium
DMSO	Dimethyl sulfoxide
DNA	Deoxyribonucleic acid
D-NAME	N(G)-Nitro-D-arginine methyl ester
EAhy926	The human umbilical vein cell line
EDTA	Ehylenediaminetetraacetate,
EGF	Epidermal Growth Factor
ELISA	Enzyme-linked immunosorbant assay
Eps15	Epidermal growth factor receptor substrate 15
eNOS	Endothelial nitric oxide synthase
Egr1	Early growth response 1
FCS	Fetal calf serum
HAS	Hyaluronan synthase
HBSS	Hank’s Balanced Salt Solution
HUVEC	Human umbilical vein endothelial cells
Hsp 70	Heat shock protein 70
IL	Interleukin
IP	Immunoprecipitation
KCl	Kaliumchlorid
kDa	kilodalton
KH_2PO_4	Kaliumhydrogenphosphat
Klf2	Krueppel-like factor 2
L-NAME	L-NG-Nitroarginine methyl ester (hydrochloride)
MAPK	Mitogen-activated protein kinase
MG132	Z-Leu-Leu-Leu-h (aldehyde)
Murf1	Muscle ring finger protein1
NaCl	Sodium chloride

$NaHCO_3$	Sodium bicarbonate
Na_2HPO_4	Disodium hydrogen phosphate
NaOH	Sodium hydroxide
Na_3VO_4	Sodium vanadate
Nedd4	Neural precursor cell expressed developmentally down-regulated protein 4
NF1	Nuclear factor I
NO	Nitric oxide
Notch1	Notch homolog 1
Nrf2	Nuclear factor like 2
OD	Optical density
PBS	Phosphate buffered saline
PCR	Polymerase chain reaction
PDH	Human pyruvate dehydrogenase
PI3K	Phosphoinositide-3-kinase
PLC	Phospholipase C
PMSF	Phenylmethylsulfonyl fluoride
POD	Horse-radish-peroxidase
RNA	Ribonucleic acid
RNAi	RNA interference
siRNA	small interfering RNA
rpm	rotations per minute
RWV	Rotating Wall Vessel
RT	Room temperature
RT-PCR	Real time polymerase chain reaction
SD	Standard Deviation
SDS	Sodiumdodecylsulfat
SSRE	Shear stress response element
vWF	von Willebrand Factor
VEGFR	Vascular endothelial growth factor receptor
TEMED	Tetramethylethylenediamine
TRE	Phorbol ester TPA responsive element
Tris	Tris-(hydroxymethyl) aminoethan
TSP1	Thrombospondin 1

Contents

1 Introduction

1.1 The vessel wall

The vessel wall consists of three concentric regions: tunica intima, tunica media and tunica adventitia (Figure 1). Tunica intima is the innermost and the thinnest (0.5-1 μm) of the layers and is built by endothelial cells. Endothelium is surrounded by internal elastic lamina. Tunica intima is covered by tunica media. Tunica media is usually the thickest and most flexible of the layers. It is thicker in the walls of arteries than in veins. It consists of concentric rings of smooth muscle cells and elastic fibers. The outermost layer in arteries and veins is tunica adventitia. It is made by fibrous connective tissue, collagen and elastic fibers. Elastic fibers allow vessels to stretch in order to prevent overexpansion due to the pressure caused by the flowing blood. In veins, smooth muscle cells may be also present in this layer. Tunica adventitia gives also strength and support to the vessel. Within this layer are also localized autonomic nerves that innervate smooth muscle cells in tunica media. Tunica media and adventitia are separated by an external elastic lamina [1].

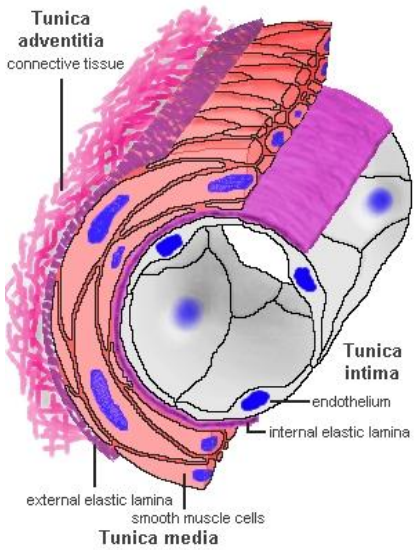

Figure 1 Structure of the vessel wall
The vascular vessel wall consists of three intimas. Tunica intima lies the innermost and is built by endothelial cells. Tunica media consists of smooth muscle cells and elastic fibers. Tunica adventitia is made of connective tissue, collagen and elastic fibers. Figure from School of Anatomy and Human Biology [2].

A crucial role in the control of many functions within vascular wall is played by endothelial cells. They participate not only in vascular homeostasis (regulation of tone)

but also are involved in blood vessel formation, coagulation and fibrinolysis or inflammatory reactions [3].

1.2 Endothelial cells

Endothelial cells cover the entire circulatory system from the heart to the smallest vessels. The estimated area of endothelial surface is about 350m^2 [4]. This continuous layer of cells serves not only as a selective, permeable barrier for many molecules but is also a "sensory organ" which integrates, transduces and responds to mechanical stimulation.

Endothelial cells actively interact with blood cells via the apical surface due to their polarization and with smooth muscle cells via their basal surface. Between endothelium and free flowing blood there seems to be an unstirred layer linked to the endothelium, the so called endothelial surface layer (supposed to be 0.5µm to more than 1µm thick) [5]. The endothelial surface layer plays an important role in the regulation of vascular permeability and modulation of inflammatory responses as well as in response to shear stress [6].

1.3 Biomechanical forces in vascular system

The blood vessel wall is constantly exposed to mechanical forces like circumferential stress and shear stress (Figure 2). Circumferential stress generated by blood pressure is perpendicular or tangential to the surface and is transferred to all layers of the vessel wall (intima, media and adventitia). Shear stress acts parallel to the vessel axis and is determined by the fluid flow rate. Shear stress affects most probably only the vascular endothelium [7].

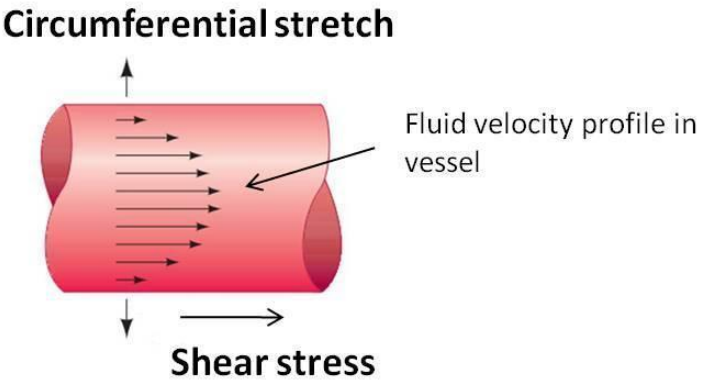

Figure 2 Schematic diagram showing forces generated by the flowing blood
Blood flowing through vessel creates circumferential stress (perpendicular to the surface) and shear stress (acts parallel to the vessel surface). The amount of shear stress acting on endothelial cells is determined by velocity profile within the vessel (shown by the arrows) and viscosity of the fluid. Figure adapted from Jones et al. [8]

In general, blood flow in the human vascular system is laminar. Velocity is increasing when closer to the center of the vessel and varies depending on the position of vessel in a vascular tree. In regions with irregular geometry like branch points, which are predilection sites of atherosclerosis, or diseased and narrowed arteries fluid flow is often turbulent or "disturbed" [9, 10].

Mainly because of the impact of atherosclerosis, the role of shear stress in endothelial cell biology has been intensively investigated over the last decades. Shear stress is crucial for endothelial cell survival, proliferation, structure and functions. Experiments performed in many laboratories clearly demonstrate that high laminar flow determines a healthy phenotype of endothelium, which is anticoagulant, antiproliferative, and serves vasodilator functions (atheroprotective). Conversely, disturbed flow (atheroprone) leads to the development of atherosclerosis (Figure 3) [11].

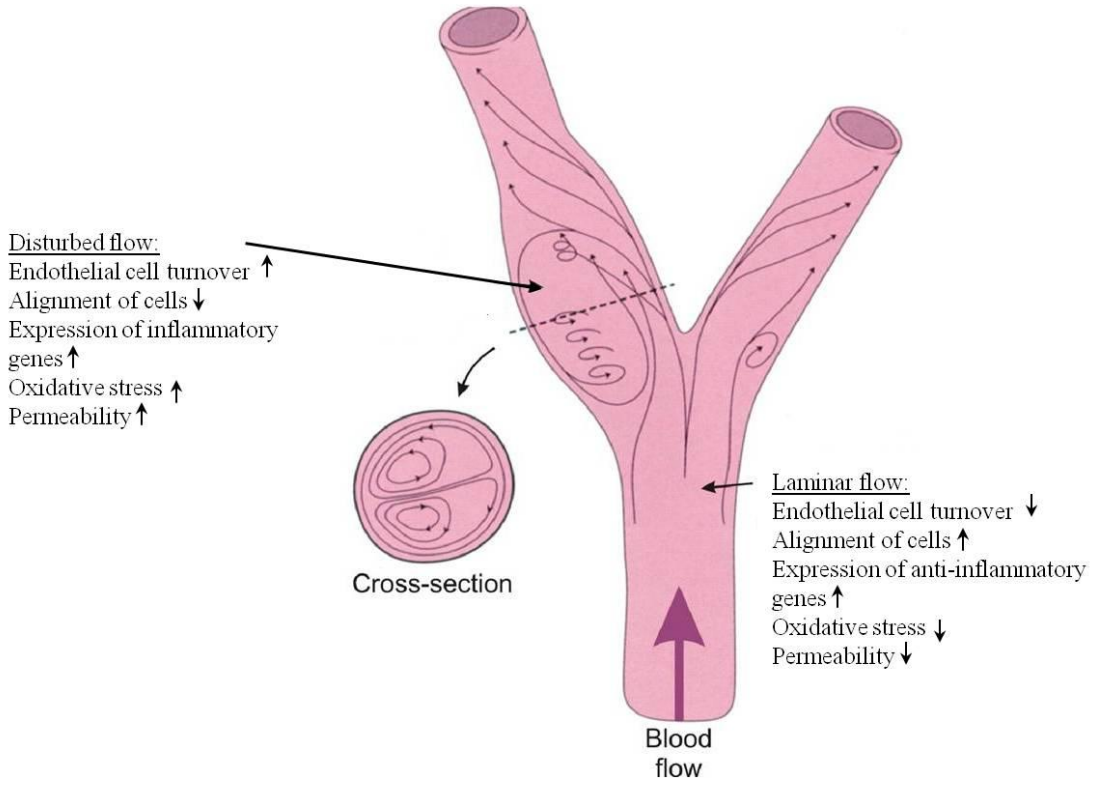

Figure 3 Schematic diagram showing the effects of different flows on endothelial cell function
In the straight part of vessels blood flow is laminar, whereas in regions with irregular geometry blood flow is often disturbed. In regions of high laminar flow endothelial cells have an atheroprotective phenotype characterized by alignment of cell in the direction of flow, low turnover, low permeability as well as low oxidative stress. Conversely, disturbed flow causes an increased permeability, leads to the high cell turnover, oxidative stress and expression of inflammatory genes. This change leads to the development of atherosclerosis. Figure adapted from Chatazisis et al. [9]

These findings stimulated series of experiments showing that different flow patterns differently impact the regulation of many genes. This allowed to state a hypothesis that endothelial cells not only "sense" mechanical forces, but also distinguish between different types of them and respond for example by changing their phenotype [12]. Although, many of such genes have been characterized, the mechanisms which endothelial cells use to adapt to changing hemodynamic conditions are still not well understood.

1.4 Angioadaptation

Mechanical forces play an essential role in the process of angioadaptation, which under physiological conditions allows for proper development and adjustment of the vascular network. In pathological states, like wound healing or inflammation, it is necessary for regeneration and repair. Angioadaptation involves remodeling, pruning, and

maintaining of existing vessels as well as building of new ones in a process called angiogenesis [13, 14] .

Angiogenesis

Angiogenesis is a physiological process resulting in the formation of a mature vascular network, which is necessary for pre- and postnatal growth and development as well as for wound healing, homeostasis of tissues, muscle training [15] and remodeling of the endometrium in adults [16]. The new vessels are created either by sprouting or intussception (known also as splitting type of angiogenesis) (Figure 4).

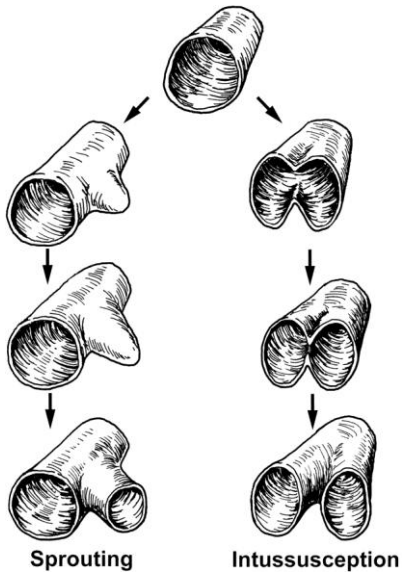

Figure 4 The new vessels are created either by sprouting or intussception (known also as splitting type of angiogenesis)
Figure from Prior et al. [17]

Sprouting angiogenesis involves several distinct steps. Initially, receptors on endothelial cells in existing vessels are activated by angiogenic growth factors, the most important of which is VEGF-A. An early step in the initiation of angiogenesis is an increase in vascular permeability. Next endothelial cells release proteolytic enzymes that degrade the basement membrane. This allows endothelial cells to escape from the vessel wall. Proliferating and migrating endothelial cells form solid sprouts which connect neighboring vessels. These sprouts then get a lumen, and with the onset of perfusion the newly formed blood vessel starts to mature. Sprouting is slow and enables new vessels to fill gaps in vasculature [18].

In intussusception a new vessel is created by splitting one single vessel into two. According to Caduff' s description, this process occurs in four steps. At first, a zone of contact between opposite capillary walls is established. In a second step intercellular junctions of endothelial cells are reorganized and the endothelial bilayer is perforated opening the way on which growth factors and cells are able to penetrate the lumen. Next, a pillar core is formed between two new vessels at the zone of contact. Pillar cores are filled with pericytes and myofibroblasts. Pericytes and myofibroblasts lay collagen fibers into the core to provide an extracellular matrix for the growing vessel. At last, vessel grows to the normal size [19].

Which type of angiogenesis occurs depends on a combination of metabolic (e.g. oxygen availability) and hemodynamic (pressure and flow) factors. Sprouting type of angiogenesis is controlled by a variety of inhibitors and stimulators in response to hypoxia, whereas changes in blood flow may promote intussception [10, 20]. It is also important to note that these two types of angiogenesis may occur in the same vessel.

1.5 The effects of microgravity on the cardiovascular system

Nowadays, together with increasing interest in the exploration of space, microgravity is more often considered as an important factor that affects the human body. Since living organisms during evolution adapted the processes described above to the mechanical environment of Earth, it is one of the most important space medicine challenges to recognize the mechanisms leading to the physiological adaptation to weightlessness and to understand how they may influence pathophysiology of diseases [21].

Several space missions confirmed a strong impact of low gravity on the cardiovascular system. NASA and ESA reports described the most dramatic changes in astronauts in the beginning of missions mainly in the vestibular and electrolyte control systems. Blood that is normally pulled into the legs is shifted into the large venous vessels in the chest, the point of least resistance in the absence of gravity. This redistribution of fluids is coupled with fluid loss because overfilled circulation adapts arterial pressure and adjusts diuresis [22]. As a result astronaut's faces are puffy and legs shrinked. It has been postulated that these changes are caused by drastic perturbation in the mechanical environment of endothelial cells, what results in altered transendothelial transport of

water and ions. Moreover, on Earth the heart operates against gravity to sustain blood flow. Without gravity the heart has less to pump and heart beat slows down. Since the body does not need strong muscles, heart tissues begin to weaken and decrease.

Microgravity has also been considered as a risk factor which may increase the development of different cardiac diseases e.g. ischemic arrhythmias, myocardial infarction, sudden cardiac death or atherosclerosis [23, 24]. The risk of developing such incidents in astronauts is very difficult to determine, mainly because of the small size and variation in astronauts population (sex, age, race, culture, occupation). Due to this problem many data and observations are extrapolated either from experiments performed in different models of microgravity simulation in humans and animals or from similar population like military and civil aviators. First investigations based on autopsy revision allowed to conclude that from 710 pilots who died in aviation accidents, 61% had a form of coronary atherosclerosis [25]. Similar studies based on 6500 autopsies revision from deaths at the aircraft accidents showed that 13% of cases were diagnosed with already pre-existing heart dysfunction. Within this group 89.1% suffered from atherosclerosis [26]. Currently, this hypothesis finds support in Doppler ultrasound measurements during parabolic flights. Results of these experiments have shown that exposure to microgravity leads to the fluctuations in blood flow and pressure [27]. It has been proposed that changes in flow profiles may have similar effects on endothelial cells phenotype as oscillatory shear stress on ground and contribute to the development of dysfunction by inducing inflammatory response and oxidative stress [28].

Changes in blood flow during exposure to microgravity lead to the differential adaptation of vessels from different anatomical regions. For example in hindlimb unloaded rats differences in forelimb and hindlimbs were observed [29]. After four weeks of suspension the lumen diameter and the cross sectional area of the arteries (femoral and anterior tibial) were decreased, whereas in forelimbs (common carotid and basilar arteries) both increased. Additional investigations showed that shape and alignment of endothelial cells decreased in length and increase in width in femoral arteries, suggesting a change in applied shear stress and increased blood flow toward the head [30]. Beside structural changes, arteries undergo functional changes like decreased vasoreactivity in hindquarter arteries [31].

The remodeling of vessel occurs also in muscle-atrophy induced by hindlimb unloading as simulation of weightlessness. Structural adaptation of muscles as well as microvasculature varies between muscle types. One of the most affected muscles is soleus, a weight bearing skeletal muscle. Several investigations confirmed atrophy of this muscle by 35% after 14 days [32] up to 50% after 5 weeks of unloading [33]. The reduced blood flow to resting and exercised soleus muscle was observed after 14 days [34]. Additionally, analysed number of capillaries was decreased already during first week of experiment [35, 36] and was about 40% lower after 5 weeks [33].

Up to date, regulation of only some of several possible molecules which may contribute to the observed changes has been investigated. The downregulation of angiopoietin-1, angiopoietin-2 and their receptor (Tie-2) as well as reduced VEGF receptors were related with capillary regression [37]. Studies by Roudier et al. revealed that VEGF-A was not affected and VEGF–B increased at two time points (3rd and 7th day of unloading), the significant increase in TSP1 was associated with capillary regression. In contrast, in plantaris muscles where the original number of capillaries was maintained, the VEGF–B increased (7th and 9th day of unloading), while VEGF-A and TSP1 were not affected [38]. This finding also supports an earlier hypothesis that the integrated balance between pro- and anti-angiogenic signals play a crucial role in the regulation of angiogenesis [39].

The reduction in blood flow and capillarization limits delivery of oxygen to the muscles and contributes to the reduced aerobic capacity. This may explain why muscle training performed as a countermeasure for microgravity is not effective [40].

1.6 Mechanosensivity of endothelial cells

The process which cells use to identify and transduce mechanical forces into biological responses is called mechanotransduction [41]. As many studies have shown the biochemical response may occur within seconds, or minutes or its effects may be measurable after several hours (Figure 5) [42].

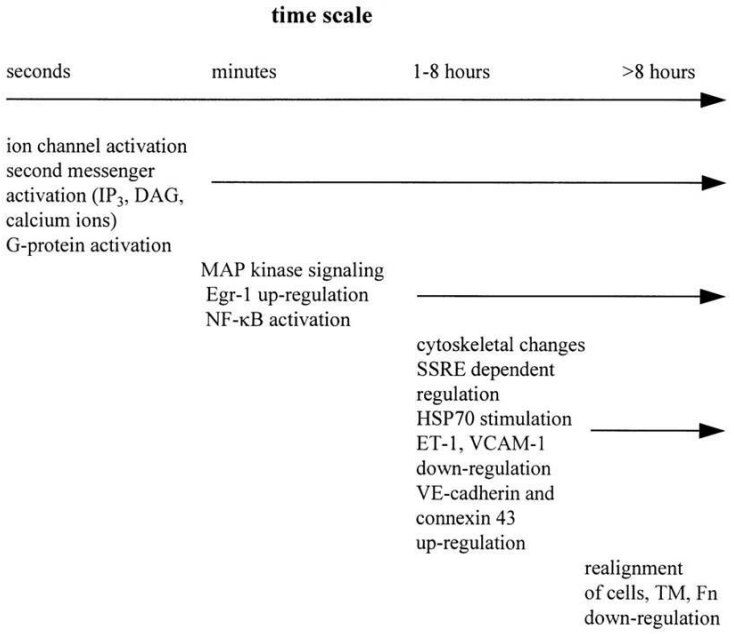

Figure 5 Biomechanical response to shear stress
Shear stress activates ion channels, second messengers and G-proteins within seconds. After minutes signaling via MAPK and transcription factors like EGR-1 and NFkB are activated. Within a few hours the cytoskeleton is rearranged, regulated shear stress responsive element (SSRE) as well as expression of ET-1, VCAM-1, VE-cadherin. After several hours realignment of cells is visible. Figure from Braddock et al. [42]

The process of mechanotransduction involves three specific steps. First, mechanoreceptors like ion channels, focal adhesion sites, integrins, G-protein coupled receptors and tyrosine kinases present on or somehow linked to endothelial cell surfaces detect mechanical stimulations (Figure 6). During the next step signaling pathways like: phosphatidylinositol 3-kinase/Akt pathway (PI3K/Akt), the mitogen-activated protein kinases (MAPK) ERK1/2, JNK, p38 are activated [42]. These signaling pathways transduce biomechnical stimulation to the nucleus. Cytoskeleton has been found to play an important role in the mediation of shear stress signaling by providing a scaffold that allows signaling molecules from inside and outside of the cell to interact [43].

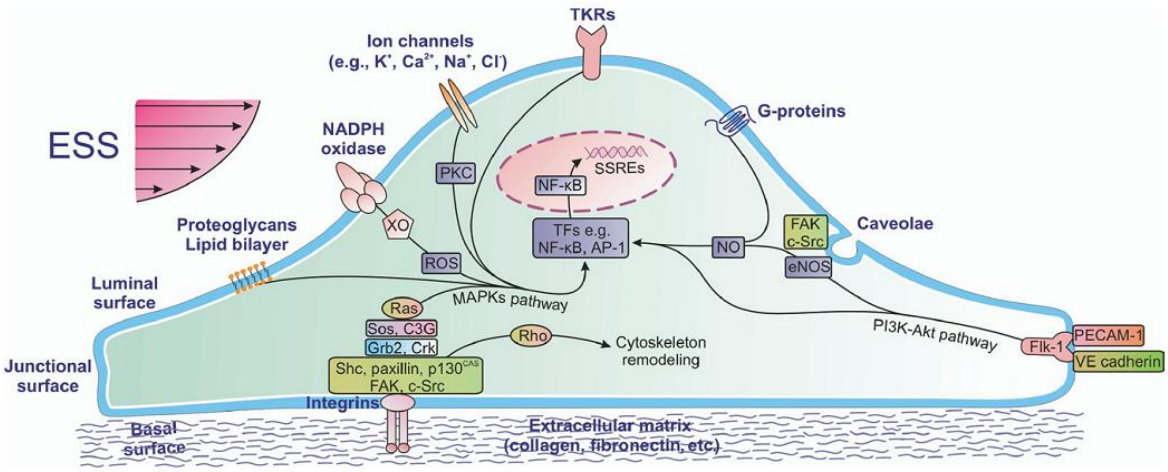

Figure 6 Schematic diagram showing shear stress acting on endothelial cell surfaces
Stimulation of mechanoreceptors by shear stress (ESS) leads to the activation of signaling cascades. Through several pathways the signal is transmitted to the nucleus. Here transcription factors are activated. They bind to the promoter of specific genes and lead to the regulation of their expression. Figure from Chatzizisis et al. [9]

In a last step, activated signaling cascades lead to the phosphorylation of different transcription factors, which bind at promoters of many genes, regulating cell morphology, migration, proliferation or apoptosis. The transcription factors which were found to participate in response to shear stress are: activator protein (AP-1), nuclear factor–kappa B (NF-κB), early growth response-1 (egr1) [44]. Additionally, the regulation of transcription can be mediated through the shear stress-sensitive *cis*- elements at the promoter regions. For example platelet-derived growth factor posses nucleotide sequence GAGACC called “shear stress response element” (SSRE) that is necessary for shear stress induced regulation of PDGF-B mRNA [45]. Transcription factor which interacts with this sequence is NF-κB [46]. The SSRE element was also found in the promoters of ICAM-1, tPA, NOSIII and TGFβ [47].

1.7 Microgravity and shear stress regulated gene and protein expression

As described above, mechanical stress activates many signalling cascades which are responsible for changes in gene expression.

Up to date only the expressions of some of several endothelial genes have been investigated under microgravity. Experiments performed under simulated and real microgravity revealed reorganization of the endothelial cytoskeleton. The increase of

cytokeratin, accumulation of collagen type I and III as well as alterations of the cytoskeletal alpha- and beta-tubulins and F-actin were detected [48, 49].
Strongly upregulated was heat shock protein 70 [50, 51] and one of the cytokines: IL-6 [50], whereas IL-1a was downregulated [50-53]. Moreover, the expression of vasolidators NO synathase and prostacyclines were increased. Investigated was also the expression of molecules involved in angiogenesis. Lack of regulation in expression of metalloproteinases and their inhibitors as well as Il-8 and FGF suggests that microgravity induces an anti-angiogenic phenotype [54].

The only available gene array study comparing cells exposed to real microgravity condition, to simulated microgravity and hypergravity was performed by Hammond in 2000, who reported that during six day long experiments performed in space (Flight STS-90 neurolab) more than 1632 genes changed more than 2 fold, whereas in the Rotating Wall Vessel 914 were changed. Genes which altered their expression were responsible for adhesion, apoptosis and cytoskeleton. Among them one of the most strongly increased was the expression of E3 ligase- NEDD4 [55]. NEDD4 is involved in targeting many proteins for degradation what may indicate that the proteasome-ubiquitin system may play an important role in the degradation of proteins under microgravity conditions.

Number of reports revealed that shear stress strongly impacts regulation of endothelial genes. For example McCormick et al.[56] in her studies based on microarray showed that shear stress (25 dyn/ cm^2) applied for 6 h and 24 h caused changes in expression in 52 out of 4000 investigated genes. In the group of 32 upregulated genes were antioxidants cytochrome P450 and heme oxygenase-1, transcription factors like glucocorticoid-induced leucine zipper protein as well as heat shock protein 70. Strongly decreased were genes involved in vascular tone homeostasis- endothelin-1 and caveolin-1 as well as cytoskeletal alfa tubulin.
Earlier studies using more traditional approaches like PCR, northern and immunoblotting techniques also identified many shear stress modulated genes. For example eNOS was upregulated at 1 h by 3-9 dyn/ cm^2 shear stress [57]. Thrombomodulin was downregulated by moderate (15 dyn/ cm^2) and elevated (36 dyn/ cm^2) shear stress after 6 h and 9 h [58], Tissue factor- transiently upregulated under 12 dyn/ cm^2 [59] and ADAMTS1 was upregulated at 6 dyn/ cm^2 [60]. Several investigations also revealed that

the type of shear led to the different patterns in expression of genes such as Klf2, Cx43 or Ang2 [12].

1.8 NEDD4

The group of NEDD4 proteins consists of nine members closely related to each other: NEDD4-1, NEDD4-2, SMURF1, SMURF2, ITCH, WWP1, WWP2, NEDL1, NEDL2. This group belongs to a family of HECT ubiquitin protein ligases (E3). E3 ligases recognize specific substrates and mediate transfer of ubiquitin [61].

In general, ubiqitination is a multistep process which involves cascades of three enzymes. Ubiquitin activating enzyme (E1) activates ubiquitin in presence of ATP. The activated ubiquitin is than transferred to cystein at the active site of the ubiquitin conjugating enzyme (E2) by transesterification. (E3) ubiquitin protein ligase binds the first ubiquitin molecule to the protein substrate via an isopeptide bond between the target potein and ubiquitin. Continuous addition of ubiquitins thus forming a polyubiquitin chain labels a protein for degradation by proteasomes, whereas mono-ubiquitination of proteins leads to a change in their function or cellular localization [62].

The NEDD4 proteins consist of an N-terminal Calcium binding domain (C2), two to four protein-protein interaction domains (WW) and carboxyl-terminal HECT domain. C2 domain is probably involved in the translocation of proteins to phospholipids of the membrane in response to changes in the concentration of cytosolic Ca^{2+}. WW domains and C-terminal domains are responsible for protein-protein interactions with PY motifs of target proteins. Different WW domains of the same protein may interact with a variety of different proteins. HECT domain transfers ubiquitin to target proteins [63, 64].

The NEDD4 members were found to regulate cell signaling, viral budding and protein trafficking. One of the most interesting members of this family is neural precursor cell expressed, developmentally down-regulated 4-2 (NEDD4-2). This gene was initially identified as a highly expressed transcript in the mouse embryonic brain. Further investigations showed the highest NEDD4-2 expression during neurogenesis.

One of the latest reports showed that NEDD4 knock-out mice suffer from heart defects and vasculature abnormalities [65]. It has also been reported that high expression of

NEDD4 corresponds with increased proteolysis of its targets by the ubiquitin-proteasome system in smooth muscle cells [63, 66].

NEDD4-2 interacts with several different targets. One of the first and best recognized NEDD4-2 targets is an epithelial sodium channel (ENaC) [67, 68]. Several investigations using *in vitro* overexpression systems and biochemical analyses proved that NEDD4-2 is responsible for ENaC endocytosis and degradation [69]. Additionally, *in vivo* experiments revealed that mice with mutations in the b-ENaC–PY motif developed hypertension. NEDD4 also mediates degradation of VEGFR2 and adaptor protein Grb10 inhibits this process by binding to NEDD4 [70]. Other NEDD4 targets are Notch 1 [66], bcl-10 and Eps 15. Moreover, NEDD4 has also been shown to bind to actin and interrupt the cytoskeleton [71].

NEDD4 is also involved in the turnover of gap junction protein Connexin 43 [72]. Gap junctions coordinate cell-to-cell communication and allow exchange of ions and small molecules between neighbouring cells. Besides forming gap junctions, Cx43 is present in cell membranes forming a kind of a pore, and is thus involved in connecting cytosol with extracellular space [73]. Cx43 also interacts with several proteins associated with cytoskeleton such as: N-cadherin [74, 75], b-catenin [76], vinculin [77], ZO-1 [78], but the best recognized is the interaction with tubulin via C-terminal tail [79]. It has been shown that Cx43 binds alpha and beta tubulins equally [80]. In Cx43 knock out animals [81] as well as in Cx43 siRNA cultured endothelial cells, Cx43-tubulins affected interactions led to the disruption of cell polarity which in turn impaired angiogenesis [82].

1.9 ADAMTS1

ADAMTS (a disintegrin and metallopeptidase with thrombospondin type 1 motif) proteins are a family of extracellular proteases which were found to be expressed in mammals and invertebrates [83]. ADMTS1 protein consists of the propeptide, metalloproteinase, disintegrin, and cysteine-rich domain and three domains containing thrombospondin 1 (TSP1) motifs, with a spacer after first TSP1 motif. ADAMTS1, like other members of this protein family, is synthesized as an inactive 110 kDA form. Maturation process requires two independent events. First, carried by furin, a 87 kDA active form is released which is able to anchor to the extracellular matrix. Second processing by matrix metalloproteinases (MMPs) results in a 65 kDa form which is not

able to anchor to the extracellular matrix due to the loss of two C-terminal TSP motifs and the spacer region [84].

ADAMTS1 is necessary to maintain normal growth and fertility as well as organ morphology and function. It has been shown by Mittaz et al. that knockout mice suffer from severe kidney dysfunction [85]. Studies performed by Shindo et al. revealed dysfunctions in female reproductive tract and uterine function resulting in poor fertility [86].

ADAMTS1 has been suggested to play an important role in atherosclerosis by its ability to cleave extracellular matrix proteins like versican as well as by promoting vascular smooth muscle cell migration. Immunohistological analysis performed on human aortic fatty streak lesion from the coronary artery by Jonsson-Rylander et al. showed high expression of ADAMTS1 in foam like cells and in vascular smooth muscle cells [87].

ADAMTS1 functions also as an angiogenesis inhibitor. It has been shown in cornea pocket assay that ADAMTS1 suppresses fibroblast growth factor 2- and VEGF-induced angiogenesis [88]. Overexpression of ADAMTS1 in tumor cells was linked with suppression of tumor angiogenesis and tumor growth, what required “intact catalytical activity of ADAMTS1”. It has been suggested that effects of ADAMTS1 on angiogenesis may differ not only in developmental stages or among tissues but also under pathophysiological conditions [89].

It has been shown that siRNA knockdown of ADAMTS1 increased endothelial cell proliferation [90]. Furthermore, ADAMTS1 releases anti-angiogenic peptides from TSP1 and TSP2 that cleaves thrombospondins [91].

In ADAMTS1- deficient mice with skin wounds was observed a significant increase in vessel density and delayed wound closure [91]. In diabetic mice with higher expression of ADAMTS1 angiogenesis was reduced in wound healing processes [92]. Lee et al. suggests that for the anti-angiogenic properties of ADAMTS1 the cleavage of thrombospondins is responsible. This process releases anti-angiogenic peptides [91].

As it has been reported by Hudlicka et al. angiogenesis is correlated with changes in hemodynamic forces acting on vascular wall [15, 93]. In sprouting type of angiogenesis, where blood flow in capillary sprouts is not present and vessels first need to be connected to be perfused, this lack of flow might be a signal to sustain sprouting and “conversely, the onset of blood flow in sprouts making contact to another vessel could be used to stop sprouting and to start maturation of the newly grown blood vessel” [94].

To evidence this it would be mandatory to show regulation of suitable endothelial genes by shear stress.

In earlier studies ADAMTS1 was found to be strongly regulated by shear stress in endothelial cells.[60]. Moreover, transcription factors NF-1 and SP1 which bind to the ADAMTS1 promoter [95] are shear sress dependent [96]. This may suggest that ADAMTS1 regulation by shear tress is mediated in part by these transcription factors.

2 Aims

The reduction of capillary density in microgravity- induced muscle atrophy has been observed by several studies. Molecular mechanisms leading to this change remain to be elucidated. Therefore, this study was designed at testing endothelial reactions on microgravity which are probably connected to the regulation of blood vessel growth.
According to the literature, one of the most sensitive genes responding to microgravity is NEDD4 [55]. Therefore, the aim of this work was to validate the expression of NEDD4 in endothelial cells, to investigate the impact of microgravity on it, to verify NEDD4 intractions with Cx43 as well as to identify new NEDD4-regulated and angiogenesis-related genes/proteins.

In addition, previous studies performed in our Institute revealed that ADAMTS1, which plays a pivotal role in the regulation of angiogenesis, is strongly induced by mechanical forces acting on endothelial cells, namely by shear stress. Here, it was also investigated if there is any influence of microgravity (i.e. a reduction in mechanical loading) on ADAMTS1 expression.

To better compare the experiments, both, NEDD4 and ADAMTS1, were likewise tested under conditions of increased shear stress and of microgravity. By the same time, this did allow for a better control of a side effect of the Rotating Wall Vessel, i.e. a small increase in shear stress.

Furthermore, to more closely resemble human *in vivo* conditions, a new cone and plate apparatus was built and evaluated, and shear stress experiments were extended to real flow profiles.

The results of these studies are expected to provide a better understanding of mechanisms which can contribute not only to the development of different pathological situation observed in astronauts, but also for patients during long bed rest.

3 Material and Methods

3.1 Material

3.1.1 Chemical compounds

Standard chemicals were obtained from Sigma-Aldrich (Steinheim, Germany), Carl Roth (Karslruhe, Germany), Merck (Darmstadt, Germany), Biomol and Calbiochem (Darmstadt, Germany).

Cell culture media, supplements and antibiotics were ordered at PromoCell (Heidelberg, Germany) and Biochrom (Berlin, Germany).

3.1.2 PCR

PCR reagents were obtained from Promega (WI, USA). All primers were produced by MWG Biotech GmbH (Ebersberg, Germany). The sequences of primers are listed in tables below (Table 1, Table 2 and Table 3).

Table 1Primers for semi-quantitative RT-PCR

Gene	Gene bank Accesion number	Forward primer (5'-3')	Reverse primer (5'-3')	Product size (bp)
PDH	NM_001173454.1	GGTATGGATGAGGACCTGGA	CTTCCACAGCCCTCGACTAA	103
ADAMTS1	NG_008308	AGAATGGAGGGAAGTACTGTG AAGG	GGGCTACATGGAGTACCATCTA CAA	280
NEDD4	NM_006154	TTGCAGCAACAACAAGAACC	GGCCTGGTTGCTATACATGG	294

Table 2 Primers for real time RT-PCR (long products)

Gene	Gene bank Accesion number	Forward primer (5'-3')	Reverse primer (5'-3')	Product size (bp)
GAPDH	NM_002046	CCTGACCTGCCGTCTAGAAA (nucleotide position 834)	TACTCCTTGGAGGCCATGTG (nucleotide position 1109)	276
Cx43	NG_008308	AAGGGAAAGAGCGACCCTTA (nucleotide position 16970)	GCTGGTCCACAATGGCTAGT (nucleotide position 17333)	364
NEDD4	NM_006154	TTGCAGCAACAACAAGAACC (nucleotide position 632)	GGCCTGGTTGCTATACATGG (nucleotide position 925)	294
ADAMTS1	NM_006988	GGGAATGTGACAACCCAGT (nucleotide position 2206)	TTTTAGGTCGAAGGGCATT (nucleotide position 2961)	756
TSP1	NM_003246	CCTCATGAACGGGACAACT (nucleotide position 2597)	TCATCGATGTCTGGCACACT (nucleotide position 3010)	414
Klf2	NM_016270.2	CACCAAGAGTTCGCATCTGA (nucleotide position 933)	GGAGGATCGTGGTCTTTTCC (nucleotide position 1368)	436
Nrf2	NM_006164.3	TCATGATGGACTTGGAGCTG (nucleotide position 554)	TCCACTGGTTTCTGACTGGA (nucleotide position 844)	291
PGI_2s	NM_000961.3	GGCAGGTATGTCACCGTTCT (nucleotide position 265)	CTTCTGTAGCATCGCCCAAC (nucleotide position 517)	253

Table 3 Primers for real time RT-PCR (short products)

Gene	Gene bank Accesion number	Forward primer (5'-3')	Reverse primer (5'-3')	Product size (bp)
GAPDH	NM_002046	TCAAGAAGGTGGTGAAGCAG (nucleotide position 875)	CCCTGTTGCTGTAGCCAAAT (nucleotide position 1072)	198
Cx43	NG_008308	CTCGCCTATGTCTCCTCCTG (nucleotide position 7083)	TCTGGTTATCATCGGGGAAA (nucleotide position 17276)	194
NEDD4	NM_006154	GTGGGAAGAGAGGCAGGATA (nucleotide position 670)	CGTTGTGCTTGCAGTTGAAT (nucleotide position 807)	138
ADAMTS1	NM_006988	AGAATGGAGGGAAGTACTGTGAA GG (nucleotide position 2230)	GGGCTACATGGAGTACCATCTAC AA (nucleotide position 2509)	280
TSP1	NM_003246	AGATGGCCACCAGAACAATC nucleotide position 2771)	GTCATCATCGTGGTCACAGG nucleotide position 2876)	106
Klf2	NM_016270.2	AAGCCCTACCACTGCAACTG (nucleotide position 982)	GGCTACATGTGCCGTTTCAT- (nucleotide position 1154)	207
Nrf2	NM_006164.3	CAGCAGGACATGGATTTGATT (nucleotide position 595)	TTGCTCCTTTTGGAGTTGTTC- (nucleotide position 753)	158
PGI_2s	NM_000961.3	TGGACCCACACTCCTACGAC (nucleotide position 287)	GCTTCTGTGAGTGCCTGGA (nucleotide position 470)	184
Ang2	NM_001147.2	TTGGAACACTCCCTCTCGA (nucleotide position 830)	GGATGATGTGCTTGTCTT (nucleotide position 962)	133

3.1.3 Antibodies

Primary and secondary antibodies as well as their dilutions used for immunoblotting and immunostaining are listed in a Table 4.

Table 4 Primary and secondary antibodies

Antibody	Dilution	Company
NEDD4	1:5000 WB 1:500, 1:250 IF	Millipore (Billerica, USA)
Cx43	1: 1000 WB 1:500, 1:250 IF	BD Biosciences (New Jersey, USA)
ADAMTS1(H-60) ADAMTS1	1:200 IF 1:2500 WB	Santa Cruiz Biotechnology (California, USA) Triple Point Biologics, JK technology (Forest Grove, USA)
TSP1(N-20) TSP1 (Ab-4, Clone A6.1)	1:50 IF 1:250 WB	Santa Cruiz Biotechnology Neomarkers (Freemont, CA, USA)
Peroxidase-Conjugated rabbit anti mouse	1:5000 WB	DAKO (Glostrup, Denmark)
Peroxidase-Conjugated goat anti rabbit	1:5000 WB	DAKO (Glostrup, Denmark)
Peroxidase-conjugated rabbit anti goat	1:5000 WB	DAKO (Glostrup, Denmark)
Alexa Fluor 555 donkey anti goat Alexa Fluor 555 goat anti mouse	1: 2000 IF 1:2000 IF	Invitrogen (Leek Netherlands)
Alexa 488	1: 2000 IF	Invitrogen (Leek Netherlands)

3.1.4 siRNA

siRNA against NEDD4 (5'-UAGAGCCUGGCUGGGUUGUUUUG-3') was produced by MWG Biotech GmbH (Ebersberg, Germany).

3.1.5 Commercially available kits

Real time PCR SYBR green kit, RNeasy mini kit, Quiagen gel extraction kit, Mini Elute Kit were purchased from Qiagen (Hilden, Germany).

3.2 Equipment

3.2.1 **Laboratory equipment**

Western blot systems:

- Protean II, Bio- Rad Laboratories (California, USA)
- Protean II xi Cell, Bio- Rad Laboratories (California, USA)

Semi dry blotting system- Trans blot SD, Bio- Rad Laboratories (California, USA)

Thermocyclers:

- Biometra UNO Thermoblock (Göttingen, Germany)
- Rotor Gene 2000 (LTF, Wasserburg, Germany)

Photometers:

- GeneQuant, Pharmacia Biotech (Cambridge, England)
- Eppendorf 254 (Hamburg, Germany)

Centrifuges:

- 5417R Eppendorf AG (Hamburg, Germany)
- Biofuge stratos, Thermo scientific, Hearus GmbH (Hanau, Germany)

Microscopes:

- Confocal laser scanning microscope: Leica TCS SP-2, Leica Microsystems (Heidelberg, Germany)
- Fluorescencent microscope AxioVert 200 equipped with AxioCam and AxioVision 4.0 software (Carl Zeiss Jena GmbH, Jena, Germany)

Shaker- duomax 1030, Heidoplh (Schwabach, Germany)

Rotator - RS 24 Rotation, Biosan (Riga, Latvia)

Power supplies:

- Biometra standard Power pack P25 (Göttingen, Germany)
- Biorad Power PAC 300 (California, USA)

Vortex- reax top, Heidoplh (Schwabach, Germany)

Heating block- Techne DRI-block DB-2A, Sigma-Aldrich (Steinheim, Germany),

Vacuum pomp- Biometra (Göttingen, Germany)

Incubator- Hearus cytoperm 2 (Hanau, Germany)

3.2.2 **Models to study the effects of mechanical forces on cells**

3.2.2.1 Cone and plate devices

Shear stress was applied using a cone and plate device. Two types of such instruments were designed and constructed in the Institute of Physiology in Berlin. The idea is based on the apparatus built by Bussolari and Dewey [97]. The general outline of the devices is shown in Figure 7, A-B.

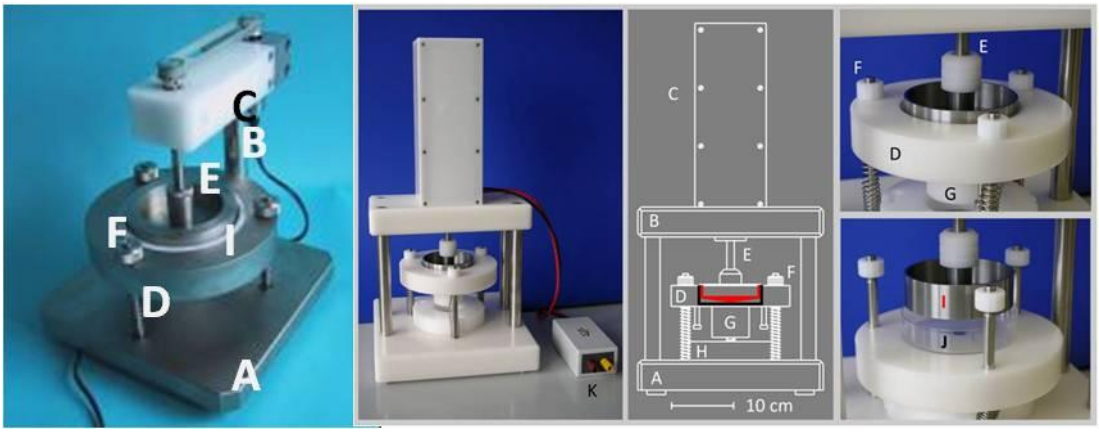

Figure 7 Cone and plate devices
These devices allow for application of different shear stresses on cells cultured in Petri dish. Both, consists of strong motor (DC) which drives cone (I, red in middle panel). The cone is inserted into culture dish (J, black in middle panel) by lifting the sliding table (D). Different flow patterns are loaded by computer into motor control box (K).

Both devices consist of a lower platform (A) which carries the shear cone arrangement (E-J) and the upper platform (B) which supports a DC motor. The rotation is transmitted by a shaft (E) to the cone (J, red in middle panel) which fits standard 100 mm culture dishes (J, black in middle panel). The culture dish is positioned with the sliding table (D) fixed with a rotating disc (H) in the lower, loading position (lower right panel). Control box (K) controls the voltage by which the motor is driven. In the first apparatus Control box (not shown) allows to manual switch/off as well as on control of rotation speed of the cone. In the second system Control box (K) is loaded with the desired velocity profile via a serial link from a computer.

When exposed to a laminar flow, uniform shear stress (τ) is provided over the entire cross-sectional area according to the formula:

$$\tau = (\omega/\alpha)\eta$$

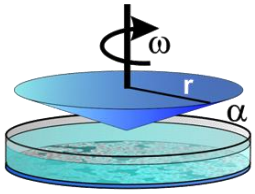

where:

- ω is the angular velocity,
- α the cone angel (1 °),
- η the viscosity of the flowing medium (0.75 cPoise at 37 °C) [98] .

This equation strictly applies only for laminar flow conditions which can be expected for the relatively low angle of the shear cone of 1° and rotational speeds up to ~ 150 rpm. This corresponds to shear stress values of up to approximately 6 dyn/ cm^2.
In order to achieve higher shear stress values the viscosity of the supernatant medium should be increased to 5 cPoise at 37°C by adding Dextran (83 mg per ml medium).

3.2.2.2 Rotating Wall Vessel bioreactor

There is no device which can exactly model space conditions, but recently the Rotating Wall Vessel has been developed to simulate some aspects of microgravity. "This device is based on the idea that sensing no weight would have similar effects as being weightless"[99].
Rotating Wall Vessel provides these condition by randomizing the gravity vector of the cells in a three dimensional space [100].
The Rotating Wall Vessel consists of culture dishes called vessels (Figure 8). Vessels are equipped with gas permeable membranes, two injection ports and drain/fill ports. Vessels are attached to the base. Speed of rotation and direction is controlled by a power supply. Vessels are rotated about their horizontal axis and the suspended cells are in a "freefall" within culture medium in order to provide exchange of nutrients, wastes and dissolved gases. This "freefall" state is achieved "by balancing sedimentation induced by gravity with centrifugation caused by the rotating vessel" [101].

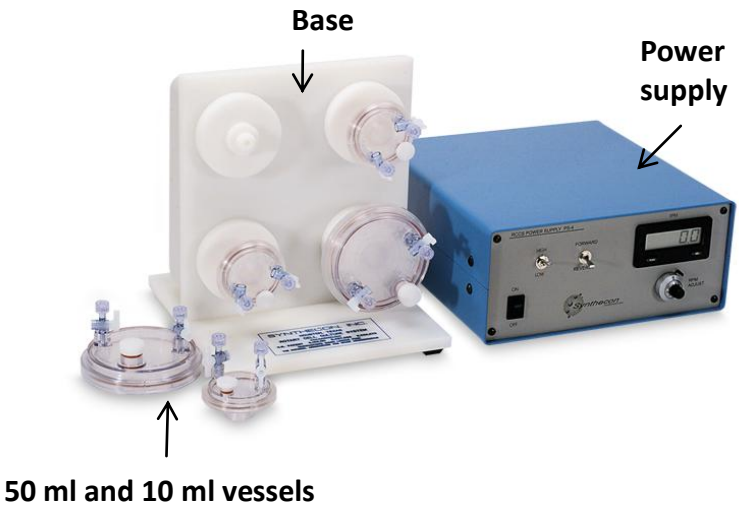

Figure 8 Rotating Wall Vessel (provided by Synthecon, Houston, Texas, USA)
Rotating Wall Vessel bioreactor consists of base and power supply. Culture dishes called vessels (50ml and 10ml volume) are mounted to the basis. The direction and rotation of speed are controlled by power supply.

In this system adherent cells are cultured on microcarrier beads which give structural support and promote 3D growth. Initial speed is adjusted to allow individual cells to pre-aggregate. The vessel has no mixing device, so cell aggregates are not destroyed. As the cell aggregates grow in size, the rotational speed is increased to compensate for increased sedimentation rates.

This unique cell culture conditions not only affect gene expression by randomizing gravity vector, but also promote cell-cell contacts and initiation of cellular signaling via specialized cell adhesion molecules.

In order to successfully produce microgravity like environment many conditions need to be optimized. Extremely important is the choice of microcarriers. Microcarriers should be spherical in shape and have a density as close as possible to the surrounding medium. To avoid particle-wall-, particle-particle collisions (which leads to lower cell adhesion to the microcarriers) and cell damage, optimal cell-microcarrier ratio and rotation speed is necessary. Adequate terminal velocity is also important for mass transport of nutrients to the cultured cells. If the velocity is minimized, nutrient delivery is reduced [102-105].

3.3 Methods

3.3.1 **Cell culture**

HUVEC

Human umbilical vein endothelial cells (HUVEC) were isolated from freshly obtained umbilical cords. First, the veins of umbilical cords were rinsed with PBS. Endothelial cells from the vein were isolated by a treatment with 0.2 % collagenase II (from Clostridium histolyticum) for 10-15 min at 37 °C. Next, cells from the veins of umibilcal cords were rinsed with Hanks´ Balanced Salt. Cell suspension was centrifuged at 1000 rpm for 5 min, the supernatant discarded and cells resuspended and cultivated to confluence in Endothelial Cell Basal Medium MV in a humidified atmosphere with 5 % CO_2 at 37 °C.

EAhy926

A permanent human cell line– EAhy926 is "a fusion of human umbilical vein endothelial cells with the permanent human cell line A549" [106]. These cells express factor VIII-related antigen.
EAhy926 cells were cultured in DMEM Medium with 10 % FCS and 1 % streptomycin\penicillin and 1 % L-glutamine in a humidified atmosphere with 5 % CO_2 at 37 °C.

Cell culture in the cone and plate apparatus

Endothelial cells (HUVEC or EAhy926) were cultured on Petri dishes. One day after cells reached confluence, Petri dishes were placed under the rotating cone of the apparatus and exposed either to constant laminar or pulsatile laminar flow.

In order to validate the cone and plate apparatus, three shear stress profiles:

- atherosclerosis susceptible (atheroprone)- shear stress oscillating between -8.4 and +3.6 dyn/ cm^2
- atherosclerosis resistant (atheroprotective) with shear stress ranging from 13.3 dyn/cm^2 to 40.7 dyn/ cm^2
- large arterial profiles as previously described by Dai et al [12]

and additionally constant flow of 5,4 dyn/ cm^2 were applied (Figure 9).

These profiles vary with respect to four main parameters with potential biological importance: mean shear stress (τ_{mean}), shear stress amplitude (τ_{ampl}), maximal rate of change in shear stress ($d\tau/dt_{max}$), directional changes of shear stress.

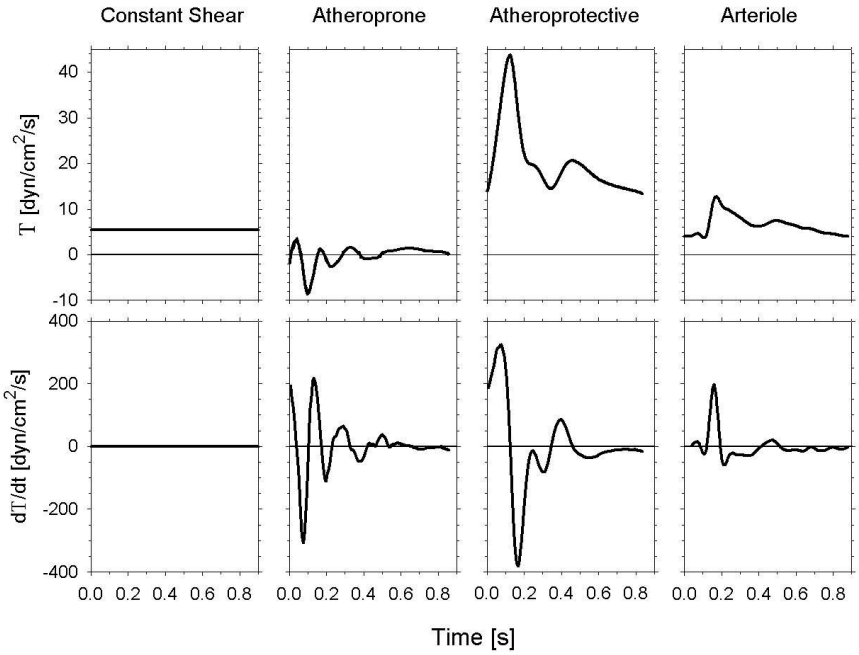

Figure 9 Flow patterns: constant, atheroprone, atheroprotective and arteriole used in experiments
For each flow pattern used in experiments shear stress (T, top panels) and the rate of change in shear stress (dT/dt, bottom panels) is shown over one heart cycle.

Cone and plate devices were kept in a humidified incubator with 5 % CO_2 at 37°C. In experiments with shear stress values higher than 6 dyn/cm^2, the viscosity of the medium in samples exposed to shear as well as in their controls was increased to 5 cPoise with dextrane.

To avoid a loss of cells after a switch from static to shear conditions, the rotational speed was continuously increased from zero to the average speed of the shear pattern applied. Control samples were cultivated under non-flow conditions for the same time.

All combinations of time and shear stress used in experiments are listed in a Table 5.

Table 5 List of experiments using cone and plate apparatus
Table specifies type of flow, time and force of endothelial cells exposure to shear stress in experiments perfrormed to study the regulation of NEDD4 and ADAMTS1.

Type of flow	NEDD4	ADAMTS1
Constant laminar	2 dyn/cm^2 - 24 h 6 dyn/cm^2 - 4 h, 15 h, 24 h 10 dyn/cm^2 - 24 h	1, 2, 3, 5.4 dyn/cm^2 – 24 h 6 dyn/cm^2 – 12 h, 24 h, 48 h 10 dyn/cm^2 - 24 h 20 dyn/cm^2 - 24 h
Pulsatile- atheroprone	24 h	24 h
Pulsatile- atheroprotective	24 h	24 h

Cell culture in the Rotating Wall Vessel

Microcarrier preparation

Cytodex 3 beads were swollen overnight in PBS, washed three times in fresh PBS and autoclaved. Beads suspension was stored at 4°C.

Cell culture

During the first 12 h endothelial cells (HUVEC or EAhy926) were occasionally rotated in both directions, followed by 12 h of slow rotation (7,5 rpm) in order to attach them to the Cytodex3 beads.

Next, speed was increased to 21 rpm. At this speed cells maintained in the upper part of the vessel, slowly falling down, without reaching walls and bottom of the culture dish. Cell were cultured in a humidified incubator at 37 °C with 5 % CO_2 for 24 h and 48 h. Control cells were seeded on the beads and kept in the flask without rotation in the same incubator.

3.3.2 Transfection of EAhy926 cells with siRNA against NEDD4

Transfection was performed according to the Dharma FECT1 transfection protocol with minor modifications. 10 µl siRNA against NEDD4 (5'-UAGAGCCUGGCUGGGUUGUUUUG-3') 100 mmol×L^{-1} stock solution or 20 µl negative control siRNA (50 µmol×L^{-1} stock solution) were incubated in 490 µl or 480 µl cell culture medium without serum and antibiotics at room temperature for 5 min. At the same time 15 µl of transfection reagent Dharma FECT1 were incubated in 485 µl cell

culture medium without serum and antibiotics at room temperature for 5 min. Next, siRNA and the transfection reagent were incubated together at room temperature for another 20 min. 4 ml complete cell culture medium was added to achieve 5 ml of transfection medium. Subconfluent EAhy926 cells were incubated in 5 ml of transfection medium in Petri dishes for 144 h in humidified atmosphere with 5% CO_2 at 37°C.

3.3.3 Treating cells with inhibitors

Proteasome inhibition

Protein degradation by proteasome was inhibited by using two inhibitors: ALLN and MG132. ALLN was prepared as 100 mmol×L^{-1} stock solution in DMSO and diluted to final concentration 40 µmol×L^{-1}. MG132 was prepared as 10 mmol×L^{-1} stock solution in DMSO and diluted to final concentrations of 20 µmol×L^{-1} and of 40 µmol×L^{-1} . EAhy926 cells were cultured in T25 flasks under static conditions or under microgravity in the Rotating Wall Vessel. One day after they reached confluency inhibitors at final concentrations were added for 3 h, 6 h and 9 h. Non-treated controls were incubated with the same volume of DMSO only. After incubation time, proteins were extracted according to the standard procedure described below.

Lysosome inhibition

Protein degradation via lysosome was inhibited by chloroquine at a final concentration of 100 µmol×L^{-1}. First, stock solution (100 mmol×L^{-1}) was prepared by dissolving chloroquine in aqua bidest and then diluted to final concentration. EAhy926 cells were cultured in T25 flasks under static conditions or under microgravity in the Rotating Wall Vessel. One day after they reached confluency, 100 µmol×L^{-1} chloroquine was added for 2 h and 4 h. Non-treated controls were incubated with the same volume of water. After incubation time, proteins were extracted according to the standard procedure described below.

PI3 K inhibition

Phosphoinositid 3-kinase (PI3K) was inhibited by using LY294002. First, stock solution (10 mmol×L^{-1}) was prepared in DMSO and then diluted to a final concentration of

10 μmol×L^{-1}. This represents about four times the half-effective concentration of this inhibitor.

Non-treated controls were incubated with the same volume of DMSO only. Cells were pre-incubated for 30 min and then exposed to shear stress or kept as static control for 4 h and 24 h in the presence of the inhibitor. After incubation time RNA was extracted according to the standard procedure described below.

eNOS inhibition

Endothelial nitric oxide synthase (eNOS) was inhibited using NG nitro L-arginine methyl ester (L-NAME). The inactive isomer D-NAME, served as a control. A stock solution (500 mmol×L^{-1}) was prepared in PBS. Cells were incubated at final concentrations of 500 μmol×L^{-1} . Next, cells were exposed to shear stress (6 dyn/ cm^2) or kept as static control for 24 h. After incubation time RNA was extracted according to the standard procedure described below.

3.3.4 Testing of cells with different oxygen pressure

Endothelial cells were exposed to different amounts of oxygen pressure using incubator regulated to varying oxygen fractions: 3 % (21 mmHg), 5.6 % (40 mmHg), 14 % (100 mmHg) and 21 % (150 mmHg) calculated for humidified atmosphere at 37 °C and 30 m above sea level. Next, RNA was extracted according to the standard procedure described below.

3.3.5 Gene expression analysis

RNA isolation

Cells were harvested with 0.05 % Trypsin/ 0.02 % EDTA, centrifuged and frozen in liquid nitrogen. RNA was isolated using RNeasy mini kit according to the manufacturer instructions. The amount of isolated RNA was estimated with a photometer.

Reverse transcription

2 μg of total RNA and 1 μg of oligo(dT) primers were incubated for 8 min at 70°C and chilled on ice. cDNA was produced using M-MLV reverse transcriptase and 10 mmol×L^{-1}

dNTP in 25 µl of total volume for 1 h at 42 °C. The enzyme was inactivated at 70 °C for 10 min.

Semi quantitative PCR

1 µl of reverse transcription reaction mix was used for PCR. PCR mix contained 10 mmol×L^{-1} Tris–HCl 1 % (v/v) Triton X-100, 1.5 mmol×L^{-1} MgCl2, 50 mmol×L^{-1} KCl, 200 µmol×L^{-1} dNTP and 1.0 U Taq DNA polymerase. Primers (Table 6) added at final concentrations of 0.5 µmol×L^{-1} for NEDD4, 0.3 µmol×L^{-1} for ADAMTS1, 0.2 µmol×L^{-1} for PDH. PCR conditions for each primer pair (Table 6) were optimized separately to remain in the exponential phase of amplification. PDH was amplified using the same samples and PCR mix in separate reaction tubes to normalize the results. Non-template and no-RT controls were run for all reactions. PCR products were separated on agarose gels and detected by staining with ethidium bromide.

Table 6 PCR protocol

Gene	Initial denaturation	Denaturation	Annealing	Extension	Final extension	Number of amplification cycles
ADAMTS1	94°C for 60s	94°C for 30s	60°C for 30s	72°C for 75s	72°C for 300s	29
PDH	94°C for 60s	94°C for 30s	60°C for 30s	72°C for 75s	72°C for 300s	29
NEDD4	94°C for 60s	94°C for 30s	56°C for 30s	72°C for 60s	72°C for 300s	35

Real time PCR

External standards for RT-PCR were produced using PCR conditions described above and primer pairs listed in a Table 2. PCR was run for 40 cycles. Reaction products were analysed on agarose gel and than isolated either from agarose gel using Qiaquick Gel extraction kit or from PCR reaction tube using Mini elute kit and diluted to 10^8–10^2 copies/µl.

Amplification reactions (20 µL final volume) contained 10^8–10^2 copies/µl of standard dilutions as a template, primers pairs (at final concentration of 0.3 µmol×L^{-1}) with sequences listed in a Table 3, 10 µl Master mix SYBR-Green and 5 µl od RNase free

water. PCR was run for 45 cycles using a Rotor Gene 2000 cycler. Conditions of real time PCR are presented in a Table 7.

Samples from all experiments were run as 1 µl cDNA as described above. Amplification products were controlled by melting curves. No-RT- and non-template controls were run for all reactions. The values of NEDD4, Cx43 and ADAMTS1,TSP1, klf2, nrf2 and PGI_2s were normalized to the corresponding GAPDH values.

Table 7 Real time RT-PCR protocol

Gene	Initial denaturation	Denaturation	Annealing	Extension
GAPDH	94°C for 900s 94°C for 900s	94°C for 30s 94°C for 30s	60°C for 30s 56°C for 30s	72°C for 75s 72°C for 60s
ADAMTS1	94°C for 900s	94°C for 30s	60°C for 30s	72°C for 75s
NEDD4	94°C for 900s	94°C for 30s	56°C for 30s	72°C for 60s
TSP1	94°C for 900s	94°C for 30s	56°C for 30s	72°C for 60s
Cx43	94°C for 900s	94°C for 30s	56°C for 30s	72°C for 60s
Klf2	94°C for 900s	94°C for 30s	56°C for 30s	72°C for 60s
Nrf2	94°C for 900s	94°C for 30s	56°C for 30s	72°C for 60s
PGI_2s	94°C for 900s	94°C for 30s	56°C for 30s	72°C for 60s

3.3.6 Protein analysis

Protein extraction

HUVEC or EAhy926 cells were cooled on ice, washed three times with ice cold PBS and suspended with cell scraper in 350 µl extraction buffer containing 1% Triton X-100, 20 mmol×L^{-1} sodium phosphate buffer (pH 7.8), 150 mmol×L^{-1} NaCl, 2.5 mmol×L^{-1}

EDTA, 1 mmol×L^{-1} Na_2VO_4, 50 mmol×L^{-1} NaF, and protease inhibitors (1 mmol×L^{-1} PMSF, 0.02 µg/µl aprotinin, 0.02 µg/µl leupeptin, and 0.02 µg/µl pepstatin A, and homogenized using needle and syringe. After 15 min incubation on ice, extracts were centrifuged at 19800 rpm for 15 min. Supernatant was transferred to a new tube. Protein concentration was determined using Bradford-kit.

Immunoblotting

40 µg or 50 µg of protein extracts were mixed with Laemmli sample buffer (50 mmol/l sodium phosphate, 100 mmol/l DTT, 2% SDS, 10% glycerol, and 0.1% bromophenol-Blue) [107] and heated for 3 min at 95 °C. After electrophoretic separation on 10 % gels, proteins were transferred to the nitrocellulose membrane. Membrane was blocked with 5 % dry milk powder in PBST (0.1% v/v Tween 20 in PBS) buffer overnight at 4 °C. Membranes were cut according to the molecular weight. Part containing proteins with molecular weight above 75 kDa was incubated for 3 h with anti-NEDD4 antibody. Specifity of the 104 kD band detected by the NEDD4 antibody was confirmed by mass-spectrometry. Part containing proteins with lower molecular weight was incubated for 3 h with anti-Cx43 antibody at room temperature. Blot membranes for ADAMTS1 and TSP1 analysis were incubated with anti-ADAMTS1 antibody or anti-TSP1 antibody for 2 h at room temperature.

After incubation time membranes were washed three times in PBST buffer 5 min each, secondary antibody were applied for 45 min. Unbound antibodies were removed by five incubations with washing buffer (PBST) 5 min each. Equal protein loading was confirmed by Ponceau staining. Blots were developed by chemiluminescence using ECL immunoblotting analysis system for varying times. Films were scanned and densitometric quantification was performed using Quantity 1D analysis Programme.

Co-Immunoprecipitation

1,5 mg protein extract was incubated for 2 h with antibodies at 4 °C, then 35 µl protein sepharose A was added into each tube. Extracts were rotated at 4 °C. After 2,5 h tubes were shortly centrifuged, supernatant was collected and 4x washed in protein extraction buffer followed by short centrifugation after each washing. Precipitations of complexes were performed by using 20 µl of 2x Laemmli buffer. Precipitates were electrophoretically

separated either on gradient gels or 8 % acrylamide gels, than stained with silver or immunoblotted.

Silver staining

Gels were fixed overnight in fixing solution (40 % (v/v) methanol and 10 % (v/v) acetic acid in aqua bidest). Next, washed in wash solution (30 % (v/v) ethanol in aqua bidest) twice 20 min each, followed by three times washing in water (30 min each). Gels were incubated for 1 min in sensitizer solution (0,02 % (w/v) natrium triosulfat) and washed three times in water exactly for 20 sec. Incubation with 0,15 % (w/v) silver nitrate was performed at 4 °C for 20 min. Next gels were washed three times in water 20 sec, each washing. Gels were developed in developing solution (2 % (w/v) Natriumcarbonat, 0,0005 % natriumthiosulfat, 0,04 % (v/v) formaldehyde) for 3-5 min, followed by washing two times in water (30 sec each washing). Reaction was stopped by using stop solution (0,5 % (w/v) glycin in aqua bidest).

Immunocytochemistry

Endothelial cells were grown on cover slips (12 mm diameter) until they reached confluence. Then, cells were washed three times in PBS, fixed in ice-cold methanol for 20 min, washed three times in PBS. Cells were incubated with primary antibody (NEDD4 1:250 and 1:500 and Cx43 1:250 and 1:500) at room temperature, washed in PBS and incubated with secondary antibody Alexa 488 (1:2000) or Alexa 555 (1:2000).
For co-immunostaining, a first antibody against NEDD4 was applied, followed by washing and incubation with secondary antibody-Alexa. Next second primary antibody against Cx43 was applied. After 1 h incubation cells were washed and secondary antibody was added. For negative control- cells were incubated with secondary antibody only.

3.3.7 Scratch wound assay

Human Umbilical Vein Endothelial Cells were grown to 100% confluence in Petri dishes. Then, the monolayer was scratched using a pipette [108]. During cultivation cells were allowed to migrate and proliferate. The medium used in these experiments was either freshly prepared or conditioned for 24 h with HUVEC cultured under static or exposed to

(6 dyn/ cm^2) laminar flow. Medium from cells exposed to shear stress was transfected with the siRNA 24 h earlier before shear stress exposure or used without transfection. The initial scratch was documented as a photograph using a Nikon Diaphot inversion microscope equipped with Hoffman´s modulation contrast and a corresponding objective (plan 4/0.13 DL, 160/-, Phl, Nikon). Pictures were taken with a Canon camera. Cell migration was measured by comparing an initial photo with photos following 4 h and 24 h incubation time. Scratch width was measured offline using ImageJ 1.34s program for histometry.

3.3.8 **Proliferation assay**

To analyze proliferation and viability of endothelial cells cultured in the Rotating Wall Vessel for 24 h Trypan blue staining was performed. Cytodex 3 beads were allowed to settle and culture medium was removed. Beads were washed three times in 15 ml PBS, 5 min each. Next, beads were incubated with Trypsin/EDTA at 37 °C with slow rotation.
After 5 min the action of trypsin was stopped by addition of cell culture medium containing serum. The detached cells were separated from Cytodex 3 by filtering through a 100 µm filter. Cell proliferation was evaluated by staining cells with Trypan blue and counting viable cells in Neubauer chamber [50].

3.4 Statistical analysis

In experiments using Human Umbilical Vein Endothelial Cells “n” refers to the number of umbilical cords from which HUVEC were isolated. In experiments using EAhy926 cell line “n” refers to the number of experiments. Data are given as mean ± SD from at least three independent experiments. Statistical analysis was performed using Sigma Plot software (Systat Software Inc., San Jose, CA, USA). Statistical analysis was done using students one-tailed- or two-tailed t-test, for either paired or unpaired samples, as appropriate. Statistical significance was set at a value of $*p \leq 0.05$.

4 Results

4.1 Optimization and evaluation of models used to study endothelial gene expression under mechanical stress

4.1.1 Evaluation of cone and plate apparatus

To test the ability of the cone and plate appatatus to produce different flow patterns which affect the expression of Klf2-, nrf2- and PGI_2-mRNA, endothelial cells were exposed to atheroprone, atheroprotective and arteriolar profiles as well as to constant laminar flow (5,4 dyn/cm^2) for 24 h (as described in Materials and Methods).

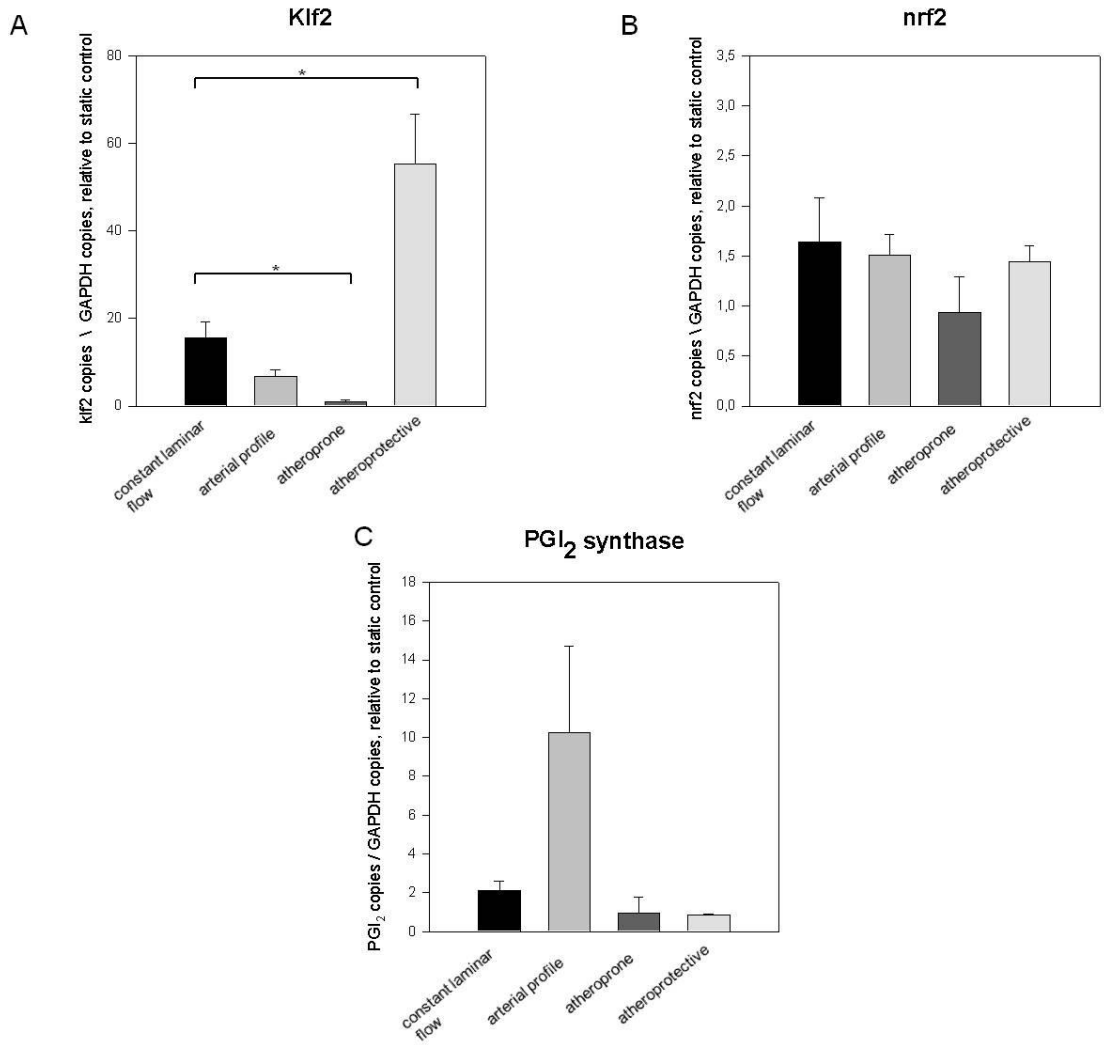

Figure 10 Effect of different shear stress profiles on expression of A) Klf2, B) nrf2 and C) PGI_2 synthase genes
Endothelial cells were exposed to laminar flow, arteriolar profile as well as atheroprone and atheroprotective for 24 h. Control cells were kept in a Petri dish. Expression of Klf2 mRNA, nrf2 mRNA, and PGI2s mRNA were analysed by real time RT-PCR. Results are given as mean ± SD, n=4, *$p \leq 0.05$, vs. constant laminar flow. Results are expressed as fold of the corresponding static control cultures.

RNA was extracted and real time RT-PCR was performed. Results of these experiments revealed the greatest regulation of Klf2 by atheroprotective profile when compared to constant and arteriolar shear stress profile. Nrf2 mRNA was not regulated by any shear stress profile. PGI_2 synthase was induced only by arteriolar profile (Figure 10).

4.1.2 Optimization of the cell culture in the Rotating Wall Vessel

Rotating Wall Vessel was validated by investigating endothelial cells morphology (Figure 11), proliferation and viability as well as expression of genes. Microscopic observation did not show any capillary-like structure formation.

In order to investigate proliferation rate, endothelial cells were cultured in the Rotating Wall Vessel for 24 h and stained with Trypan blue.

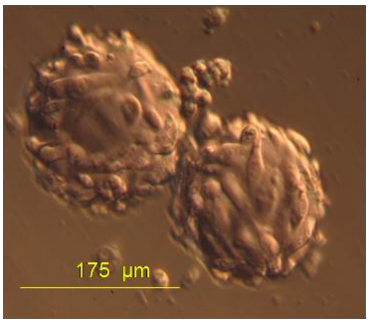

Figure 11 Cytodex 3 beads covered with endothelial cells after 24 h of exposure to simulated microgravity in the Rotating Wall Vessel

Figure 12 illustrates that endothelial cells exposed to microgravity grew more than 60 % faster in comparison to control cells.

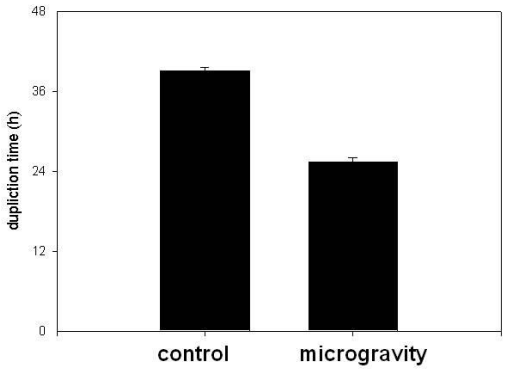

Figure 12 Duplication time of endothelial cells cultured as a static control and in microgravity
Endothelial cells were attached to the beads and then exposed to microgravity for 24 h. Control cells (1×g).) were kept without rotation. Cells stained with Trypan blue were counted using Neubauer chamber. Results are given as mean ± SE, n=3.

Regulation of EGF and IL-6 expression after 24 h and 48 h of exposure to microgravity was also tested. Results of real time RT-PCR demonstrate that EGF as well as IL-6 expression increased after exposure to microgravity when compared to 1×g control (Figure 13, A-B).

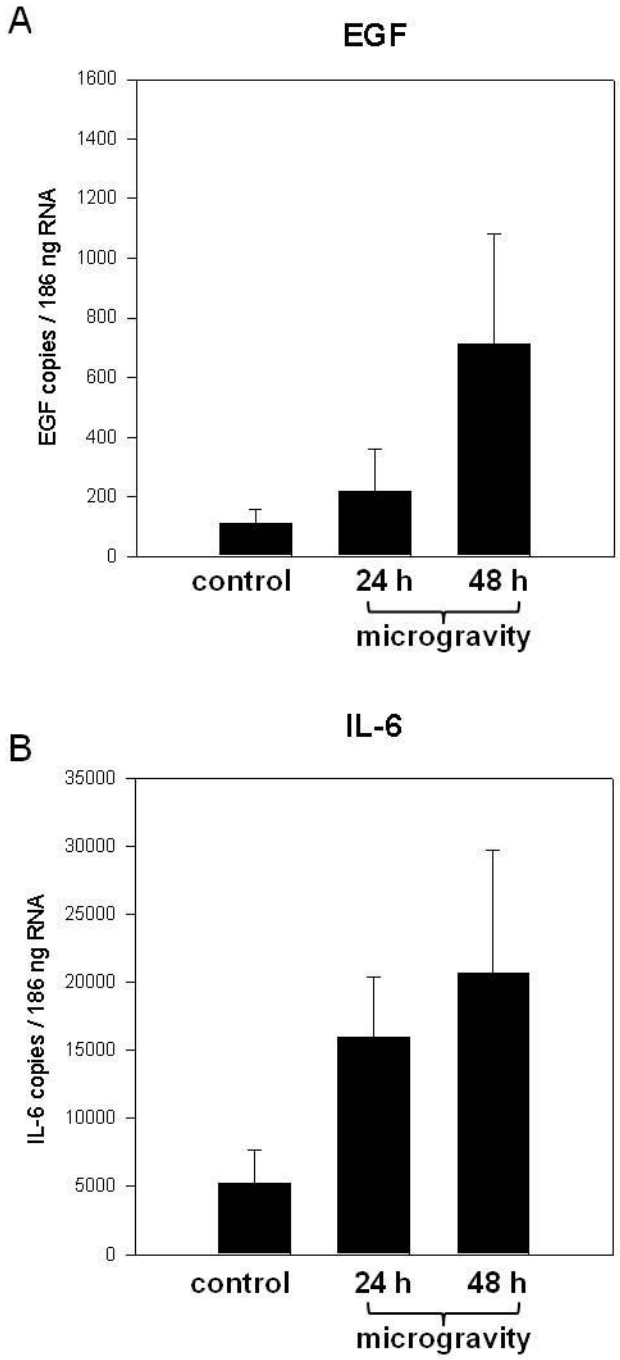

Figure 13 Effects of microgravity on A) EGF and B) Il-6 expression.
Endothelial cells were attached to the beads and then exposed to microgravity for 24 h and 48 h or kept as a control (1×g). Expression of EGF mRNA, IL-6 mRNA was analysed by real time RT-PCR. Results are given as mean ± SD, n=3.

4.2 Expression of NEDD4 in endothelial cells

To verify NEDD4 expression in HUVEC and EAhy926 cells, PCR and immunoblotting analysis were performed. Figure 14, A represents the result of semi quantitative PCR. PCR samples run on 1,5 % agarose gel revealed a band of 294 bp which corresponds with NEDD4 in both cell types. The results of immunoblotting performed with anti-NEDD4 antibody for HUVEC and EAhy926 cells showed a band at 104 kDA (Figure 14, B).

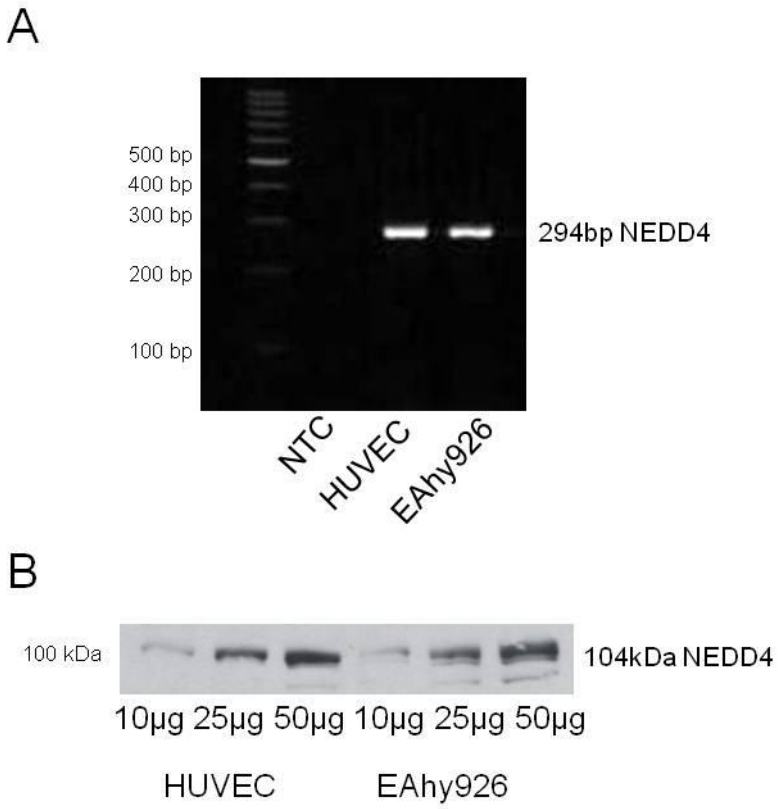

Figure 14 NEDD4 is expressed in HUVEC and EAhy926 cells

A) The results of semiquantitative PCR. Non template control- NTC (line 1), a band of 294 bp corresponds with NEDD4 in HUVEC (line 2) and EAhy 926 cell (line 3).

B) The results of immunoblotting analysis performed in HUVEC and EA926 cells using anti-NEDD4 antibody with 10, 25 and 50 microgram of total protein loading.

4.3 Interactions of NEDD4 with Cx43 in endothelial cells

To verify whether NEDD4 binds to Cx43, co-immunostainig, siRNA and immunoprecipitation experiments were performed.

Immunostaining

Cells were seeded on coverslips. One day after they reached confluency, immunostaining was performed. Images were taken using a scanning confocal microscope. Endothelial cells expressed Cx43 (red) with a typical punctate staining pattern (Figure 15, A). NEDD4 (green) staining was mainly observed in the cytoplasm (Figure 15, B), with a smaller contribution of NEDD4 being located at the cell border. The merged images showed co-localization of NEDD4 and Cx43 (yellow) at the plasma membrane at an extent of approx. 10 % of NEDD4 (Figure 15, C).

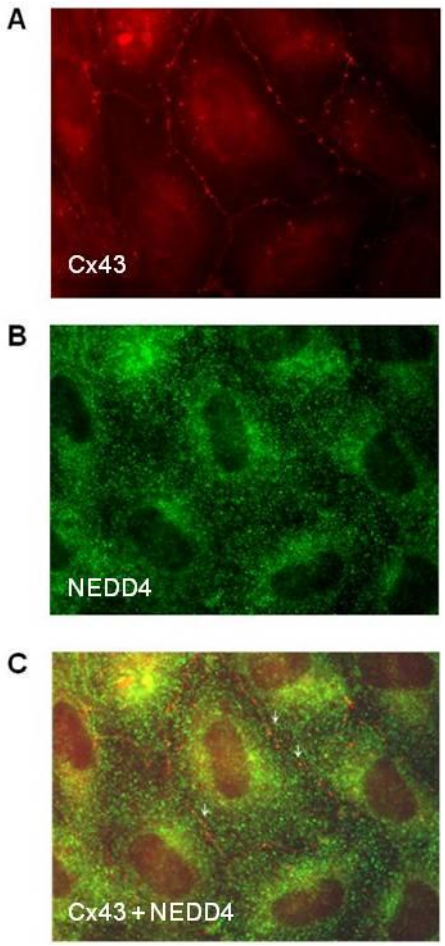

Figure 15 Localisation of NEDD4 and Cx43
EAhy 926 cells were double labeled for NEDD4 (green, B, C) and Cx 43 (red, A, C).
Cx43 and NEDD4 are co localized at the plasma membrane-associated structures (C).

Immunoprecipitation

To reveal any interaction between NEDD4 and Cx43 co- immunoprecipitation was preformed. The whole cell lysates were precipitated using the anti-NEDD4 antibody. The complexes of NEDD4 were analysed by immunoblotting with anti-Cx43 antibody. Figure 16 represents NEDD4 and associated Cx43.

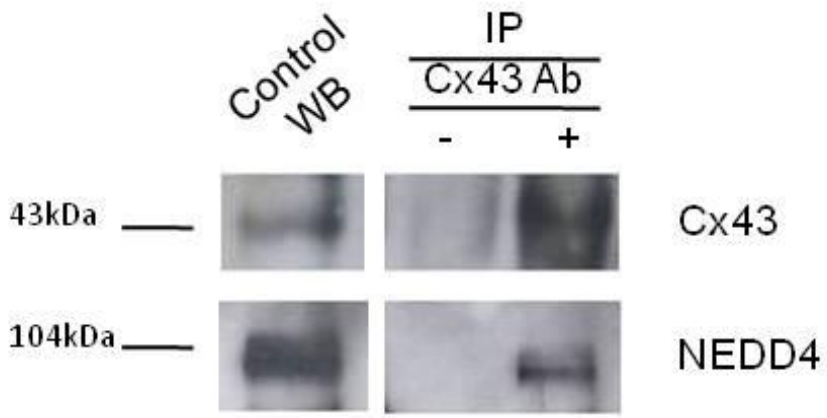

Figure 16 Co-precipitation of NEDD4 with Cx43
Anti- Cx43 antibody was used to immunoprecipitate protein complexes in Eahy926 cells lysates. Cx43 and NEDD4 were visualized by immunoblotting with an anti-Cx43- or anti-NEDD4 antibody, respectively. The results are representative for three experiments.

siRNA

In order to show whether NEDD4 influences Cx43 expression, endothelial cells were treated with negative control or siRNA against NEDD4. After 144 h of incubation, proteins were isolated. The NEDD4 and Cx43 protein were analysed by immunoblotting. Figure 17 shows successful knock-down of NEDD4 and the corresponding increase of Cx43 protein in comparison with the un-treated control.

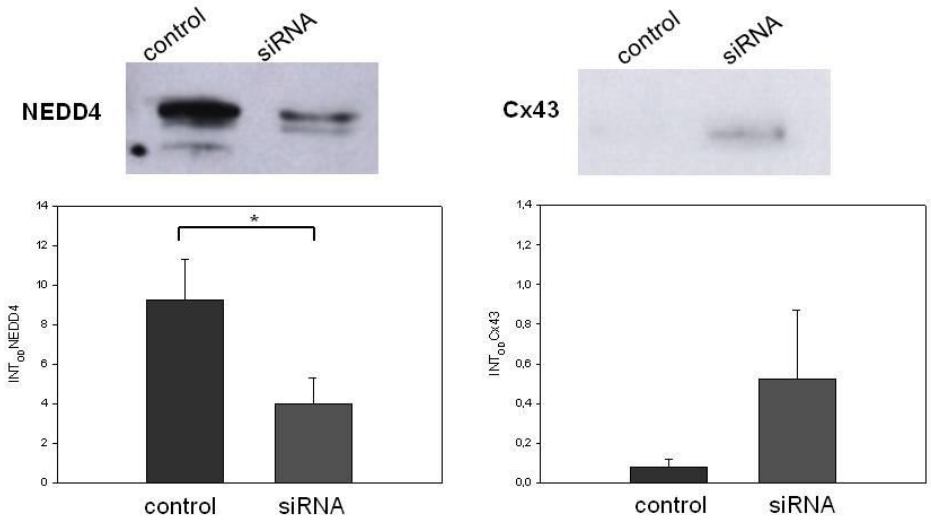

Figure 17 The effect of NEDD4 knockdown on Cx43 expression
Negative control siRNA (control) or siRNA against NEDD4 (siRNA) was transfected into EAhy926 and the expression of NEDD4 and Cx43 protein was detected by immunoblotting after 144 h. Figure shows representative results of NEDD4 and Cx43 expression analysed by immunoblotting and measured optical density of NEDD4 and Cx43.Equal loading was confirmed by Pounceau staining. Data are given as mean± SD, n=3, *$p \leq 0.05$, vs. control.

4.4 Impact of proteasomal and lysosomal inhibitors on Cx43 level

In order to block different pathways of protein degradation, cells were treated with two different proteasome and one lysosome inhibitor/s. After each time point cells were collected and whole cell lysates were subjected to immunoblotting analysis using anti-Cx43 antibody.

Figure 18 shows inhibition of Cx43 degradation by 40 $\mu mol \times L^{-1}$ ALLN. Incubation for 3 h and 6 h did not have any effect, whereas 9 h nearly tripled the amount of Cx43 in comparison with control cells.

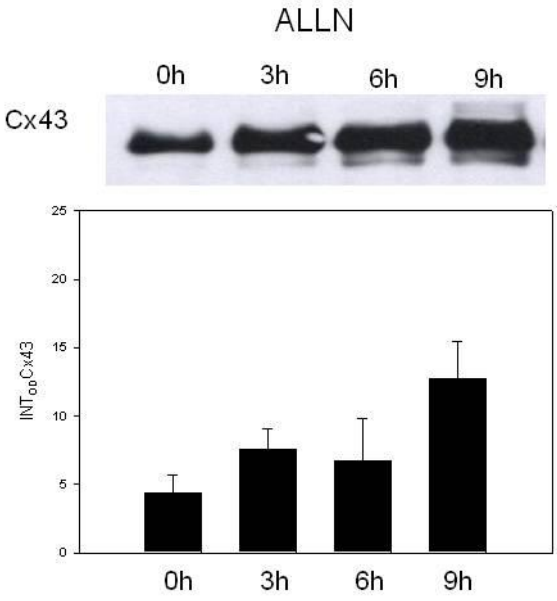

Figure 18 Inhibition of Cx43 degradation by ALLN
Cells were treated with proteasome inhibitor- 40 μmol×L^{-1} ALLN for 3 h, 6 h and 9 h. Cx43 protein level was analysed by immunoblotting. Representative results of Cx43 level analysed by immunoblotting are shown in the upper part. The corresponding statistical values from four experiments are shown below. Equal loading was confirmed by Pounceau staining. Data are given as mean± SD, n=4, *$p \leq 0.05$, vs. control.

MG132 inhibitor at the concentration of 40 μmol×L^{-1} was lethal for cells. Half lower concentration (20 μmol×L^{-1}) led to Cx43 accumulation after 9 h of incubation (Figure 19).

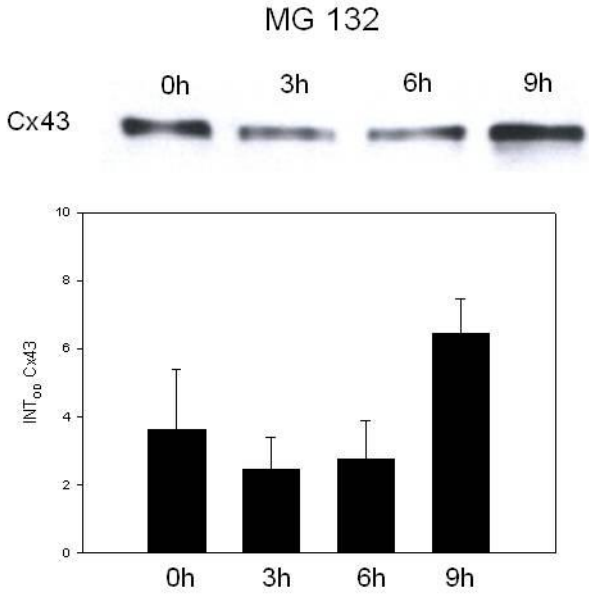

Figure 19 Inhibition of Cx43 degradation by MG 132
Cells were treated with proteasome inhibitor- 20 μmol×L^{-1} MG132 for 3 h, 6 h and 9 h. Cx43 protein level was analysed by immunoblotting. Representative results of Cx43 level analysed by immunoblotting are shown in the upper part. The corresponding statistical values from four experiments are shown below. Equal loading was confirmed by Pounceau staining. Data are given as mean± SD, n=4.

Next Cx43 degradation via lysosome was examined. 100 µmol×L^{-1} of chloroquine was used for 2 h and 4 h. As immunoblotting analysis showed chloroquine failed to inhibit Cx43 degradation at this two time points (Figure 20).

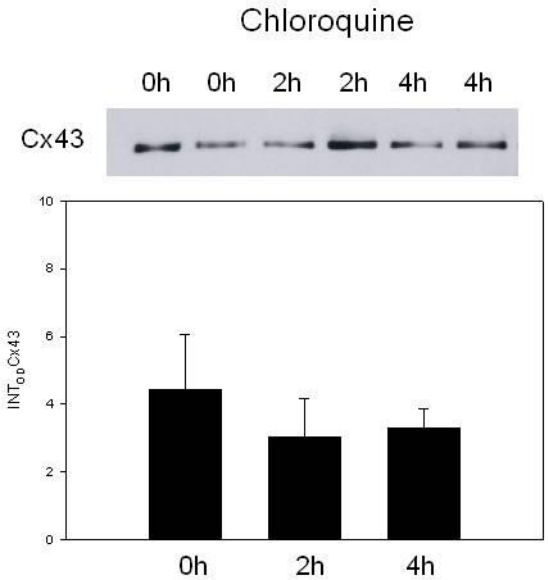

Figure 20 Inhibition of Cx43 degradation by chloroquine
Cells were treated with 100 µmol×L^{-1} chloroquine for 2 h and 4 h. Cx43 protein level was analysed by immunoblotting. Representative results of Cx43 level analysed by immunoblotting are shown in the upper part. The corresponding statistical values from four experiments are shown below. Equal loading was confirmed by Pounceau staining. Data are given as mean± SD, n=4.

4.5 Identification of NEDD4 binding partners

Since we showed for the first time NEDD4 expression in endothelial cells, we also intended to identify new NEDD4 binding partners. As a screening method, co-immunoprecipitation analysis was performed.

Total cell lysates were precipitated with anti-NEDD4 antibody or without antibody as a control. Additional negative controls were performed with HAS3 antibody. Protein extracts (before washing) and precipitates after four times of washing were loaded on the polyacrylamide gel and electrophoretically separated. This experiment showed specific bands bound at molecular weights of about 150 kDa, 110 kDa and 70 kDa as shown in Figure 21. These bands were isolated from the gel, destained and analysed by mass spectrometry.

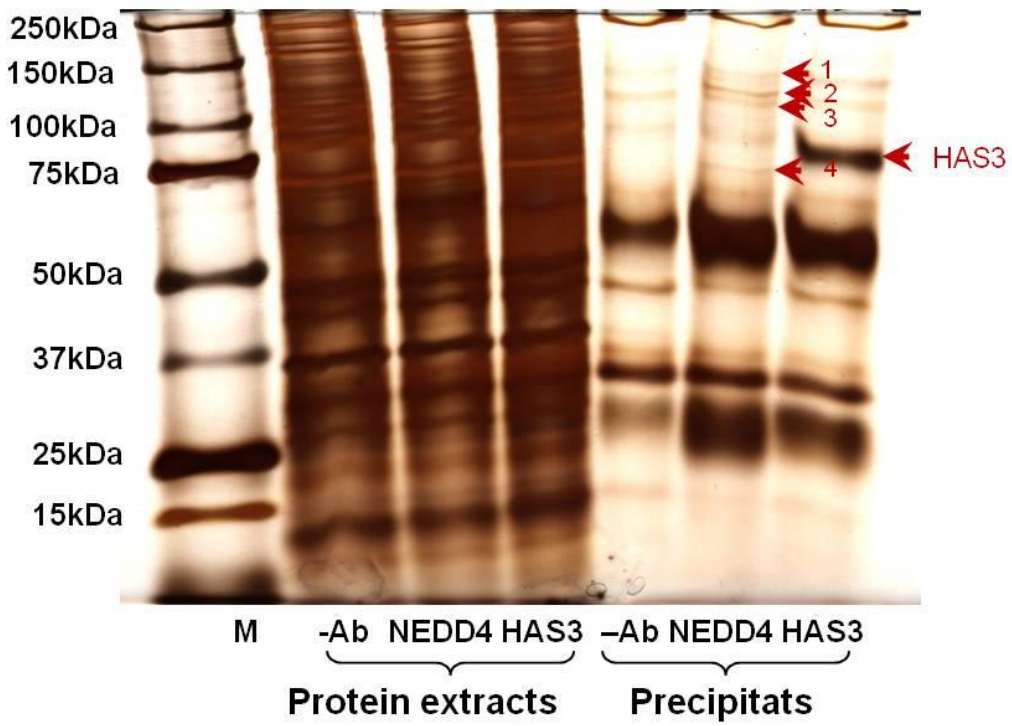

Figure 21 Possible NEDD4 binding partners
Total cell lysates (protein extracts) were either incubated without antibody (-Ab), with anti-NEDD4 antibody (NEDD4), or HAS3 antibody (HAS3). Protein extracts and precipitates were electrophoretically separated on 8% polyacrylamide gel and stained with silver. Marked bands (arrow and number) were subjected to mass spectrometric analysis.

This analysis revealed that extracted samples most probably corresponded with:

Band 1- P11142- Heat shock cognate 71 kDa protein (Heat shock 70 kDa protein 8)

Band 2- P46934- E3 ubiquitin-protein ligase NEDD4 (EC 6.3.2.-)

Band 3- O00308- NEDD4-like E3 ubiquitin-protein ligase WWP2 (EC 6.3.2.-)

Band 4- O95817- Bcl-2-associated athanogene 3 (BAG-3)

4.6 Impact of mechanical forces on NEDD4 expression

4.6.1 **Regulation of NEDD4 by laminar flow**

NEDD4 expression was analysed in shear stress-treated cells for different times and forces of treatment. First, endothelial cells were exposed to 6 dyn/ cm^2 constant laminar flow for 4 h, 15 h and 24 h (Figure 22, A-C). Results obtained from real time RT-PCR showed that only at 4h NEDD4 mRNA slightly increased. Interestingly, NEDD4 protein at the same time decreased. Both of the observed changes were not statistically significant.

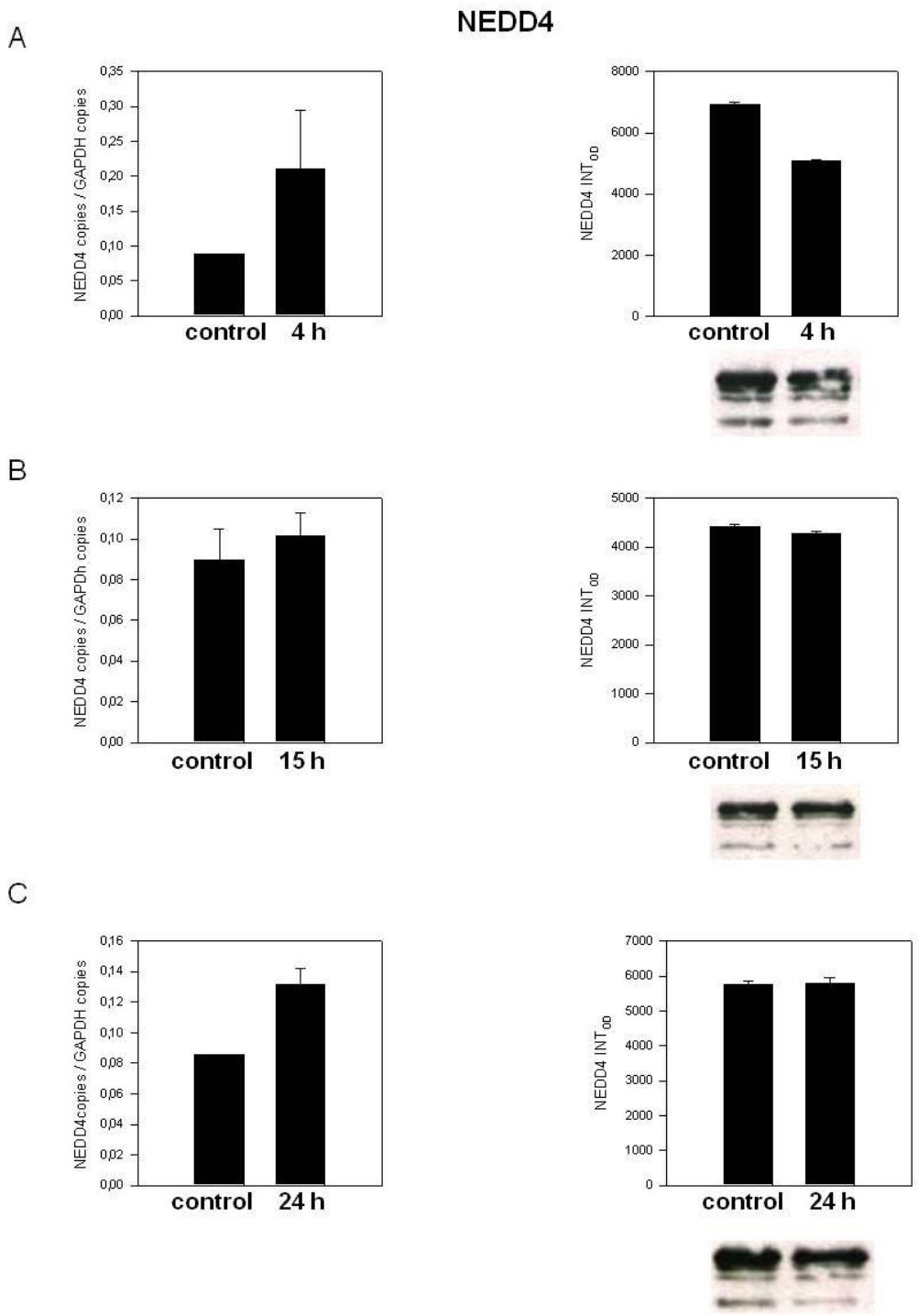

Figure 22 Expression of NEDD4 as a function of time
Endothelial cells were exposed to constant laminar flow (6 dyn/ cm^2) for A) 4 h, B) 15 h, and C) 24 h or kept as a static control.
Left panels show NEDD4 mRNA expression analysed by real time RT-PCR. Data are given as mean ± SD, n=3.
Right panels show measured optical density of NEDD4 expression analysed by immunoblotting. Additionally, representative blots are shown below figures. Equal loading was confirmed by Pounceau staining. Data are given as mean ± SD, n=3.

In a next set of experiments, constant laminar flow of 2 dyn/ cm^2, 6 dyn/ cm^2 and 10 dyn/ cm^2 was applied for 24 h. As shown below NEDD4 mRNA and protein expression did not change (Figure 23, A-C).

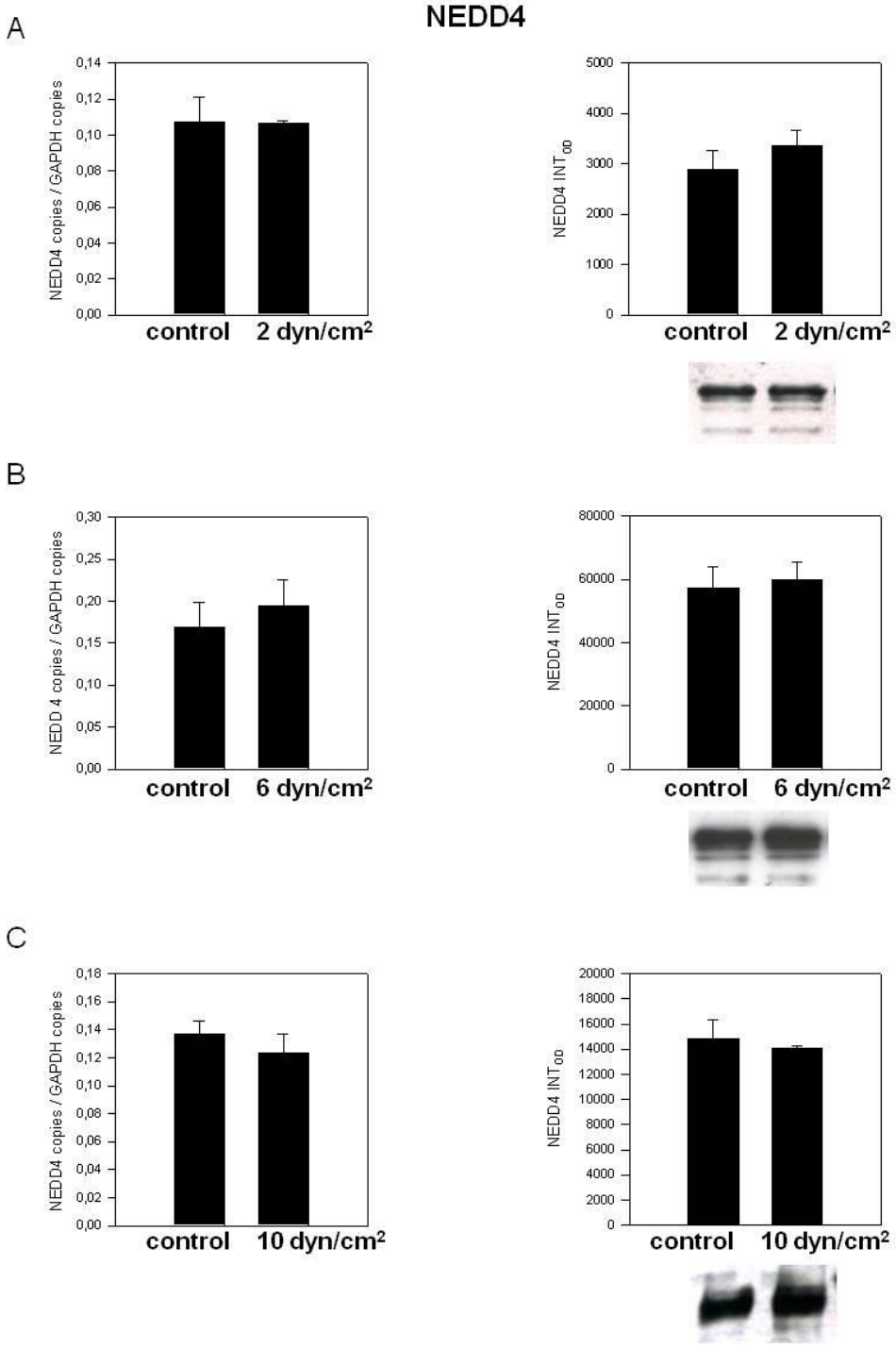

Figure 23 Expression of NEDD4 as a function of force
Endothelial cells were exposed to A) 2 dyn/ cm^2, B) 6 dyn/ cm^2, and C) 10 dyn/ cm^2 constant laminar flow for 24 h or kept as a static control.
Left panels show NEDD4 mRNA expression analysed by real time RT-PCR. Data are given as mean ± SD, n=3.
Right panels show measured optical density of NEDD4 expression analysed by immunoblotting. Additionally, representative blots are shown below figures. Data are given as mean ± SD, n=3.

Endothelial cells were also exposed to different flow patterns for 24 h. The NEDD4 mRNA expression was analysed by real time RT-PCR. As Figure 24 demonstrates, NEDD4 was highly upregulated under atheroprotective flow when compared to constant laminar flow.

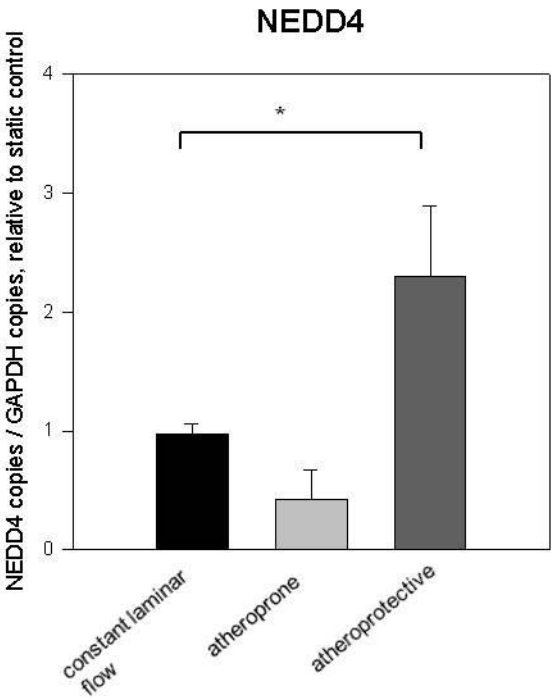

Figure 24 Influence of different flow patterns on NEDD4 expression
Endothelial cells were exposed to constant laminar flow (5,4 dyn/ cm^2) as well as atheroprone and atheroprotective flow for 24 h. Control cells were kept without flow. Nedd4 expression was determined by real time RT-PCR. Results are given as mean ± SD, n=4, *$p \leq 0.05$, vs. constant laminar flow. Results are expressed as fold of the corresponding static control.

4.6.2 Regulation of NEDD4 by PI3K and NO signalling pathways

To test if they contribute to the shear stress sensitivity of NEDD4, two well known mechanosensitive enzymes resp. signal transduction pathways were blocked by specific inhibitors. So, PI3K was inhibited by 10 $\mu mol \times L^{-1}$ LY294002 and cells were exposed to 6 dyn/ cm^2 laminar flow for 4 h and 24 h, respectively. Figure 25 illustrates that NEDD4 mRNA did not change when exposed to shear stress or kept under static culture conditions, both in the presence of specific PI3K inhibitor LY294002.

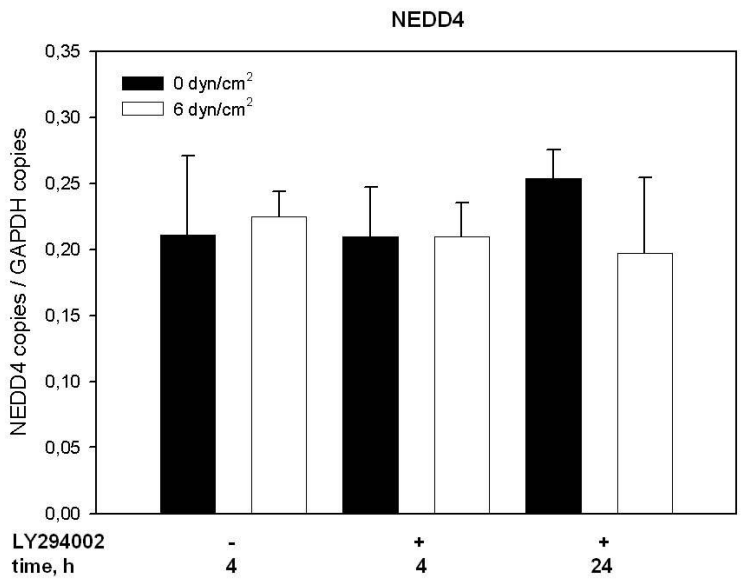

Figure 25 Impact of PI3K on NEDD4 expression
Cells were treated with 10 µmol×L^{-1} LY294002 inhibitor and either exposed to laminar flow (6 dyn/ cm^2 for 4 h and 24 h) or kept as a static cell culture. Control cells where cultured without inhibitor. NEDD4 mRNA expression was analysed by real time RT-PCR. Data are given as ± SD, n=3.

In addition, nitric oxide production was blocked by using 500 µmol×L-1 L-NAME. As a control 500 µmol×L^{-1} D-NAME was used. In these experiments cells were exposed to 6 dyn/ cm^2 shear stress for 4 h. Real time RT-PCR results indicated that NEDD4 mRNA expression was not affected (Figure 26).

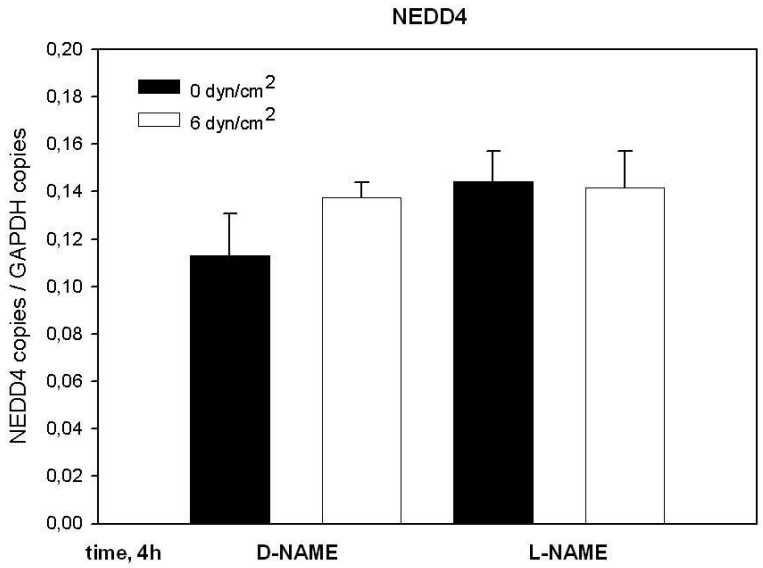

Figure 26 Impact of nitric oxide on NEDD4 expression
Cells were treated with 500 µmol×L^{-1} L-NAME inhibitor and 500 µmol×L^{-1} inactive isomer D-NAME as a control and either exposed to 6 dyn/ cm^2 for 4 h or kept as a static cell culture. Control cells where cultured without inhibitor. NEDD4 mRNA expression was analysed by real time RT-PCR. Data are given as ± SD, n=3.

4.6.3 **Regulation of Cx43 expression by laminar flow**

Results presented above demonstrated that NEDD4 binds to Cx43. The same set of samples from experiments using cone and plate system was used to analyse Cx43 expression. The expression of Cx43mRNA and protein did not change significantly. Figure 27 shows a results from experiments performed under 6 dyn/ cm^2 for 24 h.

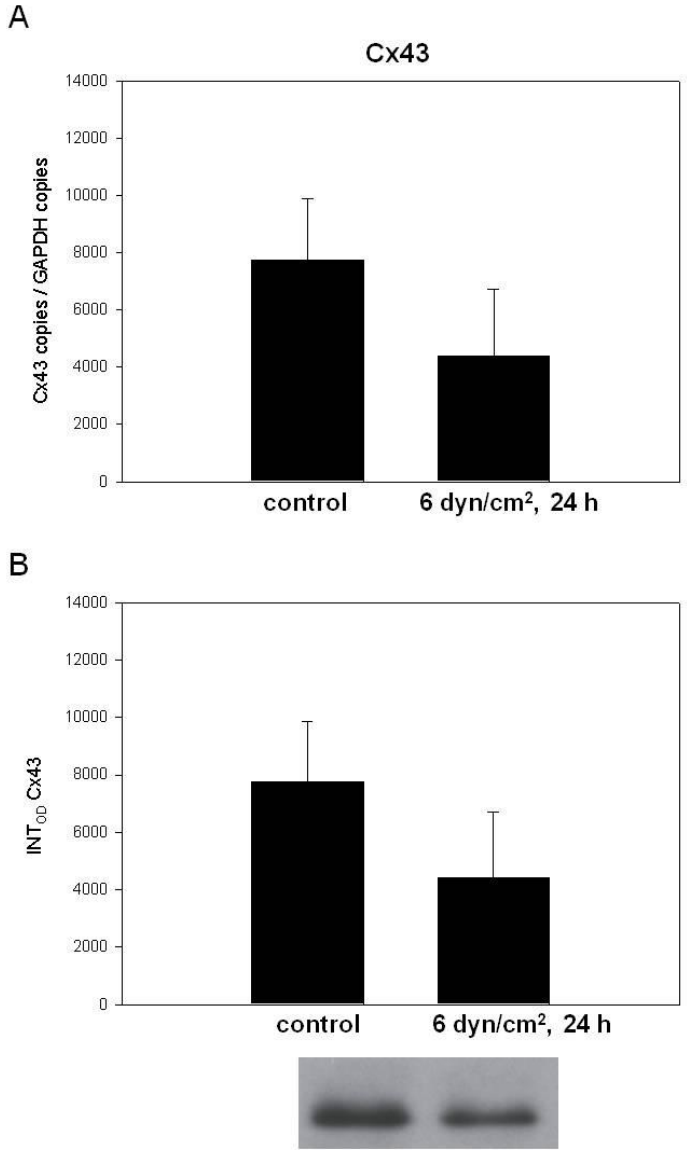

Figure 27 Effect of constant laminar flow on Cx43 expression
Endothelial cells were exposed to constant laminar flow (6 dyn/ cm^2) for 24 h.
A) shows Cx43 mRNA expression analysed by real time RT-PCR. Data are given as mean ± SE, n=5.
B) shows measured optical density of Cx43 protein expression analysed by immunoblotting. Additionally, representative blots are shown below figure. Data are given as mean ± SD, n=3.

To test whether higher NEDD4 expression under atheroprotective flow profile impacts Cx43 regulation, the same set of samples was run as real time RT-PCR for Cx43 mRNA expression. Figure 28 shows that Cx43 mRNA did not significantly differ between profiles.

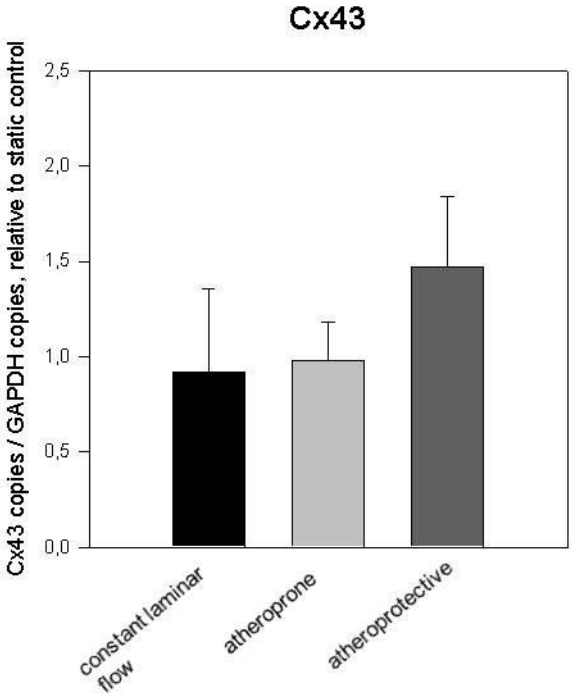

Figure 28 Influence of different flow patterns on Cx43 expression
Endothelial cells were exposed to constant laminar (5,4 dyn/ cm^2) as well as atheroprone and atheroprotective flow for 24 h. Control cells were kept in a Petri dish. Expression of Cx43 mRNA was analysed by real time RT-PCR. Results are given as mean ± SD, n=4. Results are expressed as fold of the corresponding static control cultures.

4.6.4 Impact of microgravity on NEDD4 and Cx43 expression

In order to study the impact of microgravity on NEDD4 as well as its possible effects on Cx43 regulation in endothelial cells, Rotating Wall Vessel was used.

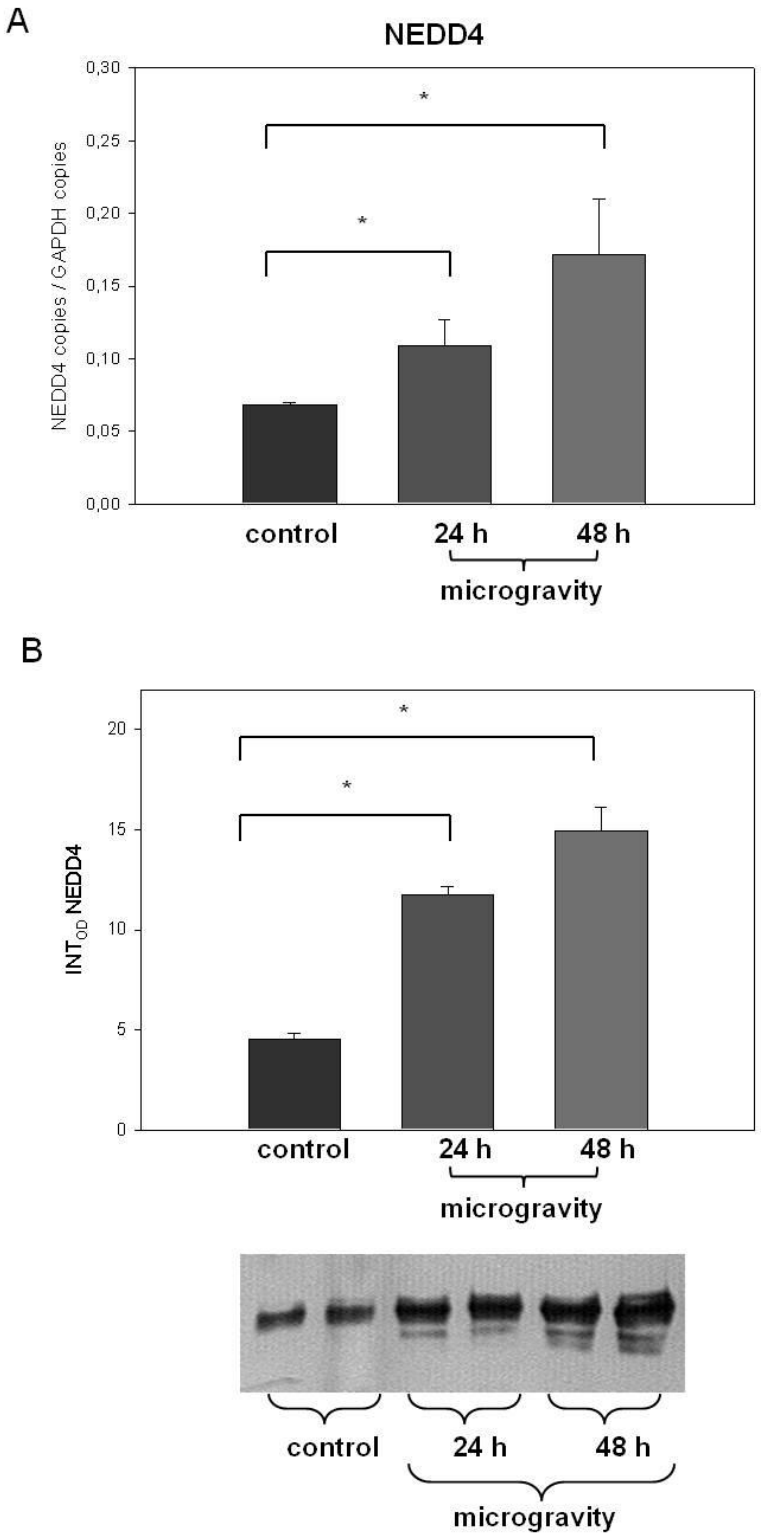

Figure 29 Impact of microgravity on NEDD4 expression
Endothelial cells were attached to the beads for 24 h and then exposed to microgravity for 24 h and 48 h, or kept as a control under 1×g.
A) Expression of NEDD4 mRNA was analysed by real time RT-PCR. Data are given as mean ± SD, n=4, * $p \leq 0.05$, vs. control (1×g).
B) Protein expression was analysed by immunoblotting with anti-NEDD4 antibody. Represantative blot is shown below figure. Equal loading was confirmed by Pounceau staining. Data are given as mean ± SD, n=4, * $p \leq 0.05$, vs. control (1×g).

NEDD4 mRNA (Figure 29, A) and protein (Figure 29, B) were significantly induced already after first 24 h of microgravity and additional 24 h caused an even higher increase in both.

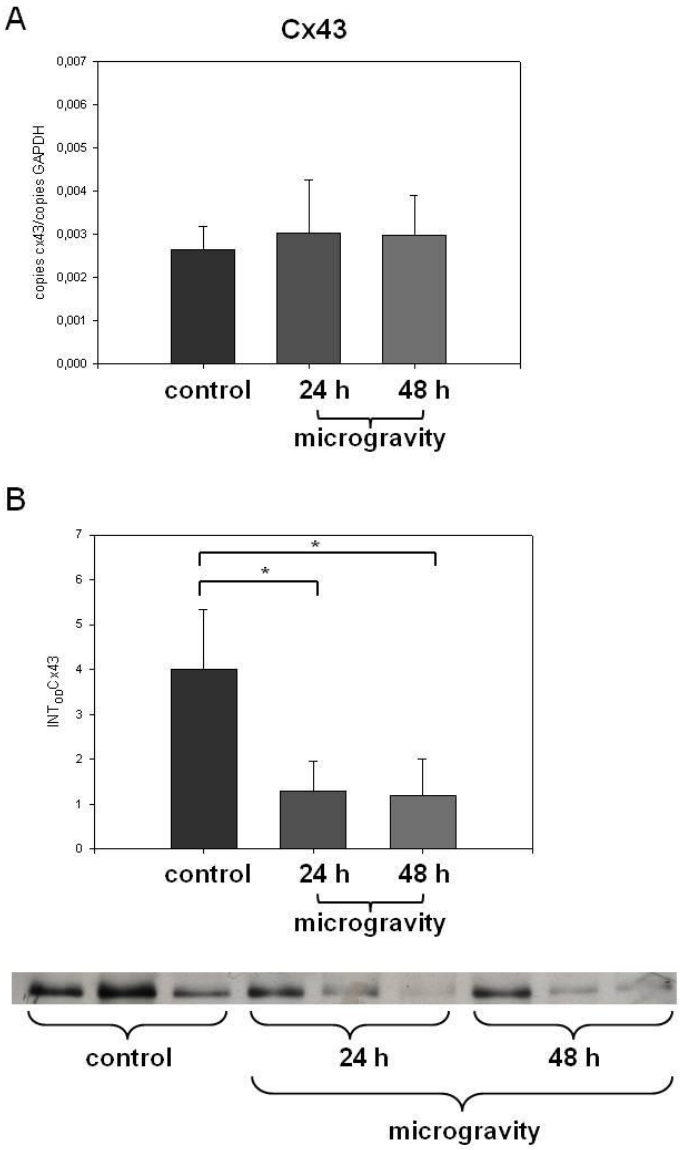

Figure 30 Impact of microgravity on Cx43 expression
Endothelial cells were attached to the beads and then exposed to microgravity for 24 h and 48 h or kept as a 1×g control.
A) Expression of Cx43 mRNA was analysed by real time RT-PCR. Data are given as mean ± SD, n=4.
B) Protein expression was analysed by immunoblotting with ant-Cx43 antibody. Represantative blot is shown below figure. Equal loading was confirmed by Pounceau staining . Data are given as mean ± SD, n=4, * $p \leq 0.05$, vs. control (1×g).

Cx43 mRNA was not affected by microgravity for 24 h and 48 h (Figure 30, A) but Cx43 protein decreased notably after first 24 h and kept the same level of expression to the end of experiment (Figure 30, B).

4.7 Impact of mechanical forces on ADAMTS1 expression

4.7.1 **Regulation of ADAMTS1 by laminar flow**

In order to test whether ADAMTS1 is sensitive to mechanical forces, endothelial cells were exposed to 6 dyn/ cm^2 of shear stress produced by laminar flow for different times and analysed by semiquantitative duplex RT-PCR for the expression of ADAMTS1 mRNA. ADAMTS1 expression was increased within the first eight hours and remained elevated for up to 48 h (Figure 31, A) in comparison with corresponding (cells isolated from the same umbilical cord) static controls (Figure 31, B).

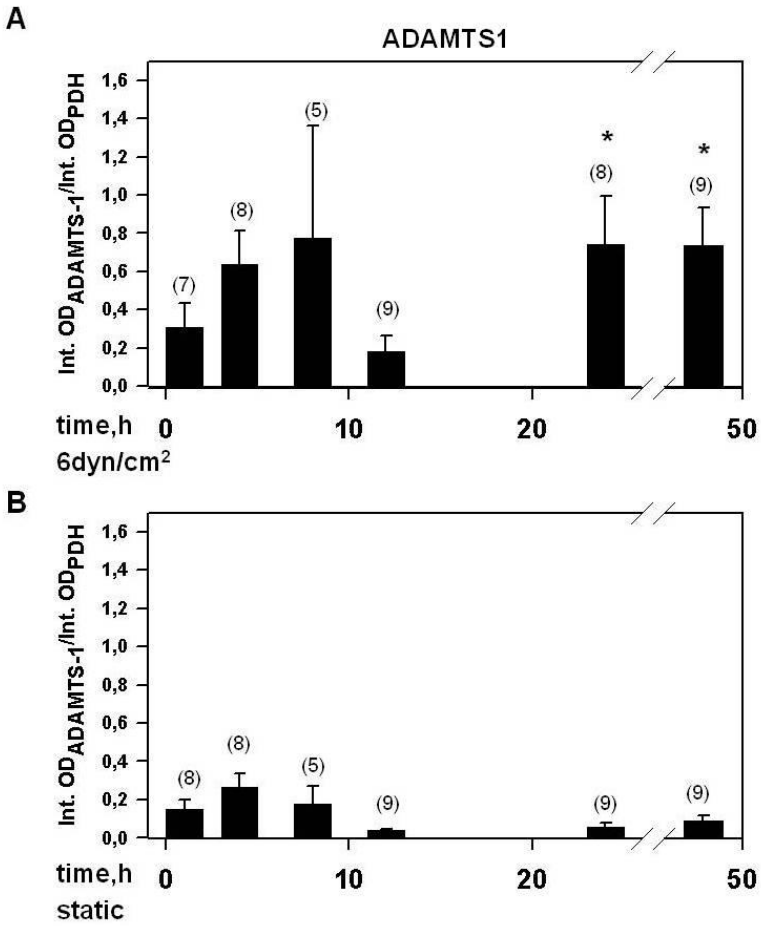

Figure 31 Expression of ADAMTS1 in endothelial cells as a function of time.
Endothelial cells were exposed to constant laminar flow (6 dyn /cm^2) for different times as indicated and then analysed by semiquantitative duplex RT-PCR (panel A). The corresponding no-flow controls are shown in panel B. Data are given as mean ± SD, numbers of independent experiments are given in brackets on top of each bar, * $p \leq 0.05$. Significance (A) was tested for shear stress treated samples versus paired static control samples (B).

Next, different shear forces of 1 dyn/ cm^2, 2 dyn/ cm^2, 3 dyn/ cm^2, and 5,4 dyn/ cm^2 were applied for 24 h. Shear stress-induced upregulation of ADAMTS1 mRNA was observed from 2 dyn/ cm^2 onwards (Figure 32).

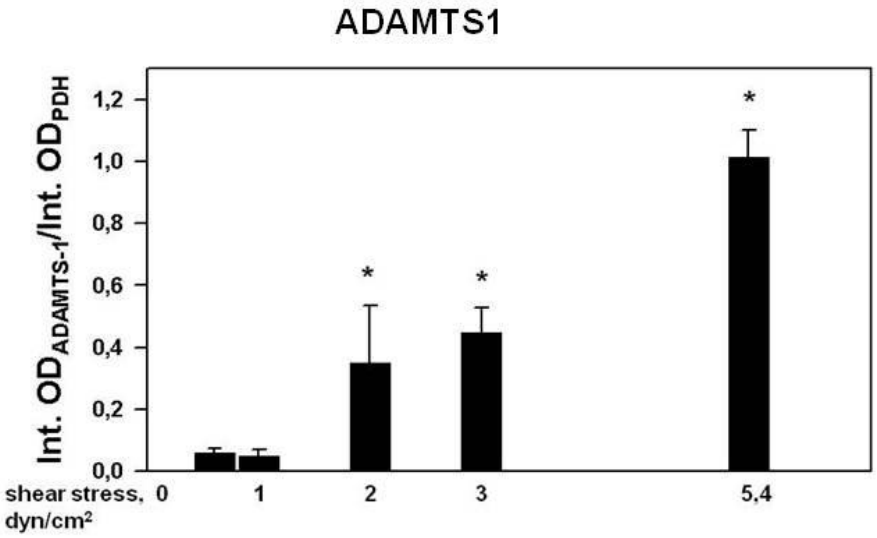

Figure 32 Expression of ADAMTS1 in endothelial cells as a function of shear stress
Endothelial cells were exposed to 1 dyn/ cm^2, 2 dyn/ cm^2, 3 dyn/ cm^2, and 5,4 dyn/ cm^2 of shear stress for 24 h. ADAMTS1 expression was analysed by semiquantitative duplex RT-PCR. Data are given as mean± SD, n=4, *$p \leq 0.05$. Significance was tested for shear stress treated samples against low shear stress of 1 dyn/ cm^2.

To simulate vessel occlusion, exposure of cells to 6 dyn/ cm^2 shear stress was stopped after 24 h in some cell cultures, and ADAMTS1 mRNA expression was investigated by semi-quantitative duplex RT-PCR 1 h, 4 h and 24 h later. As Figure 33 shows ADAMTS1 mRNA was reduced to near static control conditions within 4 h following flow stop.

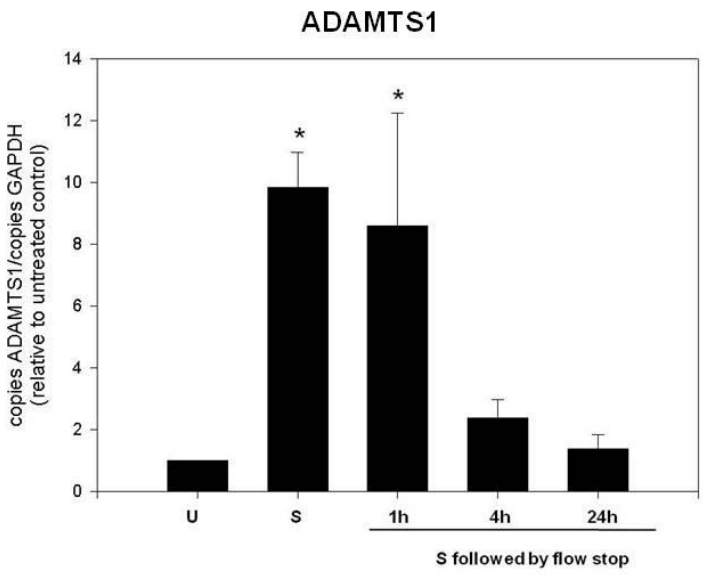

Figure 33 Expression of ADAMTS1 following flow stop
Endothelial cells were exposed to constant laminar flow (S) of or kept as static control (U). In some samples ADAMTS1 expression was analysed 1 h, 4 h or 24 h following flow stop. Samples were analysed by real time RT-PCR. Data are given as mean ± SD, n=5, * $p \leq 0.05$. Significance was tested for shear stress treated samples against untreated controls.

Further investigations by real time RT-PCR of endothelial cells exposed to different flow patterns revealed that the increase of ADAMTS1 was a bit higher using an atheroprotective flow profile than under constant laminar flow. Under an “atheroprone profile” ADAMTS1 mRNA was similarly low expressed as with no-flow culture conditions (Figure 34).

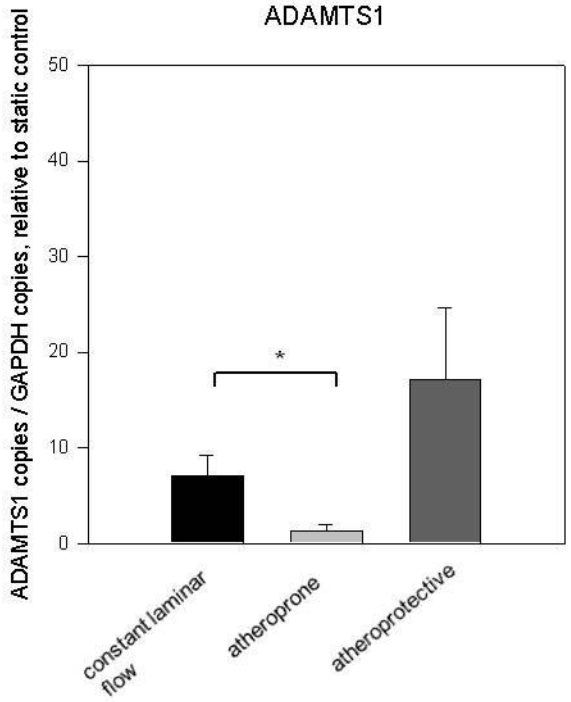

Figure 34 Effect of different flow patterns on ADAMTS1 expression
Endothelial cells were exposed to constant laminar flow as well as atheroprone and atheroprotective flow profiles for 24 h. Control cells were kept in a Petri dish. Samples were analysed by real time RT-PCR. Results are given as mean ± SD, n=4, * $p \leq 0.05$, vs. constant laminar flow. Results are expressed as fold of the corresponding static control cultures.

4.7.2 Inhibition of PI3K and eNOS on shear stress-induced ADAMTS1 expression

To investigate if mechanosensitive pathways may be involved in the induction of ADMATS1 by shear stress, endothelial cells were exposed to 6 dyn/ cm^2 shear stress for 24 h in the presence of specific inhibitors for PI3K and eNOS signaling pathways or kept either with inactive analogues or without these inhibitors as controls. ADAMTS1 mRNA was then analysed by quantitative real-time RT-PCR.

PI3 kinase was inhibited by using 10 µmol×L-1 LY294002. During this experiment baseline and shear stress-induced mRNA of ADAMTS1 were both significantly reduced (Figure 35).

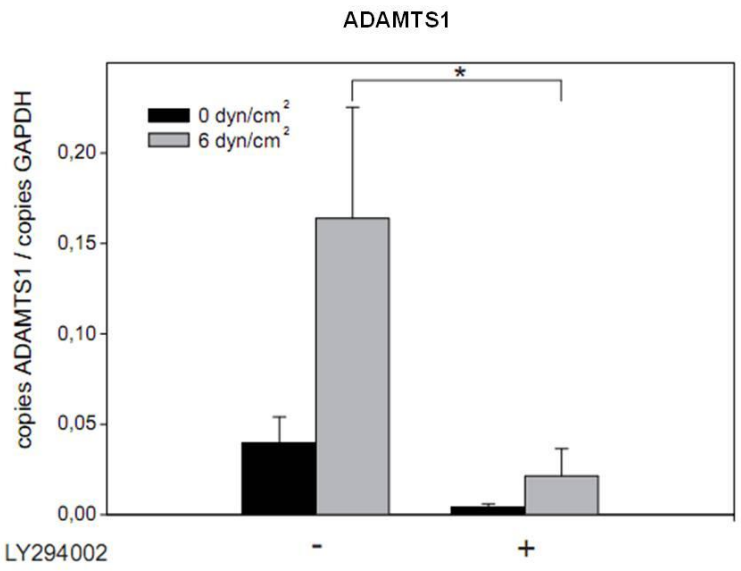

Figure 35 Impact of PI3K on shear stress dependent regulation of ADAMTS1
Endothelial cells were exposed to 6 dyn/ cm^2 shear stress or kept as static controls for 24 h in the presence of 10 $\mu mol \times L^{-1}$ LY 294002 inhibitor. Samples were analysed by real time RT-PCR. Data are given as mean ± SD, n=5,* $p \leq 0.05$, vs. control.

Inhibition of eNOS with L-NAME, using D-NAME as an inactive control also suppressed the shear stress-induced expression of ADAMTS1 (Figure 36).

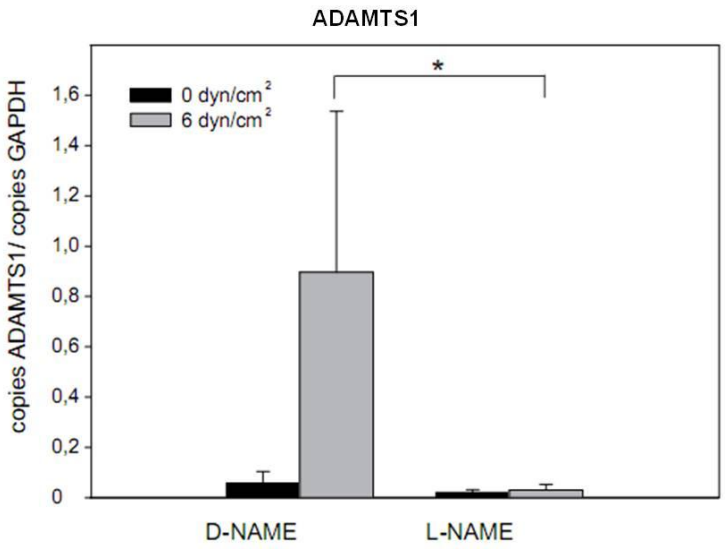

Figure 36 Impact of nitric oxide on shear stress-dependent regulation of ADAMTS1
Endothelial cells were exposed to 6 dyn/ cm^2 or kept as static control for 24 h in the presence of 500 $\mu mol \times L^{-1}$ L-NAME inhibitor or its inactive analogue (500 $\mu mol \times L^{-1}$ D-NAME). Data are given as mean ± SD, n=5,* $p \leq 0.05$, vs. control.

4.7.3 Regulation of ADAMTS1 expression by oxygen pressure

Since hypoxia induces sprouting type of angiogenesis, it was interesting to test ADAMTS1 expression in relation to oxygen pressure. Endothelial cells exposed to oxygen pressures lower than 100 mmHg P_{O2} significantly reduced ADAMTS1 mRNA expression (Figure 37, A).

In order to investigate conditions which are typical for arteries (10 dyn/ cm^2, 100 mmHg $p0_2$, 24 h), veins (2 dyn/ cm^2, 40 mmHg $p0_2$, 24 h) and capillary sprouts (0 dyn/ cm^2, 20 mmHg $p0_2$, 24 h) cells were exposed to a combination of shear stress and oxygen pressure. Results of these experiments revealed that simulated capillary- and vein like conditions did not affect ADAMTS1 mRNA expression, whereas arterial like conditions strongly upregulated ADAMTS1 mRNA (Figure 37, B).

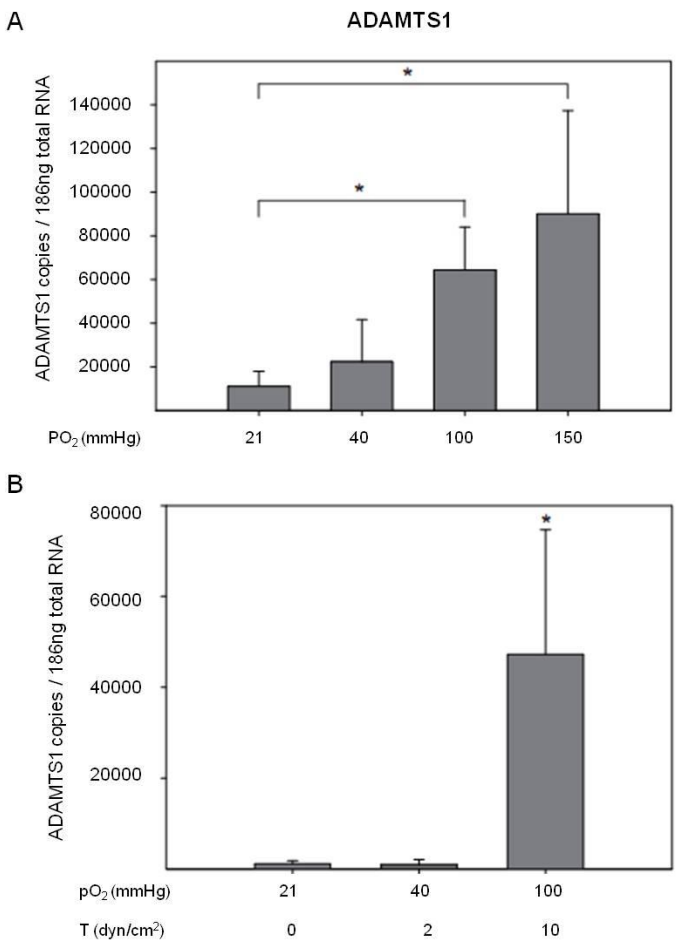

Figure 37 ADAMTS1 expression is affected by oxygen pressure and combinations with shear stress
A) Endothelial cells were cultured at different oxygen pressures.
B) Endothelial cells were cultured at combinations of shear stress with oxygen pressure according to the typical conditions in capillaries ($pO_2$20 mmHg, shear stress 0 dyn/ cm^2), different veins (pO_2 40 mmHg, shear stress 2 dyn/ cm^2) and arteries (pO_2 100 mmHg, shear stress 10 dyn/ cm^2).
Samples were analysed by quantitative real-time RT-PCR. Results are presented as mean ± SD, n=5, * $p \leq 0.05$.

4.7.4 ADAMTS1 cleaves TSP1 to 70 kDA fragments under shear stress

To investigate whether under shear stress ADAMTS1 cleaves TSP1 and produce a fragment with anti-angiogenic properties, cells were exposed to 6 dyn/ cm^2 for 24 h or kept under static conditions. Whole cell lysates were analysed by immunoblotting using anti-TSP1 antibodies. The results indicated that under flow conditions there is a significant increase of a 70 kDA fragment, and decrease of full length 180 kDA TSP1 (Figure 38).

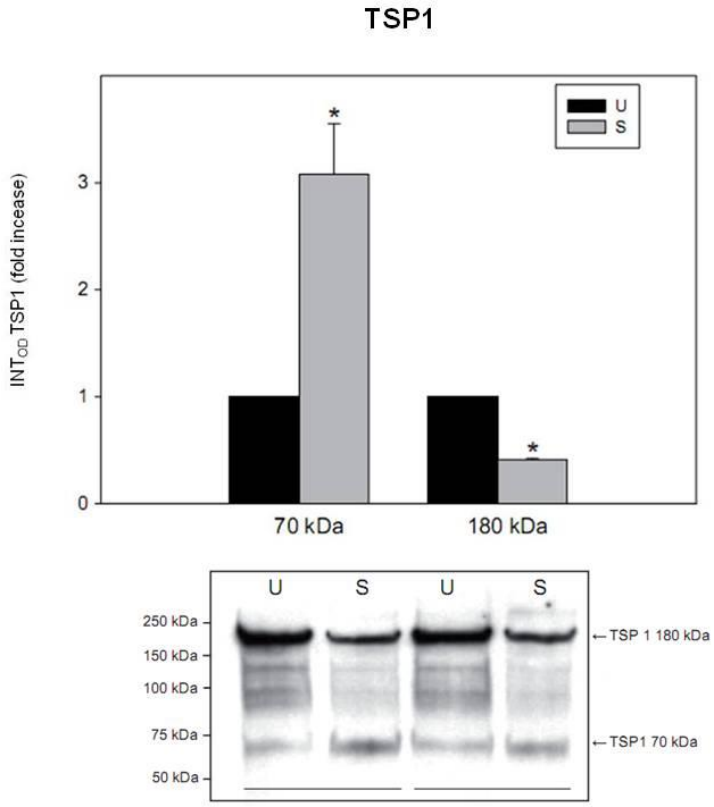

Figure 38 TSP1 is cleaved to smaller fragments by ADAMTS1 under shear stress
HUVEC cells were exposed to 6 dyn/ cm^2 for 24 h (S) or kept as static controls (U). TSP1 was analysed by immunoblotting. Figure shows measured optical density of the 180 kDA and 70 kDA TSP1 as a fold increase. Below are shown representative blots. Results are shown as mean ± SD, n=3,* $p \leq 0.05$.

4.7.5 Medium conditioned by shear stress treated HUVEC inhibits cell cratch closure

Conditioned cell culture medium was collected from experiments where cells were exposed to shear stress as well as from static controls and used in scratch wound assay. Endothelial cells monolayers were scratched and scratch closure was observed. Medium from cells exposed to shear stress inhibited scratch closure whereas medium from control cells did not affect this process (Figure 39).

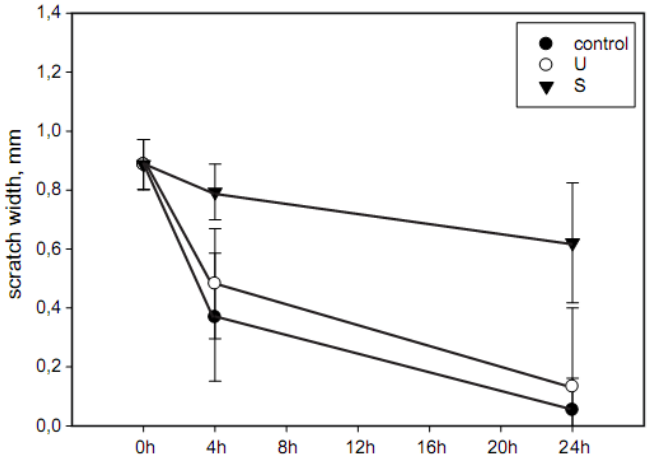

Figure 39 The scratch wound closure in HUVEC
HUVEC monolayers were scratched and the wound closure was observed in cell culture with freshly prepared medium (control), conditioned medium from HUVEC exposed to 6 dyn/cm^2 for 24 h (S) or static conditions (U). Results are shown as mean ±S D, n=3.

4.7.6 Impact of microgravity on ADAMTS1 and TSP1 expression

It was also interesting to test whether ADAMTS1 and TSP1 are sensitive to microgravity. Endothelial cells were exposed to simulated microgravity by culturing in the Rotating Wall Vessel. Expression of ADAMTS1 mRNA was investigated by real time RT-PCR after 24 h and 48 h of exposure and compared to ground controls. As Figure 40 illustrates, ADAMTS1 was strongly upregulated after 24 h, but within next 24 h decreased, reaching nearly control level at the end of the experiment.

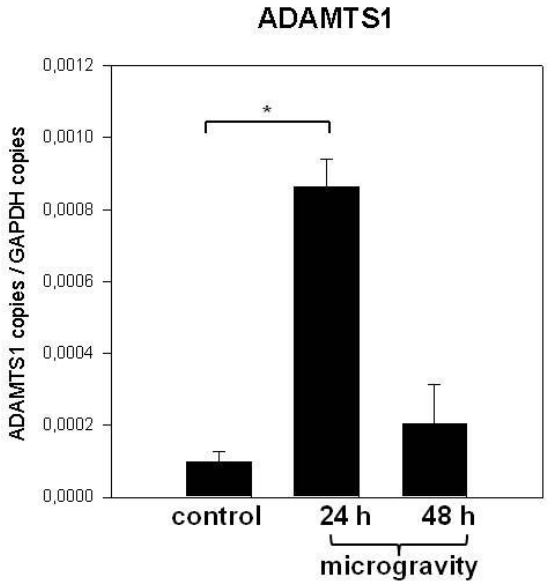

Figure 40 Impact of microgravity on ADAMTS1 expression
Endothelial cells were exposed to microgravity for 24 h and 48 h. Control cells were kept as control (1×g). Expression of ADAMTS1 mRNA was analysed by real time RT-PCR. Data are given as mean ± SD, n=3, *$p \leq 0.05$, vs. control (1×g).

TSP1 revealed different expression patterns when exposed to microgravity. TSP1 mRNA expression did not change within first 24 h, but additional exposure led to an increase (Figure 41).

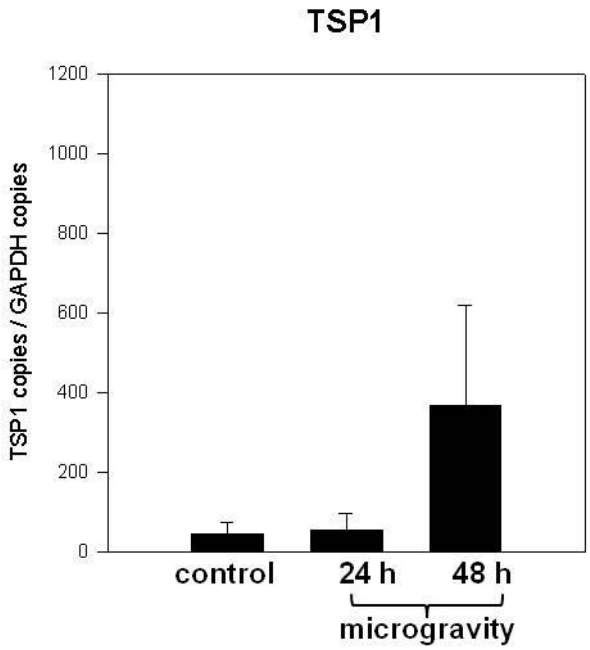

Figure 41 Impact of microgravity on TSP1
Endothelial cells were exposed to microgravity for 24 h hand 48 h. Control cells were kept as control (1×g). Expression of TSP1 was analysed by real time RT-PCR. Data are given as mean ± SD, n=3.

5 Discussion

5.1 Cone and plate system as a model to study shear stress

In the last several years together with the increasing number of reports on the effects of shear stress on endothelial cell behavior, the need for devices generating shear stress has been increasing. There are two types of devices used to expose cells to shear stress. First, parallel plate flow chamber and capillary tube flow viscosimeter which consists of a chamber with grown cells. Shear stress is generated by forcing a fluid through a chamber by a pump or hydrostatic head. Second class includes devices with a rotating disc or cone, which moves on top of the culture medium and transmits shear stress to the cells.

In comparison with flow chambers, the cone and plate devices are simpler to operate. Moreover, the size of apparatus allows performing standard cell culture technique under controlled conditions in the incubator. Cells are grown on a standard Petri dish (10 cm) which allows isolating sufficient amounts of RNA and proteins to investigate changes in genes and proteins expression. Important to note is also that applied shear stress is homogenous on a whole area and the device is able to produce high range of shear stresses.

Cone and plate apparatus has few disadvantages. Since this is an open system, the risk of contamination of samples with bacteria and fungi is higher. Therefore, the time of exposure in performed experiments was no longer than 24 h. Another limitation which occurs commonly is that application of higher shear stress leads to the turbulent flow. This problem may be overcome by addition of substances that increase the viscosity of the flowing medium, e.g. Dextran. In this studies Dextran was added when applied shear stress was higher then 6 dyn/ cm^2. It has also been observed that application of high shear may cause detachment of cells from the bottom of Petri dish. In order to solve this problem in our experiments shear stress application was smoothly increased at the beginning of each experiment.

Cone and plate devices used to perform experiments presented in this thesis were designed and built in the Institute of Physiology in Berlin-Dahlem. The first cone and

plate apparatus ever in use at the institute had already been evaluated earlier. The microscopic observation reveled that endothelial cells align in the direction of flow within 24 h under 6 dyn/ cm^2. Moreover, expression of CNP and ET-1 under laminar flow was examined. The results showed an increase in CNP and decrease in ET-1 expression after 24 h of exposure to 6 dyn/ cm^2 [60]. This results are consistent with previous reports [109, 110].

As it has been shown by many experiments endothelial cells are able to respond by changing their phenotype to a specific shear stress profile [12]. To be able to test the influence of different shear stress profiles on endothelial cells, another version of a cone and plate apparatus was designed and built in the Institute of Physiology. By investigating regulation of expression in KLF2, nrf2 and PGI_2-synthase, we could show that our experimental setup led to comparable results with other similar devices. High expression of Klf2 under atheroprotective flow when compared to constant and arteriolar shear stress profiles was also observed by Parmar et al.[111], Dekker et al.[112], Wang et al. [113] and Dai et al.[12]. The transcription factor nrf2, whose posttranslational regulation by shear stress has been shown previously [114], was not regulated on the mRNA level by any tested flow profiles. Induction of PGI_2s expression by the small arterial profile may suggest its role in the regulation of peripheral resistance in the vascular system. It also indicates the sensivity of PGI_2s gene to the acceleration of blood flow. Relatively low expression of PGI_2s mRNA under conditions of constant laminar flow was likewise observed by Okhara et al. [115] before.

5.2 Rotating Wall Vessel as a model to study microgravity

There are two commonly used devices simulating microgravity like conditions on earth - random positioning machine, which was developed in Japan by Hoson et al. [116] and Rotating Wall Vessel, developed by Hammond et al.[104] at NASA. Rotating Wall Vessel provides some aspects of microgravity by maintaining continuous free-fall, whereas in random positioning machine cells are exposed to random speeds and orientation which randomizes the gravity vector [117]. Although microgravity in this two devices is simulated in a different way, there are studies showing that endothelial cells and papillary thyroid carcinoma cells respond [118, 119] similarly in terms of cytoskeleton organization [120] in the two model systems. Moreover, proliferation rates of human vein

endothelial cells were equally higher in the random positioning machine and in the Rotating Wall Vessel when compared to the "ground control" [121].

The Rotating Wall Vessel as a culture system has many advantages. First, in this system mechanical stress acting on cells in culture, which is more or less a suspension culture, is minimized because there is no mixing device like in spinner flasks. Second, an optimal exchange of nutrients, wastes and dissolved gases is provided by vessel rotation. Additionally, elimination of sedimentation as well as buoyancy and density driven convection creates unique culture conditions, where cells form aggregates and tissues similar to "*in vivo*" conditions. Moreover, Rotating Wall Vessel supports co-culture by bringing together different cells types and cells of different sizes. This system is also useful for simple exposure of cell suspension to different reagents. Accordingly, Rotating Wall Vessel has been successfully used not only in microgravity studies but also in different biotechnological applications like production of recombinant proteins by microbial hosts [122] or bone tissue engineering [123].

It needs to be mentioned that despite its advantages, experiments performed in the Rotating Wall Vessel have also limitations. During longer cell culture periods, as the cell aggregates grow in size, the rotational speed is increased to compensate for increased sedimentation rates. That causes an increase in shear stress acting on the cells. In our studies in order to minimize shear stress, exposure time in all experiments was limited to 48 h.

Another aspect is that cells exposed to microgravity regulate genes that are constitutively expressed on Earth. Rezwan et al. report as well as our own experiments showed that Beta2 microglobulin, 40 s ribosomal protein 17, cytoplasmatic beta actin, beta tubulin and GAPDH protein were differentially regulated by microgravity[124]. Therefore, in this work, protein analysis data were shown with Ponceau staining as a loading control.

Arguable are also applicable controls for experiments performed in the Rotating Wall Vessel. For example studies performed on Jurkat cells by Lewis et al. refer to cells grown in a traditional cell culture as a control. Such comparison is not sufficient because cells grown on beads in three dimensional space change extracellular matrix composition in comparison to traditional cell cultures, thereby affecting the expression

of many genes. A further aspect for which the traditional cell culture might be a weak control is that, Rotating Wall Vessel provides a good gas exchange. For this reason, cone and plate device is an interesting comparison group.
Our studies used as a control cells which were first seeded on microcarrier beads and then kept without rotation. The same kind of controls were used in earlier studies on endothelial cells [50, 52, 125].

According to the literature [117, 125] time averaged gravity vector acting on cell aggregates in the Rotating Wall Vessel is reduced to about 10^{-2}g, which is in contrast to real "reduced gravity". In spacecraft, due to gravity-gradients, oscillatory accelerations (created for example by mechanisms on the spacecraft and by crew movement) and conditions like solar wind, atmospheric drag or light pressure, perfect weightlessness is also difficult to achieve. Conditions which are considered to be "near weightlessness" are 10^{-4} -10^{-6}g.

As described in Materials and Methods, in order to successfully produce microgravity like environment in the Rotating Wall Vessel many requirements need to be fulfilled. To evaluate our setup, morphology, proliferation rate and expression of two genes in endothelial cells were investigated. Microscopic observations revealed similar morphology of single cells as well as three dimensional growth on multibeads aggregates as previously described by Sanford et al [126]. Additionally, both cultured cell types did not reveal any capillary –like structure formation. Duplication time of cells exposed to microgravity was 60% higher when compared to ground controls and comparable with Villa et al. report [121]. Moreover, EGF and IL6 upregulation was earlier shown by Hammond et al. [55] and Cotrupi et al. [50], respectively.

5.3 NEDD4 expression and binding to Cx43 in endothelial cells

NEDD4 expression was found in heart, lung, skeletal muscles and in cancer cell lines [63]. Primarily NEDD4 function was linked to the degradation of sodium channels [67, 68]. Later investigations showed that NEDD4 protein is able to bind to many molecules [66, 127, 128] and participate in their turnover.

The results presented here show for the first time NEDD4 expression in endothelial cells, functionally link this E3 ligase with shear stress and microgravity, and Cx43

turnover in these cells. This suggests an important role of NEDD4 in endothelial protein degradation under these conditions.

Our experiments confirmed NEDD4 expression in HUVEC as well as in EAhy926 cells. Moreover, immunostaining experiments revealed NEDD4 localization similar to previously found in human alveolar adenocarcinoma cell line cells (A549) [63] and in rat liver epithelial stem-like cells (WB-F344) [129].

Earlier experiments showed involvement of three WW domains as well as C-terminus domain in NEDD4 binding to Cx43 through multiple interactions [129]. Our immunoprecipitation analysis confirmed the ability of NEDD4 to bind Cx43 in endothelial cells. Moreover, NEDD4 knock down using siRNA technique led to an increase in total Cx43 of about 20-25% in our endothelial cell model and of about 10% in other cell types in other studies [129]. According to Leykauf et al. these results indicate an involvement of NEDD4 in the internalization of gap junctions. This suggestion was confirmed by observation showing that in cells expressing NEDD4 the amount of gap junctions plaques at the cells border was lower than in cells lacking NEDD4 [129].

5.4 Inhibition of Cx43 degradation

There are two ways for proteins to be degraded. Most cytosolic and nuclear proteins and some membrane proteins are degraded by the proteasome, whereas lysosome is responsible for degradation of membrane and extracellular material. As it has been postulated by Laing et al., both the proteasome and the lysosome are involved in Cx43 degradation [130]. In our approach we intended to determine which pathway is involved in Cx43 turnover by using different specific inhibitors. Immunoblots of the whole cell lysates of endothelial cells demonstrated that 40 $\mu mol \times L^{-1}$ ALLN blocked Cx43 degradation after 9 h of incubation and inhibition by ALLN was more effective then by MG132. Similar response to proteasome inhibitors has been observed in other cell types like: Chinese hamster ovary (CHO), normal rat kidney cell line (NRK), fibroblasts (L929) and rat Marshall mammary tumour cells (BICR-M1Rk) and in the rat v-myc transformed fetal cardiomyocyte cell line (BWEM) . Moreover, in the BWEM cells [130] and in perfused adult rat heart [131] proteasome and lysosome inhibitors led to similar accumulation of Cx43. In our experiments incubation of endothelial cells with chloroquine did not affect Cx43 level. Since only one lysosome inhibitor was used, and

the incubation time was limited to 4 h, it is difficult to determine any potential involvement of the lysosome in Cx43 degradation in endothelial cells from our data. In general, the results presented here are in accordance with experiments performed in other laboratories. In E36 cells, Cx43 accumulation by ALLN was greater when compared to accumulation by lysosome inhibitors [132] and in rat liver epithelial cells (WB-F344) chloroquine treatment did not affected Cx43.

Until now turnover and degradation of Cx43 are not well understood. Our data seem to support the hypothesis stated by Berthoud et al [133] and Laing et al [130] that domination of one pathway over the other in the Cx43 degradation might be cell type specific. Despite from the lysosome, the results presented in this work show, that in endothelial cells the proteasome pathway is involved in the degradation of Cx43.

A role of the proteasome in Cx43 degradation is also supported by other studies. In 1995 Laing and Beyer [132] using a Chinese hamster ovary cell line expressing a thermolabile E1 enzyme indicated that Cx43 might be ubiquitylated. Later investigations by Leithe et al [134] on rat liver epithelial cells revealed regulation of Cx43 ubiquitination by phosphorylation. They also found that EGF stimulates Cx43 phosphorylation thus its internalization and degradation . These EGF–induced reactions were mediated via the MAPK pathway. The authors further suggested that phosporylation of Cx43 might be a binding signal for the ubiquitin ligase.

One of Leykauf's recent studies on rat liver epithelial cells indeed demonstrated that E3 ligase NEDD4 binds to Cx43 dependent on its phophorylation state, again suggesting that phosphorylation might modulate NEDD4 binding. siRNA experiments against NEDD4 increased accumulation of Cx43 at the plasma membrane. Additionally, it has been observed in epithelial cells that NEDD4 co-localizes with Cx43 in intracellular vesicles as well as at plasma membrane which is consistence with our results [129].

5.5 NEDD4 possible interactions with BAG-3 and hsp-70

Many molecules were found to be NEDD4 targets. Our approach using co-immunoprecipitation and mass spectrometric analysis revealed new possible binding partners. One of the bound molecules was identified as a heat shock cognate 71 kDa protein (heat shock 70 kDa, protein 8), which is involved in a wide range of folding processes as well as in translocation of secretory proteins [135].

The second identified protein was BAG3. BAG3 belongs to a family of co-chaperons and its function was linked with the organization of the cytoskeleton, apoptosis and development as adaptive responses to cellular stress [136]. There is also evidence that BAG 3 may bind to hsp70 and may thus modulate folding of other regulatory proteins [137]. To detect possible interactions of NEDD4 with these two proteins two hybrid system could be used. Additionally, experiments such as immunoprecipitation, knock-down as well as immunostaining should be performed.

5.6 Regulation of NEDD4 and Cx43 expression by mechanical forces

Since this is the first study reporting NEDD4 expression in endothelial cells, as a first step to characterize its expression regulation we decided to investigate any influence of different mechanical loading conditions. Endothelial cells exposed to constant laminar flow for different times and at different shear forces, did not show any significant change in NEDD4 mRNA and protein expression. However, significant increase in NEDD4 mRNA was caused by an atheroprotective flow profile with a mean shear stress 20 dyn/ cm^2, whereas under atheroprone profile expression decreased when compared to constant laminar flow (5,4 dyn/ cm^2). Inhibition of PI3K or of nitric oxide production under shear stress for 4 h and 24 h indicated that these mechanosensitive pathways are not involved in the regulation of NEDD4. In contrast, analysis of the same samples for Cx40 and Has2 expression showed an induction in both when exposed to 6 dyn/ cm^2 for 4 h. Additionally, inhibition of PI3K downregulated Cx40 and Has2 under static and dynamic condition (6 dyn/cm^2) [6, 138]. Unfortunately, up to date there are no data available on the regulation of other HECT E3 ligases by shear stress in endothelial cells.

It has been shown above that NEDD4 binds to Cx43. Since Cx43 is known to be regulated by mechanical forces, we intended to test whether changes in NEDD4 do correspond with Cx43 expression. Our results indicated that Cx43 was not regulated by constant laminar flow up to 10 dyn/cm^2 for 24 h, with the exception of a slight decrease of mRNA at 6 dyn/ cm^2. By contrast, experiments performed by others under laminar flow showed a transient upregulation of Cx43 [139, 140]. These differences might be explained by a publication of Bao et al. His studies showed that Cx43 induction depends on the onset of flow. When (similarly to our experiments) flow was smoothly increased in order to eliminate temporal shear stress gradients, Cx43 expression did not change significantly. Oppositely, step flow increase (which contains a sharp increase and steady flow) as well as impulse flow induced Cx43 [141]. This is in agreement with other results. De Paola et al. in her *in vitro* studies using parallel flow chamber exposed bovine aortic endothelial cells to disturbed flow and observed that changes in Cx43 mRNA and protein expression were mediated by shear stress gradients rather than by shear stress alone. This was explained by the fact that cells located in the downstream area of the coverslip renormalized Cx43 in comparison to those located in the disturbed flow region exposed to highest shear stress gradients. This recovery under laminar flow might be part of an adaptation to the changed hemodynamic environment. Further studies, performed using atheroprone and atheroprotective waveforms, manifested Cx43 upregulation after 24 h under atheroprone profile. Additional Cx43 immunostaining revealed abundant expression in the perinuclear region but not uniform distribution at the cell borders like under static conditions [12, 140]. Similar atypical endothelial Cx43 immunostaining and mRNA upregulation were found in the intima of atherosclerotic lesions in humans and rabbits and, as suggested by authors, might be considered as a marker for dysfunctional Cx43-mediated gap junction intercellular communication [12, 140, 142-145].

Our in vitro studies using the cone and plate system as described, showed no significant regulation of Cx43 mRNA when exposed to atheroprone and atheroprotective flow profiles. Up to date we did not test Cx43 protein expression under these conditions. However, we observed strong NEDD4 induction under conditions of an atheroprotective flow profile and based on the available reports on Cx43 protein regulation by an atheroprotective profile, one may suggest that NEDD4 might cause a decrease of Cx43 protein under these conditions. Conversely, downregulation of NEDD4 by atheroprone profiles may lead to an increase of Cx43.

Experiments performed with the Rotating Wall Vessel revealed that microgravity increased NEDD4 mRNA and protein. So, these results confirmed the previously gene array-based observation of NEDD4 expression being regulated by microgravity [55]. Studies on rat skeletal muscles exposed to hindlimb unloading for 4 days (as an alternative simulation a microgravity) likewise revealed a strong upregulation of NEDD4 [66]. In this case, the increase in NEDD4 was linked to muscle atrophy. Furthermore, this study reported that high expression of NEDD4 caused a downregulation of another target protein - Notch1 - without having an effect on other known substrates (ENaC, IGF1-R, Bcl-10, Eps15, VEGFR-2). Our analysis of NEED4 targets revealed that Cx43 was reduced, whereas IGF1R, PLCgamma1, Eps 15 or Bcl10 did not show any significant regulation by microgravity (data not shown). This and Koncarevic´s results lead to the question whether conditions of mechanical loading or -unloading like microgravity may be responsible for selective turnover of proteins in various cell types. Is it also possible that under microgravity NEDD4 binds different targets in muscle cells than in endothelial cells. In order to answer the first of these questions, few pilot experiments were performed. The whole precipitated lysates from endothelial cells which had been exposed to microgravity for 24 h, 48 h and 72 h were electrophoretically separated on gradient gels and showed that prolonged exposure to microgravity not only affects the amount of precipitated complexes, but also changed the observed protein pattern (data not shown). These preliminary results indicated that there is probably not only more protein bound to NEDD4 but other target proteins may also exist. Therefore, additional investigations should analyse this co-precipitates by mass spectrometry to identify additional putative target proteins of NEDD4. Concerning microgravity more general, our data are in agreement with one of the latest reports by Liu et al. who, using two dimensional electrophoresis revealed the induction of over 187 different proteins after 24 h of microgravity and 24 h restoration, whereas 180 proteins disappeared. After 48 h of microgravity 291 different proteins were induced and 469 proteins disappeared when compared to the “ground” control group [146].

In our investigations, only Cx43 protein, but not mRNA expression was reduced under microgravity. A similar result on loss of Cx43 was observed in the same culturing system after 72 h in NT2 cells [147]. Cx43 decrease as well as irregular distribution has also been reported in rats exposed to simulated microgravity by hind limb suspension[148].

Moreover, it has also been reported that NEDD4 binds to Cx43 in all of its phosphorylation states. Therefore, it is possible that under microgravity NEDD4 binding to Cx43 is affected by higher EGF level. This in turn may lead to the enhanced Cx43 degradation.

Cx43 is a multifunctional protein and its downregulation most likely has a series of consequences for endothelial cell functions. Cx43 builds up gap junctions that are responsible for cell to cell communication and transport of water and ions. Since altered transendothelial transport was already observed in astronauts, it is possible that dysregulation of gap junctions due to the enhanced Cx43 degradation may be involved in this process.

There is also evidence that NEDD4 may directly bind to actin and destabilize the cytoskeleton [71]. Moreover, several reports showed that Cx43 directly interacts with tubulin [79, 80]. Experiments performed *in vivo* on Cx43 knockout animals revealed that in the absence of Cx43 actin stress fibers were not oriented in the direction of cell migration. Furthermore, cells lacking Cx43 were unable to establish proper cell polarity. Studies on human aortic endothelial cells transfected with siRNA against Cx43 showed reduced length of microtubules and incomplete polygonal shape which resulted in reduced angiogenic potential [82]. These observations are in line with Lee´s et al. report who describes that proper polarity is crucial in different steps of angiogenesis starting from polarization of tip cells, through apical-basal polarity of stalk cells and migration of cells, which requires proper orientation of Golgi apparatus and microtubule organizing center [149].
Several investigations on cells exposed to microgravity also showed rearrangements of the cytoskeleton and loss of polarity [150, 151]. Moreover, earlier findings on endothelial cells exposed to microgravity in the Rotating Wall Vessel exhibited their anti-angiogenic phenotype [54].

Taking into account previous results from experiments performed on ground as well as in microgravity, it could be proposed that high NEDD4 and low Cx43 may affect the cytoskeleton as well as cell polarity. This in turn may contribute to the observed phenotype of endothelial cells under microgravity.

In our study we examined whether the degradation of Cx43 under microgravity might be blocked. Unfortunately, it was not possible to design any specific inhibitor because proteins belonging to NEDD4 E3 ligases family share similar structure. Using inhibitors of the proteasome and lysosome at the same concentration as for static cell culture experiments led to cell apoptosis already after 3 h of treatment in the Rotating Wall Vessel.

5.7 ADAMTS1 expression is regulated by mechanical forces

ADAMTS1 belongs to a family of disintegrin and metalloproteinase with thrombospondin motif. ADAMTS1 expression was detected in dermal fibroblasts and at lower levels in vascular smooth muscle cells and in endothelial cells [88, 152]. All measurements done in our group confirmed this very low expression of ADAMTS1 in endothelial cells which were grown without flow. By contrast, experiments using the cone and plate apparatus revealed strong induction of ADAMTS1 by shear stress. This was equally confirmed in two different types of endothelial cells- HUVEC and HCMEC [94, 153]. The increase of ADAMTS1 mRNA in endothelial cells became statistically significant from 2 dyn/cm^2 onwards. In most parts of the human circulation and under physiological conditions shear stress is thought not to fall under this relatively low value. ADAMTS1 protein was likewise upregulated by shear stress. This increase was comparably stronger than the induction of eNOS under the same conditions. ADAMTS1 remained elevated for at least 48 h at 6 dyn/ cm^2 proving that its regulation is not just transient but sustained. To test conditions similar to vessel occlusion, the flow was stopped and the expression of ADAMTS1 decreased, reaching the control level after 24 h. ADAMTS1 mRNA expression was also found to be differentially regulated by oscillatory flows. A somewhat stronger upregulation was caused by an atheroprotective profile than constant laminar flow (5,4 dyn/ cm^2). This might highlight that the acceleration rates of flow profiles affect the expression of endothelial genes in a way that is independent from mean shear stress. Moreover, under atheroprone flow ADAMTS1 expression was similar to static non-flow condition. This may suggest that in atheroprone regions of the vasculature ADAMTS1 is not or less expressed.

Some additional measurements showed the involvement of mechanosensitive pathways in the expression regulation of ADAMTS1. Inhibition of PI3K prevented the

upregulation of ADAMTS1 by shear stress. siRNA used to knockdown FoxO1 slightly increased the expression of ADAMTS1. Since Foxo1 is phosphorylated and activated by Akt (one step down-stream of PI3K), this result may put even more evidence to a role of the PI3K pathway in shear stress-dependent expression regulation of ADAMTS1 [94]. Induction of ADAMTS1 was also blocked by using L-NAME to inhibit nitric oxide production. This result furthermore highlighted the biological importance of the PI3K/Akt/NO pathway in the regulation of ADAMTS1 in endothelial cells.

Transcription factors Early growth response protein 1 (Egr-1) and Elk 1, both activated via the shear stress senstitive MAPK pathway, are well known to regulate the expression of ADAMTS1 [154]. In addition, experiments performed earlier demonstrated that activation of Egr1 and elk1 depends on the activity of PI3K, $NO^{\cdot}$, and PLC [155, 156]. Since the results presented here showed a role of nitric oxide production and PI3K activation in shear stress-dependent induction of ADAMTS1 this suggests that the classical MAPK pathway is also part of a flow-dependent regulation of angioadaptation (and – more specific – angiogenesis).

ADAMTS1 expression was directly correlated with oxygen pressure. Both, no flow or low flow conditions are usually connected with hypoxia in capillary sprouts *in vivo*. Therefore shear stress-dependent expression regulation of ADAMTS1 may be enhanced due to accompanying changes in oxygen pressure. Conversely, it has been reported that in endothelial cells VEGF-A is induced in hypoxia and VEGF-A induced the expression of ADAMTS1 in a PKC-dependent manner [90]. In agreement with our results are experiments performed on fibroblasts (ARPE) as well as chondrosarcoma cells showing no significant increase of ADAMTS1 during hypoxia [157, 158].

Since ADAMTS1 is known to possess anti-angiogenic properties, we tested whether under shear stress ADAMTS1 cleaves TSP1. The results indicated that ADAMTS1 under shear stress effectively cleaved TSP1 to its 70 kDA fragments, accompagnied by a decrease of the 180 kDa form of TSP1. This allowed confirming two different studies. First, the decrease of not-cleaved TSP1 under shear stress had allready been shown before [159]. The downregulation was significant already at 2 dyn/ cm^2 and at higher laminar flow this effect was pronounced. This suppression was maintained for at least 72 h of shear stress (no longer times tested) and reversed after flow within 24 h. Second, among three different anti-angiogenic mechanisms of ADAMTS1 which had been

discussed before [88, 89, 91], our data put more strength to ADAMTS1-dependent cleavage of TSP1 as the anti-angiogenic mechanism involved. Accordingly, conditioned medium from shear stress exposed cells reduced scratch wound closure in a TSP1- and ADAMTS1-dependent manner. The decreased wound closure in cell monolayers is a hallmark of (mainly) slower cell migration and (to a lesser extent) proliferation. Both of these processes play an important role in capillary sprouting. As shown by Hohberg et al.[94] slower scratch wound closure depends on TSP1 and is reduced in experiments using siRNA against ADAMTS1. The effects on delayed wound closure compared to those on cell number in the same culturing system showed that the effects observed in the scratch wound assay are probably caused by inhibition of migration. This is in agreement with previously report by Lee et al. [160]. Their work revealed effects of ADAMTS1 on cell migration during metastasis. The same group showed that TSP1 knockdown increased cell proliferation, which is as well in agreement with Hohberg et al. [94]. Our as well as Xu's observations showed ADAMTS1 knockdown accompanied by a slight increase in proliferation [90]. Interestingly, results obtained in other laboratory found reduced proliferation after TSP1 knockdown [161].

The results obtained on endothelial cell culture led to the conclusion that ADAMTS1 expression is high in regions with high flow, whereas low expression is expected in regions without flow, such as capillary sprouts. Further experiments using intravital microscopy of the rat mesenteric vascular network allowed proving this concept. High expression of ADAMTS1 was observed in the connected blood vessels experiencing relatively high shear stress, whereas non-perfused capillary sprouts were characterized by a substantially lower expression of ADAMTS1 [94]. Because ADAMTS1 has anti-angiogenic properties, its low expression in capillary sprouts may promote angiogenesis and thus maintain the progress of sprouting. Conversely, in blood vessels with high shear stress ADAMTS1 probably contributes to the stabilization of these mature blood vessels. High expression of ADAMTS1, in vessels which are well oxygenized and experiencing high blood flow, may participate in the inhibition of unnecessary sprouting or may favor vessel growth of the splitting type of angiogenesis, as it was recognized in skeletal muscles [15]. Additionally to ADAMTS1, the expression of Ang2 was also investigated. Ang2 demonstrated opposite staining characteristics in comparison to ADAMTS1, showing highest expression in capillary sprouts. This supports earlier experiments performed in our Institute [162]. Presence of Ang2 in capillary sprouts lacking

blood flow probably supports sprouting, whereas Ang2 suppression under flow following the onset of perfusion participates in vessels stabilization.

Interestingly, ADAMTS1 was found to play an important role during invasion of endothelial cells into 3D collagen matrices and both, mRNA and protein, were increased during the first 24 h of cell invasion [163]. In this case ADAMTS1 was found to be associated with the plasma membrane and degradation of collagen [164]. This could be in agreement with our finding that ADAMTS1 is strongly upregulated during the first 24 h of microgravity experiments, because in these experiments the cells were cultured on Cytodex 3 beads covered with collagen and grew in three dimensional space. Similar to the observed downregulation of ADAMTS1 at later time points of microgravity, such a decrease has also been reported in muscles of mice exposed to tail suspension [165]. Low ADAMTS1 expression at combinations of low flow with hypoxia as shown above most probably not occurred in our experiments with simulated microgravity, because cells were well oxygenated in the Rotating Wall Vessel.

Additionally, we also investigated regulation of TSP1 expression under microgravity. This result showed an upregulation of TSP1 after 48 h of exposure. Similar result (137% increase in TSP1 expression) was observed after 5 days on hindlimb unloading in the soleus muscle experiencing capillary regression by Roudier et al [38]. The 1.5 fold increase in TSP1 expression was also demonstrated by gene array studies of the murine osteoblasts exposed to simulated microgravity for 3 days [99].

5.8 Concluding remarks

Capillary regression during muscle atrophy has been observed in several models of microgravity as well as in real space. Since we were interested in studying primary effects of microgravity on endothelial gene expression which may be involved in these changes, we performed experiments with primary isolated human endothelial cells using the Rotating Wall Vessel to simulate microgravity.

To sum up all of our results to a combined conclusion, previously unknown cellular regulation characteristics were demonstrated, contributing to a microgravity-induced anti-angiogenic endothelial phenotype. Although controversies remain in the literature regarding the effects of each of the molecules tested on the growing of new blood vessels, there is a preponderance of pro-angiogenic activity of endothelial Cx43 and of anti-angiogenic effects of ADAMTS1 and TSP1. The increase of NEDD4 and consequently enhanced Cx43 degradation during microgravity thus most probably counteracts angiogenesis, since, for instance, low Cx43 was found to affect cytoskeleton and cell polarity and thus contributes to impaired angiogenesis [166-168]. This effect will even be enhanced by the observed increase in anti-angiogenic molecules ADAMTS1 (at 24 h of microgravity) and TSP1 (at 48 h of microgravity).

This conclusion is supported by the fact, that endothelial cells grown in the Rotating Wall Vessel did not show any capillary tube like structures, when observed under the microscope. By contrast, endothelial cells co-cultured with other cell types started to form tube like structures. For example in co-culture with macrophages capillary like structures were visible after 9 days [169], whereas in experiments with retina cells tube like structures appeared after 18-36 h [170]. These findings may result from angiogenic factors which are secreted by these co-cultured cells into the cell culture medium, and thus turn the angiogenic switch [171-173].

It is well documented, that the regulation of angiogenesis strongly depends on a balance between a variety of pro- and anti-angiogenic signals [39]. Previous investigations suggest that microgravity does not induce a pro-angiogenic phenotype in HUVEC because no increase of angiogenic growth factors such as VEGF-A, FGF and IL-8 was detected. So,

these earlier results are complemented by our experiments and especially by the demonstration of NEDD4-dependent mechanisms.

In addition, each of the investigated genes showed distinct expression patterns in response to different mechanical forces applied. This is in line with previous reports showing that endothelial cells are able to distinguish between different mechanical stimuli and adapt to them by changing their phenotype [12].

5.9 Perspectives

To deal with the limitations of the presented study and the new questions which arose from its results, it should be investigated whether the microgravity-dependent regulation of NEDD4, Cx43, ADAMTS1, and TSP1 observed *in vitro*, does likewise occur in capillaries of atrophied muscles *in vivo* either following space flight or prolong bed rest. Moreover, mechanosensitive signaling pathways involved in the regulation of NEDD4 during microgravity need to be identified. Additional target proteins of NEDD4 in endothelial cells, as they were indicated by some preliminary measurements in our study, are waiting for confirmation and characterization. Further examination should aim at including possible interactions of NEDD4 with the cytoskeleton. With respect to the inhibition of angiogenesis under microgravity, more complete sets of angiogenesis regulating factors should be included in further investigations to give more conclusive results on the “angiogenic switch”. While only very few “favoured” people will ever become astronauts in the near future, a substantial larger number will suffer from atheriosclerosis. Thus, more attention should be given to a possible involvement of NEDD4 in the regulation of Cx43 at atheroprone sites of blood vessels, since Cx40 is supposed to be replaced by Cx43 at these sites, which might then somehow speed up the progress of the disease.

6 List of references

(1) Levy BI, Tedgui A. *Biology of the arterial wall*. Dordrecht [u.a.] : Kluwer Acad. Publ, ©1999.; 1999.

(2) School of Anatomy and Human Biology - The University of Western Australia. Blue Histology - Vascular System. *http://www lab anhb uwa edu au/mb140/CorePages/Vascular/Vascular htm)* 2009.

(3) Michiels C. Endothelial cell functions. *J Cell Physiol* 2003 September;196(3):430-43.

(4) Pries AR, Kuebler WM. Normal endothelium. *Handb Exp Pharmacol* 2006;(176 Pt 1):1-40.

(5) Pries AR, Secomb TW, Gaehtgens P. The endothelial surface layer. *Pflugers Arch* 2000 September;440(5):653-66.

(6) Maroski J, Vorderwulbecke BJ, Fiedorowicz K, Da Silva-Azevedo L, Siegel G, Marki A, Pries AR, Zakrzewicz A. Shear stress increases endothelial hyaluronan synthase 2 and hyaluronan synthesis especially in regard to an atheroprotective flow profile. *Exp Physiol* 2011 September;96(9):977-86.

(7) Papaioannou TG, Stefanadis C. Vascular wall shear stress: basic principles and methods. *Hellenic J Cardiol* 2005 January;46(1):9-15.

(8) Jones EA, le NF, Eichmann A. What determines blood vessel structure? Genetic prespecification vs. hemodynamics. *Physiology (Bethesda)* 2006 December;21:388-95.

(9) Chatzizisis YS, Coskun AU, Jonas M, Edelman ER, Feldman CL, Stone PH. Role of endothelial shear stress in the natural history of coronary atherosclerosis and vascular remodeling: molecular, cellular, and vascular behavior. *J Am Coll Cardiol* 2007 June 26;49(25):2379-93.

(10) Styp-Rekowska B, Hlushchuk R, Pries AR, Djonov V. Intussusceptive angiogenesis: pillars against the blood flow. *Acta Physiol (Oxf)* 2011 July;202(3):213-23.

(11) Garcia-Cardena G, Comander J, Anderson KR, Blackman BR, Gimbrone MA, Jr. Biomechanical activation of vascular endothelium as a determinant of its functional phenotype. *Proc Natl Acad Sci U S A* 2001 April 10;98(8):4478-85.

(12) Dai G, Kaazempur-Mofrad MR, Natarajan S, Zhang Y, Vaughn S, Blackman BR, Kamm RD, Garcia-Cardena G, Gimbrone MA, Jr. Distinct endothelial phenotypes evoked by arterial waveforms derived from atherosclerosis-susceptible and -resistant regions of human vasculature. *Proc Natl Acad Sci U S A* 2004 October 12;101(41):14871-6.

(13) Pries AR, Reglin B, Secomb TW. Remodeling of blood vessels: responses of diameter and wall thickness to hemodynamic and metabolic stimuli. *Hypertension* 2005 October;46(4):725-31.

(14) Pries AR, Secomb TW. Modeling structural adaptation of microcirculation. *Microcirculation* 2008 November;15(8):753-64.

(15) Hudlicka O, Brown MD. Adaptation of skeletal muscle microvasculature to increased or decreased blood flow: role of shear stress, nitric oxide and vascular endothelial growth factor. *J Vasc Res* 2009;46(5):504-12.

(16) Ferrara N. VEGF-A: a critical regulator of blood vessel growth. *Eur Cytokine Netw* 2009 December;20(4):158-63.

(17) Prior BM, Yang HT, Terjung RL. What makes vessels grow with exercise training? *J Appl Physiol* 2004 September;97(3):1119-28.

(18) Burri PH, Hlushchuk R, Djonov V. Intussusceptive angiogenesis: its emergence, its characteristics, and its significance. *Dev Dyn* 2004 November;231(3):474-88.

(19) Caduff JH, Fischer LC, Burri PH. Scanning electron microscope study of the developing microvasculature in the postnatal rat lung. *Anat Rec* 1986 October;216(2):154-64.

(20) Kurz H, Burri PH, Djonov VG. Angiogenesis and vascular remodeling by intussusception: from form to function. *News Physiol Sci* 2003 April;18:65-70.

(21) Williams DR. The biomedical challenges of space flight. *Annu Rev Med* 2003;54:245-56.

(22) Kirsch K, Gunga H-C. Current aspects of microgravity research. *A world without microgravity*. 2001. p. 35-110.

(23) Hamilton DR, Murray JD, Kapoor D, Kirkpatrick AW. Cardiac health for astronauts: current selection standards and their limitations. *Aviat Space Environ Med* 2005 July;76(7):615-26.

(24) Barratt Michael, Pool Sam. Principle of clinical medicine for space flight. 2008.

(25) Booze CF, Stags CM. A comparison of postmortem coronary atherosclerosis findings in general aviation pilot fatalities. *Aviat Space Environ Med* 1987;58:297-300.

(26) Pettyjohn FS, McMeekin RR. Coronary artery disease and preventive cardiology in aviation medicine. *Aviat Space Environ Med* 1975;46(10):1299-304.

(27) Bennett BS, Stein F, Kassam MS, Dunphy PT, Johnston KW. Cerebral blood flow velocities by transcranial Doppler during parabolic flight. *Journal of Clinical Pharmacology* 1999;915-9.

(28) Buckland D. Hemodynamics and Free Radical Production in High Gravity Shifts in the Human Cardiovascular System. 2003. Report No.: Georgia Tech Biomedical Microgravity Research Team.

(29) Zhang LF. Vascular adaptation to microgravity: what have we learned? *J Appl Physiol* 2001 December;91(6):2415-30.

(30) Mao QW, Zhang LF, Ma J. Differential remodeling changes of medium-sized arteries from different body parts in tail-suspended rats and their reversibility. *Space Med MedicalEng* 1999;12:92-6.

(31) Zhang LN, Zhang LF, Ma J. Simulated microgravity enhances vasoconstrictor responsiveness of rat basilar artery. *J Appl Physiol* 2001 June;90(6):2296-305.

(32) Schrage WG, Woodman CR, Laughlin MH. Hindlimb unweighting alters endothelium-dependent vasodilation and ecNOS expression in soleus arterioles. *J Appl Physiol* 2000 October;89(4):1483-90.

(33) Desplanches D, Favier R, Sempore B, Hoppeler H. Whole body and muscle respiratory capacity with dobutamine and hindlimb suspension. *J Appl Physiol* 1991 December;71(6):2419-24.

(34) Delp MD, Colleran PN, Wilkerson MK, McCurdy MR, Muller-Delp J. Structural and functional remodeling of skeletal muscle microvasculature is induced by simulated microgravity. *Am J Physiol Heart Circ Physiol* 2000 June;278(6):H1866-H1873.

(35) Kano Y, Shimegi S, Takahashi H, Masuda K, Katsuta S. Changes in capillary luminal diameter in rat soleus muscle after hind-limb suspension. *Acta Physiol Scand* 2000 August;169(4):271-6.

(36) Dapp C, Schmutz S, Hoppeler H, Fluck M. Transcriptional reprogramming and ultrastructure during atrophy and recovery of mouse soleus muscle. *Physiol Genomics* 2004 December 15;20(1):97-107.

(37) Wagatsuma A. Effect of hindlimb unweighting on expression of hypoxia-inducible factor-1alpha vascular endothelial growth factor, angiopoietin, and their receptors in mouse skeletal muscle. *Physiol Res* 2008;57(4):613-20.

(38) Roudier E, Gineste C, Wazna A, Dehghan K, Desplanches D, Birot O. Angio-adaptation in unloaded skeletal muscle: new insights into an early and muscle type-specific dynamic process. *J Physiol* 2010 November 15;588(Pt 22):4579-91.

(39) Folkman J. Angiogenesis in cancer, vascular, rheumatoid and other disease. *Nat Med* 1995 January;1(1):27-31.

(40) Garret WE, Kirkendal DT. *Exercise and sport science*. 2000.

(41) Davies PF. Flow-mediated endothelial mechanotransduction. *Physiol Rev* 1995 July;75(3):519-60.

(42) Braddock M, Schwachtgen JL, Houston P, Dickson MC, Lee MJ, Campbell CJ. Fluid Shear Stress Modulation of Gene Expression in Endothelial Cells. *News Physiol Sci* 1998 October;13:241-6.

(43) Alenghat FJ, Ingber DE. Mechanotransduction: all signals point to cytoskeleton, matrix, and integrins. *Sci STKE* 2002 February 12;2002(119):e6.

(44) Lan Q, Mercurius KO, Davies PF. Stimulation of transcription factors NF kappa B and AP1 in endothelial cells subjected to shear stress. *Biochem Biophys Res Commun* 1994 June 15;201(2):950-6.

(45) Resnick N, Gimbrone MA, Jr. Hemodynamic forces are complex regulators of endothelial gene expression. *FASEB J* 1995 July;9(10):874-82.

(46) Khachigian LM, Resnick N, Gimbrone MA, Jr., Collins T. Nuclear factor-kappa B interacts functionally with the platelet-derived growth factor B-chain shear-stress response element in vascular endothelial cells exposed to fluid shear stress. *J Clin Invest* 1995 August;96(2):1169-75.

(47) Hunt BJ, Poston L, Schachter M, Halliday A. *An Introduction to Vascular Biology: From Basic Science to Clinical Practice*. Cambridge University Press; 2002.

(48) Buravkova L, Romanov Y, Rykova M, Grigorieva O, Merzlikina N. Cell-to-cell interactions in changed gravity: ground-based and flight experiments. *Acta Astronaut* 2005;57(2-8).

(49) Infanger M, Kossmehl P, Shakibaei M, Baatout S, Witzing A, Grosse J, Bauer J, Cogoli A, Faramarzi S, Derradji H, Neefs M, Paul M, Grimm D. Induction of three-dimensional assembly and increase in apoptosis of human endothelial cells by simulated microgravity: impact of vascular endothelial growth factor. *Apoptosis* 2006 May;11(5):749-64.

(50) Cotrupi S, Ranzani D, Maier JA. Impact of modeled microgravity on microvascular endothelial cells. *Biochim Biophys Acta* 2005 December 15;1746(2):163-8.

(51) Mariotti M, Maier JA. Gravitational unloading induces an anti-angiogenic phenotype in human microvascular endothelial cells. *J Cell Biochem* 2008 May 1;104(1):129-35.

(52) Carlsson SI, Bertilaccio MT, Ballabio E, Maier JA. Endothelial stress by gravitational unloading: effects on cell growth and cytoskeletal organization. *Biochim Biophys Acta* 2003 October 21;1642(3):173-9.

(53) Griffoni C, Di MS, Fantozzi L, Zanetti C, Pippia P, Tomasi V, Spisni E. Modification of proteins secreted by endothelial cells during modeled low gravity exposure. *J Cell Biochem* 2011 January;112(1):265-72.

(54) Carlsson SI, Bertilaccio MT, Ascari I, Bradamante S, Maier JA. Modulation of human endothelial cell behaviour in simulated microgravity. *J Gravit Physiol* 2002 July;9(1):273-4.

(55) Hammond TG, Benes E, O'Reilly KC, Wolf DA, Linnehan RM, Taher A, Kaysen JH, Allen PL, Goodwin TJ. Mechanical culture conditions effect gene expression: gravity-induced changes on the space shuttle. *Physiol Genomics* 2000 September 8;3(3):163-73.

(56) McCormick SM, Eskin SG, McIntire LV, Teng CL, Lu CM, Russell CG, Chittur KK. DNA microarray reveals changes in gene expression of shear stressed human umbilical vein endothelial cells. *Proc Natl Acad Sci U S A* 2001 July 31;98(16):8955-60.

(57) Topper JN, Cai J, Falb D, Gimbrone MA, Jr. Identification of vascular endothelial genes differentially responsive to fluid mechanical stimuli: cyclooxygenase-2, manganese superoxide dismutase, and endothelial cell nitric oxide synthase are selectively up-regulated by steady laminar shear stress. *Proc Natl Acad Sci U S A* 1996 September 17;93(19):10417-22.

(58) Malek AM, Jackman R, Rosenberg RD, Izumo S. Endothelial expression of thrombomodulin is reversibly regulated by fluid shear stress. *Circ Res* 1994 May;74(5):852-60.

(59) Lin MC, mus-Jacobs F, Chen HH, Parry GC, Mackman N, Shyy JY, Chien S. Shear stress induction of the tissue factor gene. *J Clin Invest* 1997 February 15;99(4):737-44.

(60) Bongrazio M, Baumann C, Zakrzewicz A, Pries AR, Gaehtgens P. Evidence for modulation of genes involved in vascular adaptation by prolonged exposure of endothelial cells to shear stress. *Cardiovasc Res* 2000 August;47(2):384-93.

(61) Ingham RJ, Gish G, Pawson T. The Nedd4 family of E3 ubiquitin ligases: functional diversity within a common modular architecture. *Oncogene* 2004;23(11).

(62) Glickman MH, Ciechanover A. The ubiquitin-proteasome proteolytic pathway: destruction for the sake of construction. *Physiol Rev* 2002 April;82(2):373-428.

(63) Anan T, Nagata Y, Koga H, Honda Y, Yabuki N, Miyamoto C, Kuwano A, Matsuda I, Endo F, Saya H, Nakao M. Human ubiquitin-protein ligase Nedd4: expression, subcellular localization and selective interaction with ubiquitin-conjugating enzymes. *Genes Cells* 1998;3(11).

(64) Harvey KF, Kumar S. Nedd4-like proteins: an emerging family of ubiquitin-protein ligases implicated in diverse cellular functions. *Trends Cell Biol* 1999;9(5).

(65) Fouladkou F, Lu C, Jiang C, Zhou L, She Y, Walls JR, Kawabe H, Brose N, Henkelman RM, Huang A, Bruneau BG, Rotin D. The ubiquitin ligase Nedd4-1 is required for heart development and is a suppressor of thrombospondin-1. *J Biol Chem* 2010 February 26;285(9):6770-80.

(66) Koncarevic A, Jackman RW, Kandarian SC. The ubiquitin-protein ligase Nedd4 targets Notch1 in skeletal muscle and distinguishes the subset of atrophies caused by reduced muscle tension. *Faseb J* 2007;21(2).

(67) Staub O, Dho S, Henry P, Correa J, Ishikawa T, McGlade J, Rotin D. WW domains of Nedd4 bind to the proline-rich PY motifs in the epithelial Na+ channel deleted in Liddle's syndrome. *Embo J* 1996;15(10).

(68) Staub O, Gautschi I, Ishikawa T, Breitschopf K, Ciechanover A, Schild L, Rotin D. Regulation of stability and function of the epithelial Na+ channel (ENaC) by ubiquitination. *Embo J* 1997;16(21).

(69) Zhou R, Patel SV, Snyder PM. Nedd4-2 catalyzes ubiquitination and degradation of cell surface ENaC. *J Biol Chem* 2007 July 13;282(28):20207-12.

(70) Murdaca J, Treins C, Monthouel-Kartmann MN, Pontier-Bres R, Kumar S, Van OE, Giorgetti-Peraldi S. Grb10 prevents Nedd4-mediated vascular endothelial growth factor receptor-2 degradation. *J Biol Chem* 2004 June 18;279(25):26754-61.

(71) Stawiecka-Mirota M, Kaminska J, Urban-Grimal D, Haines DS, Zoladek T. Nedd4, a human ubiquitin ligase, affects actin cytoskeleton in yeast cells. *Exp Cell Res* 2008 November 1;314(18):3318-25.

(72) Ubiquitin protein ligase Nedd4 binds to connexin43 by a phosphorylation-modulated process 2006.

(73) Contreras JE, Sanchez HA, Eugenin EA, Speidel D, Theis M, Willecke K, Bukauskas FF, Bennett MV, Saez JC. Metabolic inhibition induces opening of unapposed connexin 43 gap junction hemichannels and reduces gap junctional communication in cortical astrocytes in culture. *Proc Natl Acad Sci U S A* 2002 January 8;99(1):495-500.

(74) Wei CJ, Francis R, Xu X, Lo CW. Connexin43 associated with an N-cadherin-containing multiprotein complex is required for gap junction formation in NIH3T3 cells. *J Biol Chem* 2005 May 20;280(20):19925-36.

(75) Xu X, Li WE, Huang GY, Meyer R, Chen T, Luo Y, Thomas MP, Radice GL, Lo CW. Modulation of mouse neural crest cell motility by N-cadherin and connexin 43 gap junctions. *J Cell Biol* 2001 July 9;154(1):217-30.

(76) Shaw RM, Fay AJ, Puthenveedu MA, von ZM, Jan YN, Jan LY. Microtubule plus-end-tracking proteins target gap junctions directly from the cell interior to adherens junctions. *Cell* 2007 February 9;128(3):547-60.

(77) Xu X, Francis R, Wei CJ, Linask KL, Lo CW. Connexin 43-mediated modulation of polarized cell movement and the directional migration of cardiac neural crest cells. *Development* 2006 September;133(18):3629-39.

(78) Taliana L, Benezra M, Greenberg RS, Masur SK, Bernstein AM. ZO-1: lamellipodial localization in a corneal fibroblast wound model. *Invest Ophthalmol Vis Sci* 2005 January;46(1):96-103.

(79) Giepmans BN, Verlaan I, Hengeveld T, Janssen H, Calafat J, Falk MM, Moolenaar WH. Gap junction protein connexin-43 interacts directly with microtubules. *Curr Biol* 2001 September 4;11(17):1364-8.

(80) Giepmans BN, Verlaan I, Moolenaar WH. Connexin-43 interactions with ZO-1 and alpha- and beta-tubulin. *Cell Commun Adhes* 2001;8(4-6):219-23.

(81) Rhee DY, Zhao XQ, Francis RJ, Huang GY, Mably JD, Lo CW. Connexin 43 regulates epicardial cell polarity and migration in coronary vascular development. *Development* 2009 September;136(18):3185-93.

(82) Wang HH, Kung CI, Tseng YY, Lin YC, Chen CH, Tsai CH, Yeh HI. Activation of endothelial cells to pathological status by down-regulation of connexin43. *Cardiovasc Res* 2008 August 1;79(3):509-18.

(83) Tang DG, Conti CJ. Endothelial cell development, vasculogenesis, angiogenesis, and tumor neovascularization: an update. *Semin Thromb Hemost* 2004;30(1).

(84) Rodriguez-Manzaneque JC, Milchanowski AB, Dufour EK, Leduc R, Iruela-Arispe ML. Characterization of METH-1/ADAMTS1 processing reveals two distinct active forms. *J Biol Chem* 2000 October 27;275(43):33471-9.

(85) Mittaz L, Ricardo S, Martinez G, Kola I, Kelly DJ, Little MH, Hertzog PJ, Pritchard MA. Neonatal calyceal dilation and renal fibrosis resulting from loss of Adamts-1 in mouse kidney is due to a developmental dysgenesis. *Nephrol Dial Transplant* 2005 February;20(2):419-23.

(86) Shindo T, Kurihara H, Kuno K, Yokoyama H, Wada T, Kurihara Y, Imai T, Wang Y, Ogata M, Nishimatsu H, Moriyama N, Oh-hashi Y, Morita H, Ishikawa T, Nagai R, Yazaki Y, Matsushima K. ADAMTS-1: a metalloproteinase-disintegrin essential for normal growth, fertility, and organ morphology and function. *J Clin Invest* 2000 May;105(10):1345-52.

(87) Jonsson-Rylander AC, Nilsson T, Fritsche-Danielson R, Hammarstrom A, Behrendt M, Andersson JO, Lindgren K, Andersson AK, Wallbrandt P, Rosengren B, Brodin P, Thelin A, Westin A, Hurt-Camejo E, Lee-Sogaard CH. Role of ADAMTS-1 in atherosclerosis: remodeling of carotid artery, immunohistochemistry, and proteolysis of versican. *Arterioscler Thromb Vasc Biol* 2005 January;25(1):180-5.

(88) Vazquez F, Hastings G, Ortega MA, Lane TF, Oikemus S, Lombardo M, Iruela-Arispe ML. METH-1, a human ortholog of ADAMTS-1, and METH-2 are members of a new family of proteins with angio-inhibitory activity. *J Biol Chem* 1999 August 13;274(33):23349-57.

(89) Iruela-Arispe ML, Carpizo D, Luque A. ADAMTS1: a matrix metalloprotease with angioinhibitory properties. *Ann N Y Acad Sci* 2003 May;995:183-90.

(90) Xu Z, Yu Y, Duh EJ. Vascular endothelial growth factor upregulates expression of ADAMTS1 in endothelial cells through protein kinase C signaling. *Invest Ophthalmol VisSci* 2006;47:4059-66.

(91) Lee NV, Sato M, Annis DS, Loo JA, Wu L, Mosher DF, Iruela-Arispe ML. ADAMTS1 mediates the release of antiangiogenic polypeptides from TSP1 and 2. *EMBO J* 2006 November 15;25(22):5270-83.

(92) Krampert M, Kuenzle S, Thai SN, Lee N, Iruela-Arispe ML, Werner S. ADAMTS1 proteinase is up-regulated in wounded skin and regulates migration of fibroblasts and endothelial cells. *J Biol Chem* 2005 June 24;280(25):23844-52.

(93) Skalak TC, Price RJ. The role of mechanical stresses in microvascular remodeling. *Microcirculation* 1996 June;3(2):143-65.

(94) Hohberg M, Knochel J, Hoffmann CJ, Chlench S, Wunderlich W, Alter A, Maroski J, Vorderwulbecke BJ, Da Silva-Azevedo L, Knudsen R, Lehmann R, Fiedorowicz K, Bongrazio M, Nitsche B, Hoepfner M, Styp-Rekowska B, Pries AR, Zakrzewicz A. Expression of ADAMTS1 in endothelial cells is induced by shear stress and suppressed in sprouting capillaries. *J Cell Physiol* 2011 February;226(2):350-61.

(95) Doyle KM, Russell DL, Sriraman V, Richards JS. Coordinate transcription of the ADAMTS-1 gene by luteinizing hormone and progesterone receptor. *Mol Endocrinol* 2004 October;18(10):2463-78.

(96) Chien S, Shyy JY. Effects of hemodynamic forces on gene expression and signal transduction in endothelial cells. *Biol Bull* 1998 June;194(3):390-1.

(97) Bussolari SR, Dewey CF, Jr., Gimbrone MA, Jr. Apparatus for subjecting living cells to fluid shear stress. *Rev Sci Instrum* 1982 December;53(12):1851-4.

(98) Lehoux S, Tedgui A. Cellular mechanics and gene expression in blood vessels. *J Biomech* 2003 May;36(5):631-43.

(99) Pardo SJ, Patel MJ, Sykes MC, Platt MO, Boyd NL, Sorescu GP, Xu M, van Loon JJ, Wang MD, Jo H. Simulated microgravity using the Random Positioning Machine inhibits differentiation and alters gene expression profiles of 2T3 preosteoblasts. *Am J Physiol Cell Physiol* 2005 June;288(6):C1211-C1221.

(100) Guidi A, Dubini G, Tominetti F, Raimondi M. A mechanobiologic research in a microgravity environment bioreactor. American Institute of Aeronautics and Astronomics; 2002.

(101) Gao H, Ayyaswamy PS, Ducheyne P. Dynamics of a microcarrier particle in the simulated microgravity environment of a rotating-wall vessel. *Microgravity Sci Technol* 1997;10(3):154-65.

(102) Ayyaswamy PS, Mukundakrishnan K. Optimal condition for simulating microgravity employing NASA designed rotating wall vessel. *Acta Astronautica* 2007;60:397-405.

(103) Botchwey EA, Pollack SR, Levine EM, Johnston ED, Laurencin CT. Quantitative analysis of three-dimensional fluid flow in rotating bioreactors for tissue engineering. *J Biomed Mater Res A* 2004 May 1;69(2):205-15.

(104) Hammond TG, Hammond JM. Optimized suspension culture: the rotating-wall vessel. *Am J Physiol Renal Physiol* 2001 July;281(1):F12-F25.

(105) Pollack SR, Meaney DF, Levine EM, Litt M, Johnston ED. Numerical model and experimental validation of microcarrier motion in a rotating bioreactor. *Tissue Eng* 2000 October;6(5):519-30.

(106) Edgell CJ, McDonald CC, Graham JB. Permanent cell line expressing human factor VIII-related antigen established by hybridization. *Proc Natl Acad Sci U S A* 1983 June;80(12):3734-7.

(107) King J, Laemmli UK. Polypeptides of the tail fibres of bacteriophage T4. *J Mol Biol* 1971 December 28;62(3):465-77.

(108) Alter A, Schmiedeck D, Fussnegger MR, Pries AR, Freesmeyer WB, Zakrzewicz A. Angiopoietin-1, but not platelet-derived growth factor-AB, is a cooperative stimulator of vascular endothelial growth factor A-accelerated endothelial cell scratch closure. *Ann Vasc Surg* 2009 March;23(2):239-45.

(109) Chun TH, Itoh H, Ogawa Y. Shear stress augments expression of C-type natriuretic peptide and adrenomedullin. *Hypertension* 1997;29:1296-302.

(110) Malek A, Izumo S. Physiological fluid shear stress causes downregulation of endothelin-1 mRNA in bovine aortic endothelium. *Am J Physiol* 1992 August;263(2 Pt 1):C389-C396.

(111) Parmar KM, Larman HB, Dai G, Zhang Y, Wang ET, Moorthy SN, Kratz JR, Lin Z, Jain MK, Gimbrone MA, Jr., Garcia-Cardena G. Integration of flow-dependent endothelial phenotypes by Kruppel-like factor 2. *J Clin Invest* 2006 January;116(1):49-58.

(112) Dekker RJ, van SS, Fontijn RD, Salamanca S, de Groot PG, VanBavel E, Pannekoek H, Horrevoets AJ. Prolonged fluid shear stress induces a distinct set of endothelial cell genes, most specifically lung Kruppel-like factor (KLF2). *Blood* 2002 September 1;100(5):1689-98.

(113) Wang N, Miao H, Li YS, Zhang P, Haga JH, Hu Y, Young A, Yuan S, Nguyen P, Wu CC, Chien S. Shear stress regulation of Kruppel-like factor 2 expression is flow pattern-specific. *Biochem Biophys Res Commun* 2006 March 24;341(4):1244-51.

(114) Dai G, Vaughn S, Zhang Y, Wang ET, Garcia-Cardena G, Gimbrone MA, Jr. Biomechanical forces in atherosclerosis-resistant vascular regions regulate

endothelial redox balance via phosphoinositol 3-kinase/Akt-dependent activation of Nrf2. *Circ Res* 2007 September 28;101(7):723-33.

(115) Okahara K, Sun B, Kambayashi J. Upregulation of prostacyclin synthesis-related gene expression by shear stress in vascular endothelial cells. *Arterioscler Thromb Vasc Biol* 1998 December;18(12):1922-6.

(116) Hoson T, Kamisaka S, Masuda Y, Yamashita M, Buchen B. Evaluation of the three-dimensional clinostat as a simulator of weightlessness. *Planta* 1997;203 Suppl:S187-S197.

(117) Schwarz RP, Goodwin TJ, Wolf DA. Cell culture for three-dimensional modeling in rotating-wall vessels: an application of simulated microgravity. *J Tissue Cult Methods* 1992;14(2):51-7.

(118) Grimm D, Infanger M, Westphal K, Ulbrich C, Pietsch J, Kossmehl P, Vadrucci S, Baatout S, Flick B, Paul M, Bauer J. A delayed type of three-dimensional growth of human endothelial cells under simulated weightlessness. *Tissue Eng Part A* 2009 August;15(8):2267-75.

(119) Infanger M, Kossmehl P, Shakibaei M, Bauer J, Kossmehl-Zorn S, Cogoli A, Curcio F, Oksche A, Wehland M, Kreutz R, Paul M, Grimm D. Simulated weightlessness changes the cytoskeleton and extracellular matrix proteins in papillary thyroid carcinoma cells. *Cell Tissue Res* 2006 May;324(2):267-77.

(120) Bradamante S, Barenghi L, Versari S, Villa A. From hypergravity to microgravity: Choosing the suitable simulator. *Microgravity Science and Technology* 2006;18(3-4):250-3.

(121) Villa A, Versari S, Maier JA, Bradamante S. Cell behavior in simulated microgravity: a comparison of results obtained with RWV and RPM. *Gravit Space Biol Bull* 2005 June;18(2):89-90.

(122) Qi F, Dai D, Liu Y, Kaleem I, Li C. Effects of low-shear modeled microgravity on the characterization of recombinant beta-D-glucuronidase expressed in Pichia pastoris. *Appl Biochem Biotechnol* 2011 January;163(1):162-72.

(123) Yeatts AB, Fisher JP. Bone tissue engineering bioreactors: dynamic culture and the influence of shear stress. *Bone* 2011 February;48(2):171-81.

(124) Rezvan A, Troop EM, Jain H, Simons DM, Morris DS, Allen FD, Lelkes P. DIifferential gene expression in endothelila cells: fluid shear stress stimulated vs. Rotating Wall Vessel cultured. 2003 p. 0537.

(125) Unsworth BR, Lelkes PI. Growing tissues in microgravity. *Nat Med* 1998 August;4(8):901-7.

(126) Sanford GL, Ellerson D, Melhado-Gardner C, Sroufe AE, Harris-Hooker S. Three-dimensional growth of endothelial cells in the microgravity-based rotating wall vessel bioreactor. *In Vitro Cell Dev Biol Anim* 2002 October;38(9):493-504.

(127) Chen C, Matesic LE. The Nedd4-like family of E3 ubiquitin ligases and cancer. *Cancer Metastasis Rev* 2007;26(3-4).

(128) Pham N, Rotin D. Nedd4 regulates ubiquitination and stability of the guanine-nucleotide exchange factor CNrasGEF. *J Biol Chem* 2001 December 14;276(50):46995-7003.

(129) Leykauf K, Salek M, Bomke J, Frech M, Lehmann WD, Durst M, Alonso A. Ubiquitin protein ligase Nedd4 binds to connexin43 by a phosphorylation-modulated process. *J Cell Sci* 2006;119(Pt 17).

(130) Laing JG, Tadros PN, Westphale EM, Beyer EC. Degradation of connexin43 gap junctions involves both the proteasome and the lysosome. *Exp Cell Res* 1997 November 1;236(2):482-92.

(131) Beardslee MA, Laing JG, Beyer EC, Saffitz JE. Rapid turnover of connexin43 in the adult rat heart. *Circ Res* 1998 September 21;83(6):629-35.

(132) Laing JG, Beyer EC. The gap junction protein connexin43 is degraded via the ubiquitin proteasome pathway. *J Biol Chem* 1995 November 3;270(44):26399-403.

(133) Berthoud VM, Minogue PJ, Laing JG, Beyer EC. Pathways for degradation of connexins and gap junctions. *Cardiovasc Res* 2004 May 1;62(2):256-67.

(134) Leithe E, Rivedal E. Epidermal growth factor regulates ubiquitination, internalization and proteasome-dependent degradation of connexin43. *J Cell Sci* 2004 March 1;117(Pt 7):1211-20.

(135) Mayer MP, Bukau B. Hsp70 chaperones:Cellular functions and molecular mechanism. *CMLS Cellular and Molecular Life Sciences* 2005;62:670-84.

(136) Iwasaki M, Tanaka R, Hishiya A, Homma S, Reed JC, Takayama S. BAG3 directly associates with guanine nucleotide exchange factor of Rap1, PDZGEF2, and regulates cell adhesion. *Biochem Biophys Res Commun* 2010 September 24;400(3):413-8.

(137) Rosati A, Graziano V, De L, V, Pascale M, Turco MC. BAG3: a multifaceted protein that regulates major cell pathways. *Cell Death Dis* 2011;2:e141.

(138) Vorderwulbecke BJ, Maroski J, Fiedorowicz K, Da Silva-Azevedo L, Marki A, Pries AR, Zakrzewicz A. Regulation of endothelial Connexin-40 expression by shear stress. *Am J Physiol Heart Circ Physiol* 2011 October 21.

(139) Cowan DB, Lye SJ, Langille BL. Regulation of vascular connexin43 gene expression by mechanical loads. *Circ Res* 1998 April 20;82(7):786-93.

(140) Depaola N, Davies PF, Pritchard WF, Jr., Florez L, Harbeck N, Polacek DC. Spatial and temporal regulation of gap junction connexin43 in vascular endothelial cells exposed to controlled disturbed flows in vitro. *Proc Natl Acad Sci U S A* 1999 March 16;96(6):3154-9.

(141) Bao X, Clark CB, Frangos JA. Temporal gradient in shear-induced signaling pathway: involvement of MAP kinase, c-fos, and connexin43. *Am J Physiol Heart Circ Physiol* 2000 May;278(5):H1598-H1605.

(142) Davies PF, Shi C, Depaola N, Helmke BP, Polacek DC. Hemodynamics and the focal origin of atherosclerosis: a spatial approach to endothelial structure, gene expression, and function. *Ann N Y Acad Sci* 2001 December;947:7-16.

(143) Gabriels JE, Paul DL. Connexin43 is highly localized to sites of disturbed flow in rat aortic endothelium but connexin37 and connexin40 are more uniformly distributed. *Circ Res* 1998 September 21;83(6):636-43.

(144) Kwak BR, Mulhaupt F, Veillard N, Gros DB, Mach F. Altered pattern of vascular connexin expression in atherosclerotic plaques. *Arterioscler Thromb Vasc Biol* 2002 February 1;22(2):225-30.

(145) Polacek D, Bech F, McKinsey JF, Davies PF. Connexin43 gene expression in the rabbit arterial wall: effects of hypercholesterolemia, balloon injury and their combination. *J Vasc Res* 1997 January;34(1):19-30.

(146) Liu M. Biological effects of simulated microgravity on human umbilical vein endothelial cell line HUVEC-C. Cheng Z, Liang S, Sun Y, editors. 37th COSPAR Scientific Assembly.Held 13-20 July 2008, in Montréal, Canada., p.1803 . 2008.
Ref Type: Generic

(147) Shamekh R, Cameron DF, Willing AE, Saporta S. The role of connexins in the differentiation of NT2 cells in Sertoli-NT2 cell tissue constructs grown in the rotating wall bioreactor. *Exp Brain Res* 2006 April;170(2):277-84.

(148) Liu ZX, Ma TM, Yang HH, Wu DW, Wang DS, Zhang SJ. [Impact of simulated microgravity on the expression and distribution of cardiac gap junction protein CX43]. *Space Med Med Eng (Beijing)* 2003 December;16(6):448-51.

(149) Lee CY, Bautch VL. Ups and downs of guided vessel sprouting: the role of polarity. *Physiology (Bethesda)* 2011 October;26(5):326-33.

(150) Mulholland J, Jackson KJ, Turner D. Development of suspension cultures for the study of epithelial cell polarity. *Remote Sensing Reviews* 1994;8(1-3 NASA Innovative Research Program):261-9.

(151) Nguyen B, Gabrion J, Herbute S, Oliver J, Maurel D, Davet J, Clavel B, Gharib C, Fareh J, Fagette S. Choroidal responses in microgravity. (SLS-1, SLS-2 and hindlimb suspension experiments). *Acta Astronautica* 1995;36(8-12):439-48.

(152) Glienke J, Schmitt AO, Pilarsky C, Hinzmann B, Weiss B, Rosenthal A, Thierauch KH. Differential gene expression by endothelial cells in distinct angiogenic states. *Eur J Biochem* 2000 May;267(9):2820-30.

(153) Bongrazio M, Pries AR, Zakrzewicz A. The endothelium as physiological source of properdin: role of wall shear stress. *Mol Immunol* 2003 January;39(11):669-75.

(154) Schwachtgen JL, Houston P, Campbell C, Sukhatme V, Braddock M. Fluid shear stress activation of egr-1 transcription in cultured human endothelial and epithelial cells is mediated via the extracellular signal-related kinase 1/2 mitogen-activated protein kinase pathway. *J Clin Invest* 1998 June 1;101(11):2540-9.

(155) Deora AA, Hajjar DP, Lander HM. Recruitment and activation of Raf-1 kinase by nitric oxide-activated Ras. *Biochemistry* 2000 August 15;39(32):9901-8.

(156) Ishida T, Takahashi M, Corson MA, Berk BC. Fluid shear stress-mediated signal transduction: how do endothelial cells transduce mechanical force into biological responses? *Ann N Y Acad Sci* 1997 April 15;811:12-23.

(157) Hatipoglu OF, Hirohata S, Cilek MZ, Ogawa H, Miyoshi T, Obika M, Demircan K, Shinohata R, Kusachi S, Ninomiya Y. ADAMTS1 is a unique hypoxic early response gene expressed by endothelial cells. *J Biol Chem* 2009 June 12;284(24):16325-33.

(158) Kalinski T, Krueger S, Sel S, Werner K, Ropke M, Roessner A. ADAMTS1 is regulated by interleukin-1beta, not by hypoxia, in chondrosarcoma. *Hum Pathol* 2007 January;38(1):86-94.

(159) Bongrazio M, Da Silva-Azevedo L, Bergmann EC, Baum O, Hinz B, Pries AR, Zakrzewicz A. Shear stress modulates the expression of thrombospondin-1 and CD36 in endothelial cells in vitro and during shear stress-induced angiogenesis in vivo. *Int J Immunopathol Pharmacol* 2006 January;19(1):35-48.

(160) Lee YJ, Koch M, Karl D, Torres-Collado AX, Fernando NT, Rothrock C, Kuruppu D, Ryeom S, Iruela-Arispe ML, Yoon SS. Variable inhibition of thrombospondin 1 against liver and lung metastases through differential activation of metalloproteinase ADAMTS1. *Cancer Res* 2010 February 1;70(3):948-56.

(161) Scheef EA, Sorenson CM, Sheibani N. Attenuation of proliferation and migration of retinal pericytes in the absence of thrombospondin-1. *Am J Physiol Cell Physiol* 2009 April;296(4):C724-C734.

(162) Chlench S, Mecha DN, Hohberg M, Hoffmann C, Pohlkamp T, Beyer G, Bongrazio M, Da Silva-Azevedo L, Baum O, Pries AR, Zakrzewicz A. Regulation of Foxo-1 and the angiopoietin-2/Tie2 system by shear stress. *FEBS Lett* 2007 February 20;581(4):673-80.

(163) Su SC, Mendoza EA, Kwak HI, Bayless KJ. Molecular profile of endothelial invasion of three-dimensional collagen matrices: insights into angiogenic sprout induction in wound healing. *Am J Physiol Cell Physiol* 2008 November;295(5):C1215-C1229.

(164) Rehn AP, Birch MA, Karlstrom E, Wendel M, Lind T. ADAMTS-1 increases the three-dimensional growth of osteoblasts through type I collagen processing. *Bone* 2007 August;41(2):231-8.

(165) Allen DL, Bandstra ER, Harrison BC, Thorng S, Stodieck LS, Kostenuik PJ, Morony S, Lacey DL, Hammond TG, Leinwand LL, Argraves WS, Bateman TA, Barth JL. Effects of spaceflight on murine skeletal muscle gene expression. *J Appl Physiol* 2009 February;106(2):582-95.

(166) Behrens J, Kameritsch P, Wallner S, Pohl U, Pogoda K. The carboxyl tail of Cx43 augments p38 mediated cell migration in a gap junction-independent manner. *Eur J Cell Biol* 2010 November;89(11):828-38.

(167) Gartner C, Ziegelhoffer B, Kostelka M, Stepan H, Mohr FW, Dhein S. Knock-down of endothelial connexins impairs angiogenesis. *Pharmacol Res* 2012 March;65(3):347-57.

(168) Milberg P, Klocke R, Frommeyer G, Quang TH, Dieks K, Stypmann J, Osada N, Kuhlmann M, Fehr M, Milting H, Nikol S, Waltenberger J, Breithardt G, Eckardt L. G-CSF therapy reduces myocardial repolarization reserve in the presence of increased arteriogenesis, angiogenesis and connexin 43 expression in an experimental model of pacing-induced heart failure. *Basic Res Cardiol* 2011 November;106(6):995-1008.

(169) Chen C-H. Utilization of microgravity bioreactor for differentiation and growth of human vascular endothelial cells. NASA; 1997.

(170) Dutt K, Sanford G, Harris-Hooker S, Brako L, Kumar R, Sroufe A, Melhado C. Three-dimensional model of angiogenesis: coculture of human retinal cells with bovine aortic endothelial cells in the NASA bioreactor. *Tissue Eng* 2003 October;9(5):893-908.

(171) Adamis AP, Miller JW, Bernal MT, D'Amico DJ, Folkman J, Yeo TK, Yeo KT. Increased vascular endothelial growth factor levels in the vitreous of eyes with proliferative diabetic retinopathy. *Am J Ophthalmol* 1994 October 15;118(4):445-50.

(172) Aiello LP, Avery RL, Arrigg PG, Keyt BA, Jampel HD, Shah ST, Pasquale LR, Thieme H, Iwamoto MA, Park JE, . Vascular endothelial growth factor in ocular fluid of patients with diabetic retinopathy and other retinal disorders. *N Engl J Med* 1994 December 1;331(22):1480-7.

(173) Aiello LP, Pierce EA, Foley ED, Takagi H, Chen H, Riddle L, Ferrara N, King GL, Smith LE. Suppression of retinal neovascularization in vivo by inhibition of vascular endothelial growth factor (VEGF) using soluble VEGF-receptor chimeric proteins. *Proc Natl Acad Sci U S A* 1995 November 7;92(23):10457-61.

7 Summary

The reduction of capillary density in microgravity-induced muscle atrophy has been observed by several studies. The cellular and molecular mechanisms leading to these changes remain to be recognized. Therefore, this study was designed at testing endothelial reactions on microgravity, focussing on those which are probably connected to the regulation of blood vessel growth. Since, according to published results from a gene array analysis, one of the most strongly regulated genes by microgravity is E3-ligase NEDD4, the aim of this work was to validate the impact of microgravity and shear stress (as a side effect when producing microgravity) on it, and search for NEDD4-regulated, angiogenesis-related proteins. In addition, previous studies indicated that ADAMTS1, which plays a role in the regulation of angiogenesis, is strongly induced by mechanical forces acting on endothelial cells, namely by shear stress. Here, it was tested if there is any influence of microgravity on ADAMTS1 expression.

Human Vein Endothelial Cells and EAhy926 cells were exposed to constant laminar or pulsatile laminar flow in a cone and plate device developed in the institute´s workshop. Microgravity experiments were performed in a Rotating Wall Vessel bioreactor. Both, NEDD4 and ADAMTS1, were tested under increased shear stress and microgravity. The regulation of genes and proteins was analysed by real time RT-PCR, immunoblotting, and immunoprecepitation, respectively. Additionally, cells were treated with different inhibitors either to block protein degradation or to investigate the role of mechanosensitive signalling pathways in their regulation.

NEDD4 is expressed in endothelial cells, co-precipitates with Cx43, and the increase of NEDD4 induced by microgravity correlates with a decrease in Cx43. This interaction between NEDD4 and Cx43 in human endothelial cells was confirmed by immunostaining showing co-localization and by siRNA mediated knockdown of NEDD4 which caused a decrease in Cx43. Accordingly, an increase of Cx43 was shown with inhibitors of the proteasome. However, there was no effect of constant laminar flow on NEDD4 expression. On contrary, an atheroprotective flow profile upregulated NEDD4 while an atheroprone flow profile caused the opposite effect. PI3K and $NO^{\cdot}$ production did not play a role in the regulation of NEDD4 by shear stress, so other signalling pathways will be involved. ADAMTS1 was transiently induced by

microgravity. Shear stress from 2 dyn/cm^2 onwards induced ADAMTS1, whereas atheroprone flow reduced it. Secreted to the cell culture supernatant, ADAMTS1 cleaves TSP1 to its smaller anti-angiogenic fragments. PI3K and $NO^{\cdot}$ production are clearly involved in the regulation of ADAMTS1 by shear stress. Likewise, TSP1 was somewhat later but as well transiently induced by microgravity.

Taken together, this work supports earlier observations of reduced angiogenesis under microgravity and extends them towards additional cellular mechanisms which contribute to the anti-angiogenic phenotype of endothelial cells under these conditions. Thus, the results of this study are expected to provide better understanding of mechanisms which can contribute not only to the development of different pathological situation observed in astronauts, but also for patients during long bed rest and for those who suffer from atherosclerosis.

8 Zusammenfassung

Eine reduzierte Kapillardichte bei durch Mikrogravitation ausgelöster Muskelatrophie ist in mehreren Studien beschrieben worden. Dennoch sind die zellulären und molekularen Mechanismen, die zu diesem Verlusst an Kapillaren führen, bisher unbekannt. Diese Studie hatte daher zum Ziel, Reaktionen von Endothelzellen auf Mikrogravitation zu untersuchen, insbesondere solche, für die ein Zusammenhang mit der Regulation des Blutgefäßwachstums besteht. Eine Gene-array Analyse einer anderen Gruppe hatte zuvor gezeigt, dass in Endothelzellen die E3-Ligase NEDD4 besonders deutlich durch Mikrogravitation induziert wird. Daher sollten nun diese Ergebnisse mit anderen Methoden bestätigt und auf Cx43 als Angiogenese-assoziiertes Substrat von NEDD4 ausgedehnt werden. Darüber hinaus sollte untersucht werden, ob das mechanosensitiv induzierte ADAMTS1, ein Angiogeneseinhibitor, auch eine Expressionsregulation durch Mikrogravitation erfährt.

Humane umbilikale venöse Endothelzellen und EAhy926 Zellen wurden in einem Konus-Platte-System konstanter laminarer oder pulsatil laminarer Strömung ausgesetzt. Mikrogravitation wurde mithilfe des von der NASA entwickelten „Rotating Wall Vessel“ simuliert. Anschließend wurden die Zellen mittels quantitativer real time RT-PCR, Immunoblotting und Immunpräzipitation untersucht. In weiteren Experimenten wurden die Zellen mit Inhibitoren des Proteasoms oder des Lysosoms, mit einem PI3K-Inhibitor oder L-NAME zur Hemmung der $NO^{\cdot}$-Synthese behandelt, um einen etwaigen Beitrag dieser Signalwege zur beobachteten Regulationscharakteristik zu ermitteln.

NEDD4 wird in Endothelzellen exprimiert, lässt sich mit Cx43 kopräzipitieren, und sein durch Mikrogravitation erzeugter Konzentrationsanstieg korrelliert mit dem Konzentrationsabfall von Cx43. Die Interaktion von NEDD4 und Cx43 wurde durch Kolokalisation in der konfokalen Lasermikroskopie sowie nach siRNA vermitteltem knock down von NEDD4 bestätigt. Entsprechend führte die Hemmung des Proteasoms zum Anstieg von Cx43. Konstante, laminare Strömung hatte dagegen keinen Einfluss auf die Expression von NEDD4. Wohl aber wurde NEDD4 durch ein atheroprotektives Strömungsprofil induziert, durch ein atherogenens supprimiert. PI3K und $NO^{\cdot}$ spielten dabei keine Rolle. ADAMTS1 wurde durch Mikrogravitation transient induziert. Schubspannungen über 2 dyn/cm^2 führten zu einem starken Anstieg von ADAMTS1,

während es durch ein atherogenes Strömungsprofil supprimiert wurde. In den Kulturüberstand sezerniert degradiert ADAMTS1 TSP1 zu einem antiangiogenen, 70 kDa großen Fragment. PI3K und $NO^{\cdot}$ Produktion sind gleichermaßen notwendig für die strömungsabhängige Expressionsregulation von ADAMTS1. Auch TSP1 wurde durch Mikrogravitation transient induziert.

Diese Arbeit unterstützt die bereits bestehende Auffassung von einer reduzierten Angiogenese unter den Bedingungen der Schwerelosigkeit und erweitert sie um zelluläre/molekulare Mechanismen, die zur Erklärung des antiangiogenen Phänotyps der Endothelzellen bei Schwerelosigkeit beitragen können. Diese Ergebnisse tragen daher bei zu einem besseren Verständnis pathophysiologischer Vorgänge bei Astronauten (bzw. Kosmonauten u.ä.) und – klinisch relevanter – bei Patienten mit langer Immobilisation. Wegen der Rolle von Cx43 bei der Entwicklung von Arteriosklerose könnten die hier vorgelegten Ergebnisse über NEDD4 auch in diesem Zusammenhang von Interesse sein.

9 Appendix

9.1 Acknowledgments

I thank my supervisors Prof. Axel Pries, Prof. Wolfgang Kuebler and Prof Volker Haucke for giving me a chance to work on this project. Their support and supervision were very helpful.

I thank dr. Andreas Zakrzewicz for his supervision, introducing to many laboratory techniques and many discussions. I would like also to thank for your patience and correcting all my paper work.

Special thank you to dr. Luis da Silva-Azevedo for introducing me to protein analysis methods. Luis, you were always great partner to discuss results and share books, protocols and idea with.

I would like to thank also Prof. Günter Siegel for giving me access to his great cell culture laboratory and to Mrs. Gabriele Bayer and Mrs. Angela Becker for great technical help.

I also thank Julia Hoffmann, Beata Styp-Rekowska and Stephanie Gembardt for all scientific and non-scientific discussions and all coffee breaks we had together. Girls you were really amazing over this years.

To Bernd Vorderwulbecke and Julian Maroski for being always such a great help in the lab, willing to share last few microliters of reagents and for all discussions. It was really great to work with you.

To Michael Mertens for his always good mood and sharing each box of cookies and every bar of chocolate. They do not taste the same without you.

To Yun Yin, Liming Wang, Arata Tabuchi, Nadine Klein, Nils Neye, Hannah Nickles and Bjorn Hoffmann for their help and support in every day life.

And to my parents, for their great support and believing that writing this thesis will ever have happy end.

9.2 List of publications

1. K. Fiedorowicz, L. da Silva-Azevedo, W.M Kuebler, D. Blottner, A.R. Pries, A. Zakrzewicz, "NEDD4 influences Cx43 degradation in endothelial cells under simulated microgravity conditions", in preparation
2. H. Habazettl and K. Fiedorowicz, R. Knudsen, A. Zakrzewicz, B. Styp-Rekowska, E. Ermilov, S.Hädel, A. Pries, "A shear cone device to apply realistic pulsatile shear profiles to cultured cells" submitted to Biorheology
3. Hohberg, M., Knöchel, J., Hoffmann, C.J., Chlench, S., Wunderlich ,W., Alter, A., Maroski, J., Vorderwülbecke, B.J., Silva-Azevedo, L.D., Knudsen, R., Lehmann, R., Fiedorowicz, K., Bongrazio, M., Nitsche, B., Hoepfner, M., Styp-Rekowska, B., Pries, A.R., Zakrzewicz, A., "Expression of ADAMTS1 in endothelial cells is induced by shear stress and suppressed in sprouting capillaries", J Cell Physiol. 2010, Jul 27
4. J. Maroski, B. Vorderwuelbecke, K. Fiedorowicz, L. Da Silva-Azevedo, G. Siegel, A. Marki, A. Pries and A. Zakrzewicz, "Shear stress increases endothelial hyaluronan synthase 2 and hyaluronan synthesis especially in regard to an atheroprotective flow profile", Exp Physiol. 2011, Sep;96(9):977-86
5. B. J. Vorderwülbecke, J. Maroski, K. Fiedorowicz, L. Da Silva-Azevedo, A. R. Pries, A. Zakrzewicz, "Regulation of endothelial Connexin 40 by shear stress", Am J Physiol Heart Circ Physiol. 2012, Jan;302(1):H143-52

Abstracts

1. H. Tönnies, K. Fiedorowicz, J. Olszanska, A.S. Müller, A. Gerlach, and H. Neitzel, "Automated I-FISH-Scanning Sensitively Detecting Early MDS- and AML-associated Chromosomal Imbalances in Peripheral Blood and Bone Marrow Cells of Fanconi Anemia Patients" 17th Annual Fanconi Anemia Research Fund Scientific Symposium, Switzerland, 2005
2. K. Fiedorowicz, A.Zakrzewicz, A.R. Pries, "Effects of microgravity on endothelial cells", 2nd International Conference on "Exploring the future of Vascular and inflammatory mediators", International Immunopharmacology, Berlin, Germany, 2007
3. K.Fiedorowicz, L. Da Silva Azevedo, W.M Kuebler, A. Zakrzewicz, A.R Pries "Microgravity-induced expression of ubiquitin-ligase NEDD4", German

Physiological Society, Acta Physiologica VOL.192 (supplement 663) OT1-5-8, Cologne, Germany, 2008

4. K. Fiedorowicz, L. Da Silva Azevedo, A.Zakrzewicz, A.R. Pries "Induction of NEDD4 under simulated microgravity", Experimantal Biology Congress, FASEB J. 22, 752.8, San Diego, 2008
5. K. Fiedorowicz, L. Da Silva Azevedo, A. Zakrzewicz, W.M. Kuebler, A.R. Pries "Nedd 4 mediated degradation of Cx43 under simulated microgravity" , Experimental Biology Congress, FASEB J. 2009, 22:752.8-752, New Orleans, 2009

Presentations

1. Poster: "Effects of microgravity on endothelial cells", 2nd International Conference on "Exploring the future of Vascular and inflammatory mediators", International Immunopharmacology Berlin, Germany, 2007
2. Lecture: "Microgravity-induced expression of ubiquitin-ligase NEDD4", German Physiological Society, Acta Physiologica VOL.192 (supplement 663) OT1-5-8, Cologne, Germany, 2008
3. Poster: "Induction of NEDD4 under simulated microgravity", Experimental Biology Congress, FASEB J. 22, 752.8, San Diego, USA, 2008
4. Poster: "NEDD4 mediated degradation of Cx43 under simulated microgravity", Experimental Biology Congress, FASEB J. 2009, 22:752.8-752, New Orleans, USA 2009

Congresses

1. Congress of German Society for Human Genetics, Halle, Germany, 2005
2. 24thEuropean Conference on Microcirculation, "From vascular biology to Clinical Microcirculation", Amsterdam, Netherlands, 2006
3. Experimental Biology Congress Washington, USA, 2007
4. International Conference on "Exploring the future of Vascular and inflammatory mediators" Berlin, Germany, 2007
5. German Physiological Society, Cologne, Germany, 2008
6. Experimental Biology Congress, San Diego, USA, 2008
7. Experimental Biology Congress, New Orleans, USA, 2009